

XD-A112 703

VANZETTI SYSTEMS INC. STOUGHTON MA
INFRARED DETECTION OF FAULTY SOLDER JOINTS. PHASE 2-2.(U)
MAR 82 A C TRAUB

F/6 14/5

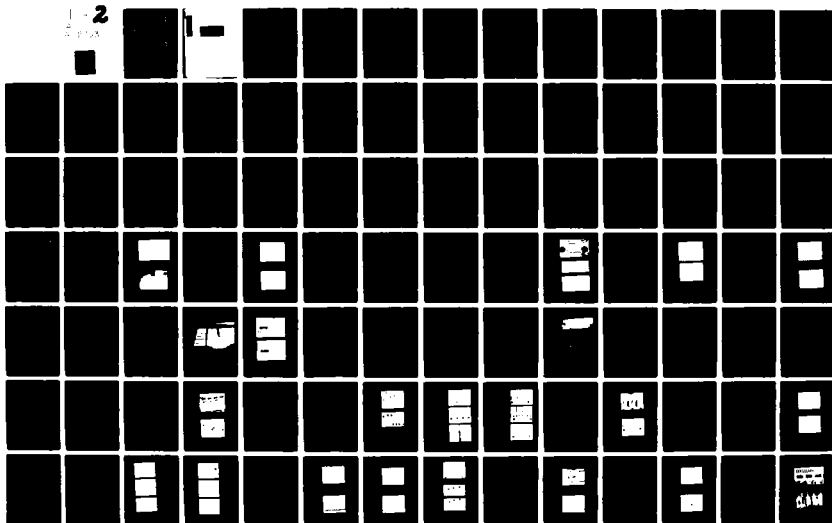
F04606-80-C-1338

NL

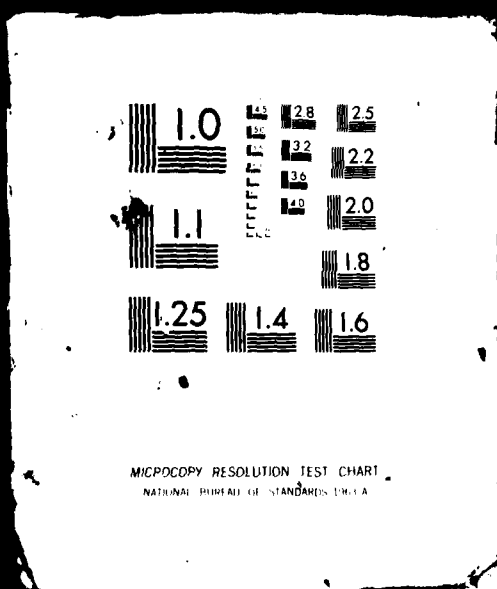
UNCLASSIFIED

2

1-2



1 OF 2
AD-
A112703

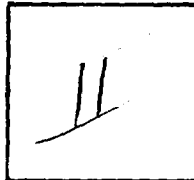


190 p.

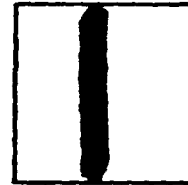
PHOTOGRAPH THIS SHEET

AD-A12703

DTIC ACCESSION NUMBER



LEVEL



INVENTORY

Infrared Detection of Faulty Solder Joints

1 Mar. 82

DOCUMENT IDENTIFICATION

Phase 2.2

Contract F04606-80-C-1338

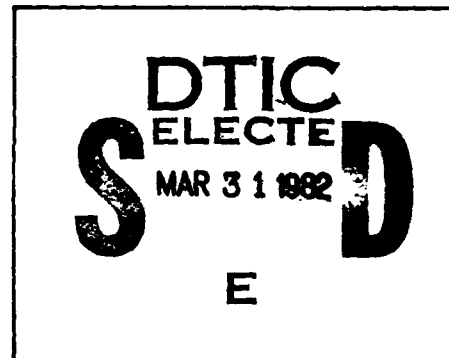
DISTRIBUTION STATEMENT A

Approved for public release
Distribution Unlimited

DISTRIBUTION STATEMENT

| | |
|--------------------|----------------------|
| ACCESSION FOR | |
| NTIS | GR&I |
| DTIC | TAB |
| UNANNOUNCED | |
| JUSTIFICATION | |
| BY | |
| DISTRIBUTION / | |
| AVAILABILITY CODES | |
| DIST | AVAIL AND/OR SPECIAL |
| A | |

DISTRIBUTION STAMP



DATE ACCESSIONED

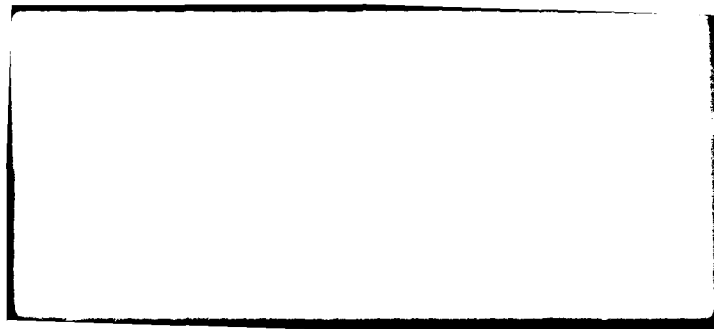


DATE RECEIVED IN DTIC

PHOTOGRAPH THIS SHEET AND RETURN TO DTIC-DDA-2

DTIC FORM 70A
OCT 79

DOCUMENT PROCESSING SHEET



①

Program Report

INFRARED DETECTION
OF
FAULTY SOLDER JOINTS
PHASE 2.2

Under

Contract No. F04606-80-C-1338

to

SM-ALC/MMIREA
SACRAMENTO, ALC
McCLELLAN AFB, CA

1 March 1982

by

Alan C. Traub
Vanzetti Systems, Inc.
Stoughton, MA 02072

APPROVED FOR PUBLIC RELEASE
DISTRIBUTION UNLIMITED

DTIC
ELEC
MAR 31 1982
E

"Original contains color
plates: All DTIC reproductions
will be in black and
white"

NOTICE

The inclusion of brand names in this report is for purposes of identifying certain materials and items of equipment which were used in the tests. Their mention is not intended to constitute an endorsement of any particular product by the United States Air Force or by the contractor.



| | |
|--------------------|-------------------------------------|
| Accession For | |
| NTIS GRA&I | <input checked="" type="checkbox"/> |
| DTIC TAB | <input type="checkbox"/> |
| Unannounced | <input type="checkbox"/> |
| Justification | |
| By | |
| Distribution/ | |
| Availability Codes | |
| Dist | Avail and/or Special |
| A | |

INFRARED DETECTION OF FAULTY SOLDER JOINTS
PHASE 2.2

Table of Contents

| | <u>Page</u> |
|--|-------------|
| List of Illustrations | v |
| List of Tables | x |
| ABSTRACT | 1 |
| 1.0 INTRODUCTION | 1 |
| 2.0 PROGRAM SUMMARY | 3 |
| 2.1 Program Activities | 4 |
| 2.2 Program Accomplishments | 5 |
| 3.0 TECHNICAL DISCUSSION | 5 |
| 3.1 Damage Tests on Laminates | 6 |
| 3.1.1 Survey of Laminate Types | 6 |
| 3.1.2 Sample Procurement and Test Preparations | 8 |
| 3.1.3 Reflectance Measurements | 9 |
| 3.1.4 Effect of Board Texture | 15 |
| 3.1.5 Ignition Point Determinations | 18 |
| 3.1.6 Softening Point Determinations | 24 |
| 3.2 Damage Prevention on Laminates | 26 |
| 3.3 Laser/thermal Testing Through Conformal Coatings | 36 |
| 3.4 Testing of Solder Joints | 44 |
| 3.4.1 Preparation of Samples | 45 |
| 3.4.2 Testing Conditions | 48 |
| 3.4.3 System Repeatability | 51 |
| 3.4.4 Method of Scoring | 56 |
| 3.4.5 Component-side Testing | 59 |
| 3.4.6 Test Results on Lap Joints | 61 |
| 3.4.6.1 Exploratory Tests | 62 |
| 3.4.6.2 Tests Using Elongated Beam Spot | 68 |
| 3.4.6.3 Focus Considerations | 71 |

| | <u>Page</u> |
|--|-------------|
| 3.4.6.4 Point by Point Testing Along the Lead Length | 75 |
| 3.4.6.5 Statistical Testing of Lap Joints | 81 |
| 3.4.6.6 Board 8B, IC 1 | 83 |
| 3.4.6.7 Board 8B, ICs 2, 3 and 4 | 89 |
| 3.4.6.8 Board 8B, ICs 5 and 6 | 97 |
| 3.4.6.9 Board 8B, ICs 7 through 12 | 98 |
| 3.4.6.10 Board 8 | 102 |
| 3.4.7 Test Results on Through-hole Joints | 111 |
| 3.4.7.1 Board 1 | 114 |
| 3.4.7.2 Board 2 | 115 |
| 3.4.7.3 Board 3 | 119 |
| 3.4.7.4 Board 4 | 120 |
| 3.4.7.5 Board 5 | 121 |
| 3.4.7.6 Board 6 | 122 |
| 3.4.7.7 Board 7 | 123 |
| 3.4.8 Summary and Discussion of Test Results | 124 |
| 3.4.8.1 Test Results on Through-hole Joints | 127 |
| 3.4.8.2 Test Results on Lap Joints | 129 |
| 3.4.8.3 Discussion of Test Results | 131 |
| 3.4.9 Specific Defect Types | 133 |
| 3.4.9.1 Internal Voids in Through-hole Joints | 134 |
| 3.4.9.2 Cracked Through-hole Joints | 137 |
| 3.5 System Optimization | 147 |
| 3.5.1 Co-alignment of Optical Axes | 149 |
| 3.5.2 Laser-beam Homogenization | 155 |
| 3.5.3 Laser-beam Power Considerations | 163 |
| 3.5.4 Other Considerations | 167 |
| 4.0 PROGRAM REVIEW | 168 |
| 5.0 RECOMMENDATIONS | 170 |
| 6.0 CONCLUSION | 171 |
| APPENDIX A | 173 |

LIST OF ILLUSTRATIONS

| Figure No. | Subject | Page |
|---------------|---|------|
| 1 | Method of measuring sample reflectance. | 14 |
| 2 | INSPECT signal vs. target temperature for a blackbody target. | 19 |
| 3 | Calculated ignition temperatures vs. emissivity for the twelve burned samples in Table 2. | 25 |
| 4 | Schematic of damage prevention and shutter control circuits. | 29 |
| 5 | Oscillogram showing effect of damage prevention circuit. | 31 |
| 6 | Photograph showing the effect of damage prevention circuit. | 31 |
| 7 | Tests similar to earlier one but with triggering threshold lowered. | 33 |
| 8 | Similar to above but with still lower threshold. | 33 |
| 9 | Alternating sequence of "good" and "cold solder" joints from No. 1 through No. 8. | 38 |
| 10 | Thermal signatures of uncoated joints. | 38 |
| 11 | Thermal signatures of same joints with silicone coating. | 38 |
| 12 | Thermal signatures of uncoated joints and of the same joints with epoxy coating. | 40 |
| 13 | Relative heating rates on Laminate Sample No. 4 with and without silicone coating. | 42 |
| 14 | Same but on Sample No. 6. | 42 |
| 15 | Component-side view of 926 solder-joint samples prepared for statistical testing. | 46 |
| 16 | Boards 8 and 8B containing 238 hand-fabricated lap joints. | 47 |

List of Illustrations
(Continued)

| Figure No. | Subject | Page |
|---------------|---|------|
| 17 | Two identical thermal passes over a row of 22 unused solder pads. | 52 |
| 18 | Twenty-four exposures on the same part of one solder joint. | 52 |
| 19 | Repeated thermal signatures at the same location on one solder joint. | 54 |
| 20 | Close-up view of solder voids on component side of board giving rise to high peaks in Figure 21. | 60 |
| 21 | Eight component-side voids and eight good joints for reference. | 60 |
| 22 | Thermal signatures of 29 test joints of various qualities. | 63 |
| 23 | Numbering and quality assessment of the 29 samples. | 63 |
| 24 | Micrographs of Samples 1 through 8. | 64 |
| 25 | Micrographs of Samples 9 through 29. | 65 |
| 26 | Blemish at center of Sample No. 15. | 67 |
| 27 | Solder joints at Pins 8 - 14 of IC No. 9, Board No. 8. | 67 |
| 28 | Thermal signatures at Pins 8 through 14 of Figure 27 with and without laser-beam spot elongation. | 70 |
| 29 | Effect of defocusing to achieve uniform thermal signatures. | 73 |
| 30 | Repeat of Figure 29 test on a different set of samples. | 74 |
| 31 | An extreme case of a "cracked joint". | 76 |
| 32 | Sequence of increasing thermal signal amplitudes from toe to heel of above lead. | 76 |
| 33 | Thermal signatures at the tip and heel of the lead shown in Figure 31. | 77 |

List of Illustrations (Continued)

| <u>Figure No.</u> | <u>Subject</u> | <u>Page</u> |
|-----------------------|---|-------------|
| 34 | A scan across the centers of the joints shown in Figure 31. | 77 |
| 35 | Test Board No. 8B, IC No. 1, Pins 1 through 6. | 78 |
| 36 | Thermal signatures at three points along two types of defective joint. | 78 |
| 37 | A lead with the toe and heel bent up, adjoined by two normal joints. | 80 |
| 38 | Thermal signatures of the toe, center and heel of the above lead. | 80 |
| 39 | A thermal scan across seven joints. | 82 |
| 40 | A view of the seven joints represented in the above thermogram. | 82 |
| 41 | ICs 1 through 3 on Board 8B. | 84 |
| 42 | Close-up view of IC 1 Pin 12 and Pin 14. | 84 |
| 43 | Scans across the toes, centers and heels of Pins 8 through 14 on IC 1 of Board 8B. | 86 |
| 44 | A "questionable" band entered on the trace of Figure 43 separates various solder-joint sections into various levels of quality. | 88 |
| 45 | Board 8B, IC 2, Pin 8. | 90 |
| 46 | Same but Pin 10. | 90 |
| 47 | Pins 8 through 14 on ICs 2, 3 and 4. | 90 |
| 48 | A defective lap joint adjoined by two good ones. | 94 |
| 49 | Two different scans of three sections on each of six joints. | 95 |
| 50 | Thermal scans across the toes, centers and heels of ICs 1 through 6 on Board 8B. | 99 |
| 51 | Thermal scans across the centers of Joints 7-1 through 12-14 on Board 8B. | 101 |

List of Illustrations
(Continued)

| Figure No. | Subject | Page |
|---------------|--|------|
| 52 | Thermal signatures of Joints 1-8 through 11-14 on Board 8. | 103 |
| 53 | Joints 3-8 through 3-14 on Board 8. | 105 |
| 54 | A second pass over some of the joints represented in Figure 52. | 105 |
| 55 | Joints 4-10 through 4-14 on Board 8. | 108 |
| 56 | Joints 11-8 through 11-14 on Board 8. | 108 |
| 57 | Appearance of the recorded data during testing of feed-through joints. | 113 |
| 58 | Effect of threshold level on trade-offs in scoring. Hypothetical case. | 125 |
| 59 | Thermal signatures and pictorial view of normal and void-type joints on Board No. 3. | 136 |
| 60 | Joints shown in Figure 49 after removal of caps. | 138 |
| 61 | Example of laser-beam damage to an earlier set of void-type samples. | 139 |
| 62 | Two lead cracks simulated by removal of solder. | 141 |
| 63 | Separate thermal scans of eight joints containing the above cracks. | 141 |
| 64 | Solder side of board at 2.5X enlargement. | 143 |
| 65 | Fourteen joints on IC 1 at 7.5X enlargement. | 143 |
| 66 | Sixteen joints on IC 2 at 7.5X enlargement. | 144 |
| 67 | Sixteen joints on IC 3 at 7.5X enlargement. | 144 |
| 68 | Thermal signatures of 46 joints including cracked ones. | 146 |
| 69 | One method of bringing the laser and detector axes into coincidence. | 151 |
| 70 | Use of a dichroic mirror to bring separate optical axes in coincidence. | 154 |

List of Illustrations
(Continued)

| <u>Figure No.</u> | <u>Subject</u> | <u>Page</u> |
|-----------------------|---|-------------|
| 71 | Spectral reflectance, transmittance and specifications for a typical dichroic mirror. | 156 |
| 72 | Near and far views of fiber optic assembly. | 161 |
| 73 | Small pit formed at corner of solder joint by laser beam. | 165 |
| 74 | Burn marks formed on substrate by laser beam. | 165 |

I

I

I

I

LIST OF TABLES

| <u>Table No.</u> | <u>Title</u> | <u>Page</u> |
|----------------------|---|-------------|
| 1 | Directional and averaged reflectance values for PC board materials (1.06 μ m). | 11 |
| 2 | Emissivities and ignition- and shutdown-temperatures for 44 samples without and with burn prevention. | 21 |
| 3 | Comparison of softening temperatures for samples. | 27 |
| 4 | Method of scoring the data on Board 2, Columns 1 - 10. | 117 |
| 5 | Scoring summary for feed-through joints. | 128 |
| 6 | Scoring summary for lap joints. | 130 |
| 7 | Comparison of laser/thermal test data with visual assessment of solder joint quality. | 148 |

Program Report

INFRARED DETECTION OF FAULTY SOLDER JOINTS PHASE 2.2

ABSTRACT

An experimental model of a laser/thermal testing system for solder joints has been evaluated during tests on 1,074 joints. Certain types of defect in through-hole and lap joints are revealed by this method, which seeks out variations in surface quality and in thermal mass. The possibility of accidental laser-beam damage to substrates was also investigated. A means of reducing this possibility was conceived and implemented. The feasibility of testing solder joints covered by a conformal coating was confirmed. Several improvements in the system design concept were effected during the course of the work.

1.0 INTRODUCTION

The effort described in this report represents a further phase in a developmental program which was begun in July, 1978 and whose purpose was the implementation of an automatic inspection system for solder joints on printed circuit boards. In this method, the joints are tested in sequence, at the rate of several per second, by the combined use of laser-beam heat injection and infrared thermal monitoring. Differences in the bulk properties or surface properties between good and bad joints are revealed as differences in their heating rates or, more simply, in the peak temperatures which are reached at the ends of exposures of fixed durations.

Earlier phases of this effort were concerned with the establishment of the feasibility of the basic concept, through testing and experimentation, and with the implementation and preliminary testing of an experimental, automated inspection system.

In Phase 2.2, we report on more extensive testing of the laboratory model and on our findings with regard to certain other questions. These questions were concerned with the possibility of accidental laser damage to the substrate material and with what measures might be used to avoid this. Another question concerned the efficacy of the testing method if it had to be carried out in the presence of a conformal coating.

Approximately 1,000 feed-through and lap-joints were used as the basis for the solder-joint tests.

During our use of the system in Phase 2.2, the need for certain improvements became apparent. One of these was the need to bring together the optical axes of the laser-beam and detector paths as they intersected the target, for these axes approached the target from slightly different angles in the breadboard system. A method of doing so was worked out during Phase 2.2 and was implemented later, bringing about the needed improvement in system performance.

A second improvement was achieved through the insertion of an optical fiber in the laser-beam path, bringing about several advantages which are discussed in Section 3.5.2.

For the reader who is unfamiliar with the details of the "laser/thermal" testing method for solder joints, we offer as Appendix A a description of this method which was prepared at an earlier time.

2.0 PROGRAM SUMMARY

This report marks the conclusion of somewhat over seven months of effort whose purpose was to:

1. Verify the capability of the laser/thermal system in detecting various types of defects in lap joints, and to do so via a large number of tests on a statistically meaningful sample size;
2. Assess the risk of laser-beam damage to circuit board parts during inspection and to determine whether such damage could be avoided by some means or other; and
3. Investigate, as per the Engineering specification, the feasibility of using the laser/thermal technique in detecting defects in feed-through joints.

Seven Monthly Status Reports have been prepared, from October 1980 through April 1981, and the purpose of this Program Report is to summarize their contents while describing the tasks that were carried out and the results thereof. The preparation of this report falls outside the scope of the contractual commitment and was carried out under Vanzetti Company sponsorship.

Here we will list, briefly, the principal activity areas during Phase 2.2, and we will follow this with a summary of the other program accomplishments besides the solder-joint test results.

2.1 Program Activities

From the program beginning, work progressed in several areas according to a program schedule which was prepared at the outset.

These areas included:

- Refurbishing of the laser/thermal system, which had been idle for several months. This included the cleaning and re-aligning of the YAG laser and of the infrared detection system optics. The detection system was also re-calibrated in order to extend its range to higher temperatures.
- A survey of available types of laminate materials and the procurement of samples for testing.
- The design and implementation of a damage-prevention circuit.
- A survey of the commonly used types of conformal coating and the procurement of samples for testing.
- The preparation of nearly 1,100 solder joint samples for testing.
- A series of activities involved with optimizing the system design concept and present operation. These included:
 1. Attempts to elongate both the laser-beam spot and the detector target area, with the conclusion that this would have to await the installation of a dichroic beamsplitter in order to bring the optical axes into coincidence;
 2. The evolution of a design concept for accomplishing this, and the preparation of a specification for a suitable beamsplitter;
 3. The installation of an optical fiber in the laser-beam path so that the beams from the YAG and HeNe lasers could be combined more effectively; and
 4. A visit to the laboratories of a major laser manufacturer where we tested the efficacy of a higher-powered laser than the present one. We concluded that nine or ten watts would be an effective level of operation.

2.2 Program Accomplishments

The principal results of the above activities, besides the solder-joint test results, were the following:

- Tests on more than 60 samples of laminate material have demonstrated that:
 1. The commonly used PC board materials are susceptible to laser-beam damage at the power levels used for solder-joint testing;
 2. There is variability in damage susceptibility from board to board, with the darker materials generally being more easily damaged;
 3. Within a given board sample, there is high variability from place to place. This is due to reflectance variations arising from the woven texture of the underlying fiber glass.
- Tests were made on the effects of conformal coatings upon laser/thermal tests of solder joints and upon board damage susceptibility. A soft (silicone) and a hard (epoxy) coating were used. In both cases, it was found that the effect of the coating was to improve the performance of the testing system by providing higher thermal signals and to reduce the heating of the laminate by providing heat-sinking.
- The damage-prevention circuit was tested and optimized. Its two-millisecond shutter-closing time was found to be completely effective in preventing laser damage to substrates at the laser power levels in present use.
- The system design concept was more firmly established by the end of the program.

3.0 TECHNICAL DISCUSSION

In this section, we will describe in some detail our investigations and findings under the various subject headings into which Phase 2.2 may be divided:

- Survey, procurement and testing of various laminate materials for laser-damage susceptibility;
- Design, implementation and testing of a damage prevention circuit for fast shutdown of the laser beam upon detection of excessive heating;
- The preparation and testing of nearly 1,100 solder joint samples of both the lap and feed-through type;
- A survey of the commonly used types of conformal coating, and the procurement, preparation and testing of a silicone type and an epoxy type;
- Optimization of the laser/thermal system design concept.

3.1 Damage Tests on Laminates

The purpose of this task was to determine damage thresholds for various laminate materials in common use as a function of laser exposure intensity and duration. The task began with a review of the various formulations, followed by the procurement and testing of samples.

3.1.1 Survey of Laminate Types

A literature review and a catalog and telephone survey of several leading manufacturers provided us with our initial information about commercially available board materials.

This effort has revealed that board materials for printed circuit use are provided in a number of formulations comprising combinations of either paper or glass fibers with either phenolic, polyester or epoxy substances. Of these, the most common board material in professional use is epoxy-glass,

whose thermal expansion properties are better matched to that of the copper films which are used on the boards, thus reducing the risk of separation during thermal cycling.

According to the manufacturers, the most common material for industrial and military applications is FR-4, a flame retardant version of G-10 which had been in wide use previously. FR-4 is usually supplied to users who request G-10 material because the latter is rarely produced. Many users, unaware of the substitution, mistakenly identify their board materials as G-10.

Apart from their being provided in various thicknesses, the major difference among the FR-4 materials is that of color. The uncolored material ranges from a straw color to pale green, but customer preferences often call for various shades of blue, black, red, dark green, white, and so forth. Because the susceptibility to laser damage can be highly dependent on color, our purpose in this program was to test as many different samples as possible.

For higher-temperature use, FR-5 is specified. This is the flame-retardant version of G-11 material, the latter being similar to G-10 but having a higher operating temperature of 150°C instead of 130°C. There is some variation among operating temperatures as specified by various manufacturers. FR-5 appears to be available only in its natural color of straw or pale green.

Both FR-4 and FR-5 are superior to common board materials in temperature resistance, impermeability to water, flexural strength, impact resistance, thermal expansion, etc., and in meeting military and Underwriters' Laboratories specifications.

Available thicknesses range typically from one-sixteenth to one-quarter inch. We expected board thickness to play a negligible role in damage susceptibility because laser-beam damage is a surface phenomenon. Our tests were therefore made on those thicknesses which were available, generally one-sixteenth inch.

3.1.2 Sample Procurement and Test Preparations

Several dozen pieces of laminate materials were obtained from various manufacturers, differing in composition and in color, but comprising FR-4 and FR-5 for the most part. Sixty samples, four inches square, were prepared and numbered, some of these being of the same material for checking purposes and some being of similar-appearing materials from different manufacturers. Some of the samples were received with copper cladding on one or both sides, and this was removed before testing. In other cases, samples were received in their original, unclad state. Those samples which had been de-clad were expected to behave differently from the unclad ones because, according to the suppliers, the bonding agent remains with the substrate when the copper is removed.

Tests of various types were performed in order to reveal such parameters as reflectance, softening temperature, ignition temperature, and effects of conformal coatings. These tests will be described in the ensuing sections.

3.1.3 Reflectance Measurements

For fixed exposure conditions, the susceptibility of a laminate material to laser-beam damage depends strongly on the absorptance of the material at the laser wavelength (1.06 μm in this case). Because of wide color variations among the samples (which depend upon the visible-band absorptivity properties), it was expected that differences would be ~~seen~~ at the laser wavelength also.

What we hoped to find was a correlation between the 1.06 μm absorptivity and the susceptibility to laser-beam damage. If such were the case, then predictions could be made about the damage susceptibility of any board material on the basis of a simple, non-destructive absorptivity measurement. Such a measurement would be carried out by use of a reflectance measurement at the laser wavelength because, for opaque samples, reflectance is known to vary in a complementary way with absorptance.

One factor which might serve to diminish the correlation would be the presence of a conformal coating or of a residual bonding layer on the laminate surface. A coated and an uncoated board of the same material would have nearly the same reflectance values if the coating were transparent at the laser wavelength. However, such a coating would most likely be absorbing at the greater wavelengths emitted by the laminate surface as it becomes warm during laser exposure. This "greenhouse effect" would interfere with the normal radiational cooling of the warmed surface, causing it to reach higher temperatures than normal.

In addition, if the coating happened to be a better thermal emitter than the substrate, it would bring about higher-than-normal infrared signals which would register as still higher temperatures at the detector.

Both of these effects would be offset by the tendency of the layer to cool the substrate by normal conductive processes.

Our procedure was to obtain an absorptivity value for each sample on the basis of a reflectance measurement. Because most of the test boards were opaque, one has only to subtract the reflectance value from "one" in order to obtain the absorptance. Some of the samples were, however, translucent and so the rule is less applicable but still useful as a general guide. For precise absorption measurements on such samples, one would make separate reflectance and transmittance measurements and would use the fact that the energy which is neither reflected nor transmitted must be absorbed.

In principle, a proper reflectance measurement requires the use of special equipment which illuminates the sample from a given direction and which collects all of the reflected radiation, regardless of direction. In the absence of such equipment, one can approximate the process by measuring the reflected amounts in several different directions and taking an average. This was the method used here, with three measurement directions being used.

The results appear in Table 1 where the first three columns are raw data derived from the three measurement positions. The differences in the three values for any one sample are an indication of the gloss characteristics of the material, with the shiny

TABLE 1. DIRECTIONAL AND AVERAGED REFLECTANCE VALUES
FOR PC BOARD MATERIALS (1.06 μm)
(Percent)

| Sample No. | Description | Direction No. 1 | Direction No. 2 | Direction No. 3 | Average |
|---------------|---|--------------------|--------------------|--------------------|---------|
| 1 | Polyply FR-4, green | 72 | 64 | 64 | 67 |
| 2 | Polyply FR-4, green | 72 | 64 | 64 | 67 |
| 3 | Polyply FR-4, blue | 64 | 75 | 69 | 69 |
| 4 | Polyply FR-4, black | 13 | 17 | 25 | 18 |
| 5 | Polyply FR-5, yellow | 78 | 71 | 70 | 73 |
| 6 | Polyclad FR-4, dk. green | 30 | 48 | 42 | 40 |
| 7 | Polyclad FR-4, dk. green | 30 | 47 | 42 | 40 |
| 8 | Polyclad FR-4, blue | 72 | 79 | 76 | 76 |
| 9 | Polyclad FR-4, blue | 72 | 82 | 78 | 77 |
| 10 | Polyclad FR-4, black | 12 | 20 | 25 | 19 |
| 11 | Polyclad FR-4, yellow | 74 | 76 | 73 | 81 |
| 12 | Polyclad FR-4, yellow | 75 | 76 | 73 | 76 |
| 13 | Polyply FR-4, pale green with watermark | 74 | 76 | 74 | 75 |
| 14 | Synthane FR-4, dk. green | 42 | 55 | 50 | 49 |
| 15 | Youngblood FR-4, grey-tan | 64 | 69 | 66 | 66 |
| 16 | Synthane FR-4, lt. green | 82 | 74 | 73 | 76 |
| 17 | Synthane FR-4, pale green | 72 | 77 | 75 | 75 |
| 18 | Synthane FR-5, orange natural, glossy | 75 | 72 | 73 | 73 |
| 19 | Synthane FR-5, yellow natural, dull | 75 | 77 | 72 | 75 |
| 20 | Synthane FR-4, black | 12 | 18 | 26 | 19 |
| 21 | CIMCLAD MA7FR phenolic, yell. | 84 | 81 | 89 | 85 |
| 22 | Oak FR-4, natural | 74 | 78 | 76 | 76 |
| 23 | Oak FR-4, natural | 72 | 77 | 75 | 75 |
| 24 | Youngblood FR-4, lt. green | 66 | 61 | 62 | 63 |
| 25 | Youngblood FR-4, lt. green | 66 | 61 | 62 | 63 |
| 26 | Polyclad FR-4, beige | 58 | 80 | 75 | 71 |
| 27 | Spaulding FR-4, green, matte, Spauldite G-10-900 | 48 | 56 | 50 | 51 |
| 28 | Keystone 2082PK phenolic | 66 | 78 | 74 | 73 |
| 29 | Kepro XXXP phenolic (P2-66) | 58 | 66 | 63 | 62 |
| 30 | NVF EG-873 SEC natural | 78 | 70 | 73 | 74 |
| 31 | Unidentified FR-4, green | 52 | 68 | 61 | 60 |
| 32 | Unidentified FR-4, green | 60 | 69 | 62 | 64 |

Continued

TABLE 1 (Continued). DIRECTIONAL AND AVERAGED REFLECTANCE
VALUES FOR PC BOARD MATERIALS AT 1.06 μ m
(Percent)

| Sample No. | Description | Direction No. | | | Avge. |
|---------------|---|---------------|----|----|-------|
| | | 1 | 2 | 3 | |
| 33 | G-E Textolite 11637U FR-4, lt. green | 86 | 66 | 67 | 73 |
| 34 | Spaulding G-10-900 FR-4 Spauldite, dk. grn. | 48 | 56 | 50 | 51 |
| 35 | Unidentified sample, may be FR-4, natural | 86 | 67 | 72 | 75 |
| 36 | Synthane FB-1011, FR-5, white | 92 | 92 | 89 | 91 |
| 37 | Synthane FB-600 FR-4, natural (pale green) | 87 | 65 | 68 | 73 |
| 38 | Synthane FB-600 FR-4, Texas green | 89 | 69 | 69 | 76 |
| 39 | Synthane FB-600 FR-4, dark blue | 87 | 88 | 84 | 86 |
| 40 | Synthane FB-600 FR-4, black | 59 | 10 | 45 | 38 |
| 41 | Polyply FR-4, tan, de-clad | 89 | 87 | 82 | 86 |
| 42 | " " " unclad (reverse side) | 88 | 83 | 84 | 85 |
| 43 | Polyply FR-4, dk. blue, de-clad | 85 | 81 | 84 | 83 |
| 44 | CIMCLAD MA7 de-clad | 88 | 82 | 92 | 87 |
| 45 | " " unclad (reverse side) | 95 | 84 | 88 | 89 |
| 46 | CIMCLAD MA7FR de-clad | 86 | 80 | 85 | 84 |
| 47 | " " unclad (reverse side) | 94 | 88 | 94 | 92 |
| 48 | CIMCLAD ACAFR de-clad | 94 | 91 | 96 | 94 |
| 49 | " " unclad (reverse side) | 97 | 89 | 96 | 94 |
| 50 | Norplex G-30 polyimide, natural, shiny | 86 | 71 | 80 | 79 |
| 51 | " " " " , dull | 87 | 72 | 82 | 80 |
| 52 | Norplex G-10FR, de-clad | 75 | 70 | 81 | 75 |
| 53 | " " , unclad (reverse side) | 72 | 64 | 77 | 71 |
| 54 | MILCLAD CA7FR de-clad | 85 | 85 | 90 | 87 |
| 55 | " " " unclad (reverse side) | 92 | 93 | 95 | 93 |
| 56 | Norplex G-60 polysulfone de-clad | 80 | 86 | 88 | 85 |
| 57 | Micaply PG 418-T Type GI polyimide | 85 | 76 | 84 | 82 |
| 58 | Micaply TG 978 triazine | 81 | 72 | 80 | 78 |
| 59 | Norplex G11FR de-clad | 82 | 69 | 82 | 78 |
| 60 | " " unclad (reverse side) | 80 | 67 | 80 | 76 |

Note: The products which are identified above were selected at random from a great many such products. Their inclusion in this table does not signify endorsement by the United States Air Force nor does the omission of any product imply a lack of endorsement.

ones reflecting more in certain directions than the matte ones.

The measurement method used the YAG laser beam as the radiation source. The beam was unfocused so as not to damage the boards during the measurements, and short pulses were used as added protection. The detector was a small silicon photodiode which was moved to various positions around the target point for the three sets of measurements. Its peak sensitivity is in the 1- μ m region. Its output was displayed on a storage oscilloscope whose vertical scale had been previously calibrated. The calibration procedure consisted of placing the "zero reflectance" and "100% reflectance" values at the bottom and top of the vertical scale. The former was the zero-voltage detector value with no light on it. The 100% value was established by measuring the laser radiation reflected from a sample of magnesium carbonate, a common laboratory reflectance standard which reflects close to 100% for visible and near-infrared radiation. Sample reflectance values were then interpolated directly from the oscilloscope face, making use of the known linearity of the detector output vs. input.

The measurement arrangement is sketched in Figure 1.

On the second page of Table 1, some of the sample numbers are used in pairs to designate opposite sides of the same sample. An example is given by Samples 41 and 42, being opposite sides of a board which had been clad on one side only and whose cladding had been removed in the target area.

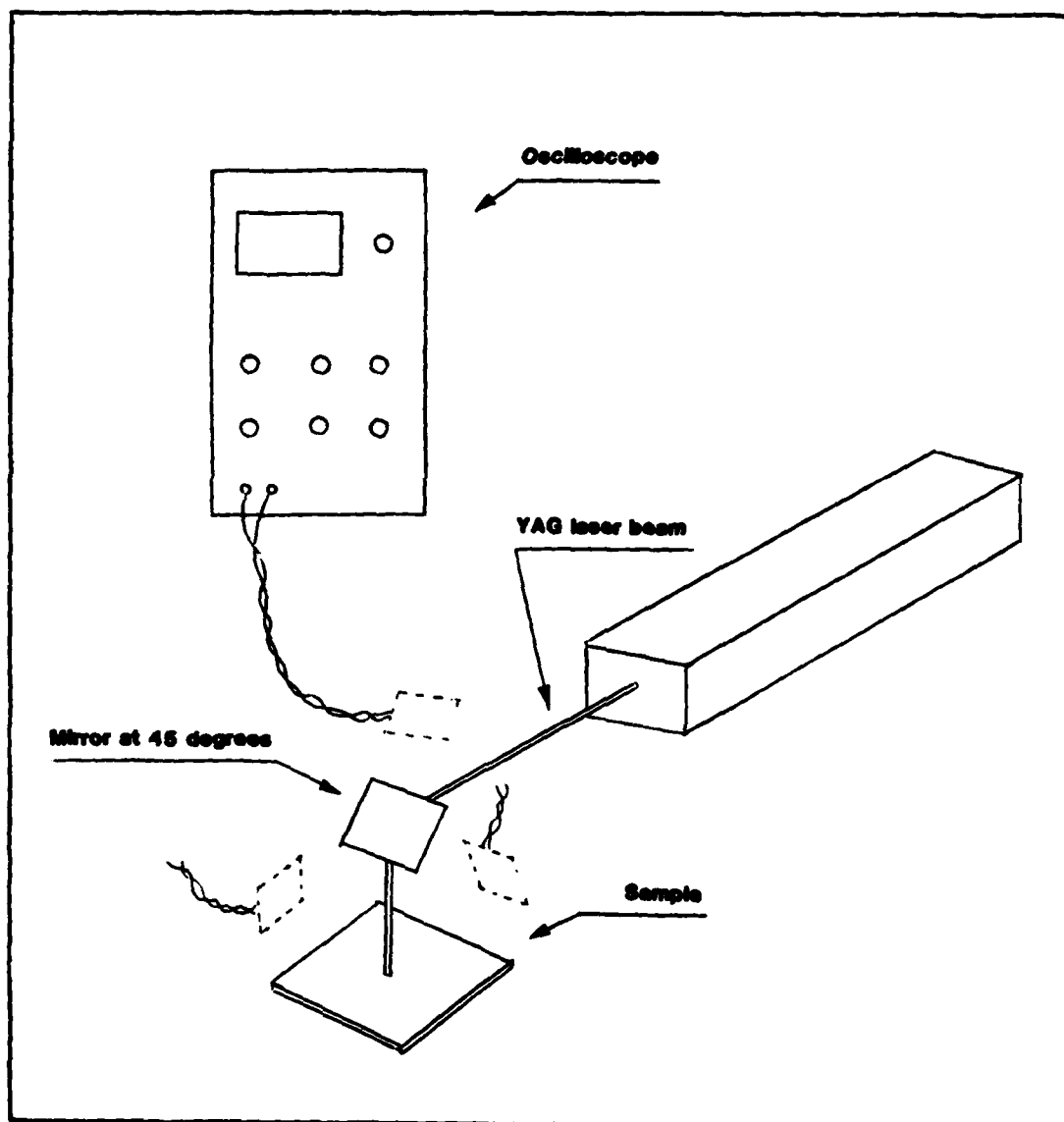


Figure 1. Method of measuring reflectance of samples with silicon detector in various positions (shown in dashed outline.)

Also listed in this part of Table 1 are some of the newer materials which are starting to be used for laminates. Samples Nos. 50 and 56 through 58 include polyimide, triazine and polysulfone which are also known, respectively, as G-30, G-40 and G-60.

As was expected, the data in the last column of Table 1 show a wide variation in reflectance values at 1.06 μm , ranging from 18% to 94%. These correspond to absorptivity values of 82% and 6%. (The boards in these two cases are essentially opaque and so the absorptivity is just "100% minus the reflectivity".) Preliminary tests did indeed show that the black Sample No. 4 was more easily laser-damaged than the other materials. Unexpectedly, the high-reflecting Sample No. 21 was also relatively easy to burn, but this may be because its phenolic/paper composition ignites at lower temperatures than the epoxy/glass materials.

The reflectance values in Table 1 form the basis for our search for a possible correlation between high absorptivity and high damage susceptibility, based on burn tests which are described in the following sections.

3.1.4 Effect of Board Texture

Our first experimental finding in the burn tests was that the textured natures of most board materials cause wide variations in damage susceptibility from place to place on a given board.

Our test procedure was to use a tightly focused laser beam (approximately 0.015" in diameter) in order to provide high intensity at the center of the beam spot, so that damage could be induced with short exposures. Various shutter durations were then used for each test board until either melting, charring or smoke could be seen visually on the board, or until the INSPECT signal showed a runaway heating condition which indicated combustion. Our first finding was that, on any one board material, widely different exposure durations were required in order to produce the same amount of damage, depending on which part of the board was exposed.

Visual examination of each board then revealed some sort of textured pattern on most of those which were translucent, when viewed by transmitted light. Almost without exception, the FR-4 boards clearly revealed a woven glass fiber pattern which was rectangular and gridlike, with a line spacing of the order of a millimeter. Phenolic board Samples Nos. 28 and 29 did not show any pattern although phenolic Sample No. 21 showed a coarse, random surface texture apparently due to large embedded fibers of material, something like the colored threads in U.S. paper currency.

The coloring matter in a board is confined to the plastic material and does not change the color of the glass fibers which are colorless and impermeable. As one views a board which is held up to the light, he sees criss-crossing light and dark lines. The dark lines are the spaces between the woven bundles of fibers. They appear darker because the observer is looking through a greater depth of colored matter.

Our reasoning led us to suspect that, on a given board, burns were produced more easily when the target spot was on a dark line between fiber bundles. We predicted that if a board were subjected to identical laser exposures at random locations in such a way that burns occurred only some of the time, then those burns which did occur would be between fiber bundles instead of on them. This suspicion was confirmed by a series of forty identical exposures at random positions on Sample No. 14, a dark green FR-4 which we had found to burn easily. Of the forty shots, only nine visible burn marks were produced. By transillumination, it was easily seen that all burns were in the spaces between fiber bundles and, in fact, most of them were at intersections of the dark lines where the absorption was the greatest.

The implication is that the reflectance values given in Table 1 are each subject to modification, depending upon whether it is a fiber bundle or a space which is being measured. The next question is, how much reflectance difference would be found between the two?

Our attempts to measure this difference between the light and dark parts of the texture pattern were not successful. In order to make the measurement, we focused the YAG laser beam to a fine spot small enough either to fit fully within a bundle of fibers or to fall into the intervening space. However, the small spot size was susceptible to minute table vibrations which are known to be present because of the air blower in the laser system. The result is random oscillations in the reflectance-detector signals

as the laser spot undergoes small excursions across the fibers. The amplitude of the oscillations corresponded to a few percent in reflectance values and therefore masked any reflectance-difference values smaller than this. Larger values than this would have been seen but were not, implying that the difference is less than a few percent.

Our conclusion, then, is that rather small absorptivity variations in a board can make a difference as to whether a burn occurs or not. This would serve to weaken any correlation which might be found between absorptivity and damage-susceptibility.

3.1.5 Ignition Point Determinations

The average temperature at which combustion would be initiated on each board material was determined in the following way.

The reflectance values in Table 1 were converted to emissivity values by subtracting them from 1. Each sample was then exposed to the laser beam and its gradual temperature rise was observed on the storage-oscilloscope display. At some point, an abrupt temperature rise would signal the onset of combustion. At this point, the amplified detector signal value was recorded. This value was then multiplied by the reciprocal of the emissivity value for that sample, yielding a value which would have been obtained if the sample had been a blackbody radiator. The blackbody value was then converted to a temperature value by use of the calibration curve of Figure 2. The resulting values are approximate because the emissivity value varies from place to place on the board; moreover, the materials are not all opaque and so

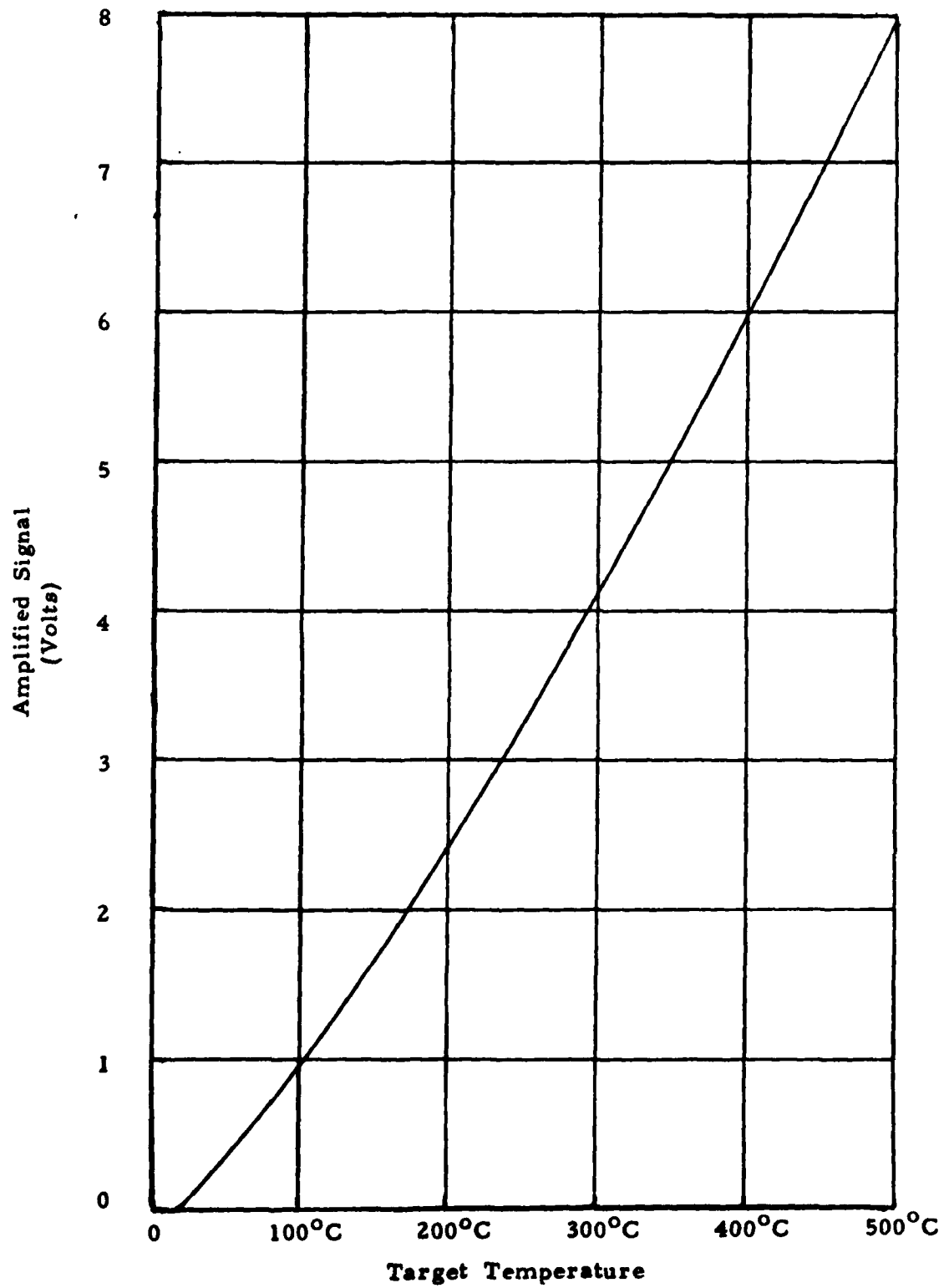


Figure 2. INSPECT signal vs. target temperature for a blackbody target.

obtaining the emissivity by subtracting the reflectivity from one is an approximation.

As a sample calculation, the reflectance value of 67% for Sample No. 2 corresponds to an emissivity of 33%, meaning that its emitted radiation at a given temperature is one-third what it would be from a blackbody of the same temperature. This board was observed to ignite when the thermal signal was 1.5 volts; had the board been a blackbody, the signal would have been 4.5 volts. From the calibration curve, a 4.5-volt blackbody signal indicates a temperature of 320°C. This, then, was the ignition temperature of the particular part of the board which was irradiated; the value would probably differ elsewhere on the board.

Ignition point data were taken for forty-four of the sixty samples and are shown in Table 2, along with their emissivity values, ϵ . In the table, the references to "burn prevention" and to "shutdown temperatures" apply to the use of a damage-prevention circuit which was implemented in parallel with these tests and which will be discussed in a later section. The effectiveness of this circuit is illustrated by the fact that the temperature values in the "Shutdown Temp." columns are substantially lower than those in the "Ignition Temp." columns, in which the damage-prevention circuit was de-activated.

In these tests, the laser-beam power was varied over the range from two to five watts to accommodate the various high and low damage susceptibilities of the targets. The darker materials

TABLE 2. EMISSIVITIES AND IGNITION- AND SHUTDOWN-TEMPERATURES FOR 44 SAMPLES WITHOUT AND WITH BURN PREVENTION.

(Degrees Centigrade)

| Sample No. | ϵ | Ignition Temp. | Shutdown Temp. | Sample No. | ϵ | Ignition Temp. | Shutdown Temp. |
|------------|------------|----------------|----------------|------------|------------|----------------|----------------|
| 1 | .33 | * | 200 | 23 | .25 | * | 315 |
| 2 | .33 | 320 | 200 | 24 | .37 | 386 | 172 |
| 3 | .31 | * | 115 | 25 | .37 | * | 192 |
| 4 | .82 | 242 | 55 | 26 | .29 | * | 80 |
| 5 | .27 | * | 300 | 27 | .49 | 410 | 72 |
| 6 | .60 | 225 | 50 | 28 | .27 | (255) | --- |
| 7 | .60 | 210 | 50 | 29 | .38 | 252 | 52 |
| 8 | .24 | 470 | 123 | 30 | .26 | (440) | --- |
| 9 | .23 | 482 | 110 | 31 | .40 | (280) | --- |
| 10 | .81 | 243 | 66 | 32 | .36 | (408) | 250 |
| 11 | .19 | * | 308 | | | | |
| 12 | .24 | * | 242 | 50 | .21 | (310) | --- |
| 13 | .25 | * | 293 | 51 | .20 | (*) | --- |
| 14 | .51 | 280 | 55 | 52 | .25 | (*) | --- |
| | | | | 53 | .29 | (322) | --- |
| 16 | .24 | * | 335 | 54 | .13 | (*) | 140 |
| 17 | .25 | * | 223 | 55 | .07 | (*) | * |
| 18 | .27 | (*) | --- | 56 | .15 | (173) | --- |
| 19 | .25 | * | 260 | 57 | .18 | (*) | --- |
| 20 | .81 | 248 | 66 | 58 | .22 | (350) | --- |
| 21 | .15 | * | 165 | 59 | .22 | (*) | --- |
| 22 | .24 | * | 320 | 60 | .24 | (350) | --- |

 ϵ = Emissivity

*Uncertain value

() = No-burn equilibrium temperature

--- = Shutdown not triggered but no burn damage

demanded the lower powers in order not to ignite instantly, whereas some of the lighter materials could not be ignited at all with the 5-watt maximum laser power which was available.

Those entries which indicate uncertain values in the combustion temperature arose from possible changes of state in the material just prior to combustion. Our calculated temperature values for these entries were unusually high, often exceeding 500°C, which corresponds to a dull red heat. This may have resulted from charring immediately prior to combustion, yielding an abrupt increase in emissivity and in the radiated power and rendering our assumed emissivity values invalid. Rather than report data of questionable value, we are simply indicating an uncertainty in these cases.

Also to be noted is that the absorptivity data were taken by use of the Nd:YAG laser and so they apply only at the 1.06 μm wavelength, whereas the temperature data were taken by a detector which is sensitive primarily in the 4 to 5- μm spectral region. It is not only conceivable but likely that the emissivities of the materials approach each other at higher values, at the greater wavelengths, so that the short wavelength absorptivity data do not apply. We shall return to this matter in a moment.

The temperature values which are enclosed in parentheses refer to samples which did not ignite at even the highest laser-beam power which was used. In this case, the indicated value refers to the equilibrium temperature which the sample finally reached before the burn-attempt was abandoned. It will be seen that various colored samples reach different equilibrium temperatures

as a result of their showing different heat-exchange properties with the environment and with nearby parts of the board. Again, the higher temperature values which are indicated for the "no burn" samples may be in doubt because of unknown emissivity changes, for it seems unlikely that ordinary board materials could withstand such temperatures.

As a matter of possible interest, a cursory burn test with a higher powered laser was conducted on a few of the samples which could not be damaged with five watts of continuous exposure. A pulsed laser was used, whose beam was focused to the 0.015" diameter spot used in the earlier tests, and each sample was exposed to a single one-joule pulse which was delivered within a two-millisecond period. This was equivalent to an average power of 500 watts during the two-millisecond exposure. For the damage-resistant samples, charred craters resulted from the pulses, having diameters from 0.022" to 0.030", or up to twice the diameter of the laser spot. When an easily-damaged black sample was exposed for comparison, its crater diameter was approximately three times the spot diameter.

We return now to the matter of the unusually high ignition temperature values which seem to be indicated for some of the samples. As was pointed out, it is possible that the materials show more uniform and high emissivities at the wavelengths where their temperatures were measured than at the 1.06- μ m wavelength where their reflectivities were measured. If this is the case, then the use of the reflectance data to "correct" the temperature readings can lead to erroneously high values. In most cases in

Table 2, we notice seemingly high ignition temperatures to be associated with low emissivities. If we consider the twelve samples which showed combustion, of the 44 samples in Table 2, we can plot their supposed ignition temperatures versus emissivity, as has been done in Figure 3. From the plot, we can observe a certain regularity in the data, leading us to believe that those samples having lower emissivities required higher starting temperatures in order to ignite. From other experience, we would not expect to find different ignition temperatures in various samples of epoxy glass due to their assorted colors; instead, the ignition temperature should be a constant of the material itself.

We therefore conclude that the assumed ignition temperature values of Table 2 may be erroneously high due either to:

1. An increase in the actual emissivity value due to charring at the moment of ignition, or
2. The improper application of short-wavelength reflectance data in the longer-wavelength thermal emission region.

3.1.6 Softening Point Determinations

In a separate test series, comparative data were obtained for the softening points of most of the laminate samples. The softening point represents a lower level of damage than does burning; it would be the temperature at which the first visible blemish might appear.

Initial tests were conducted by use of the laser beam at low power. When inconsistent results were obtained, a different heating method was devised. In this method, a hot soldering iron was

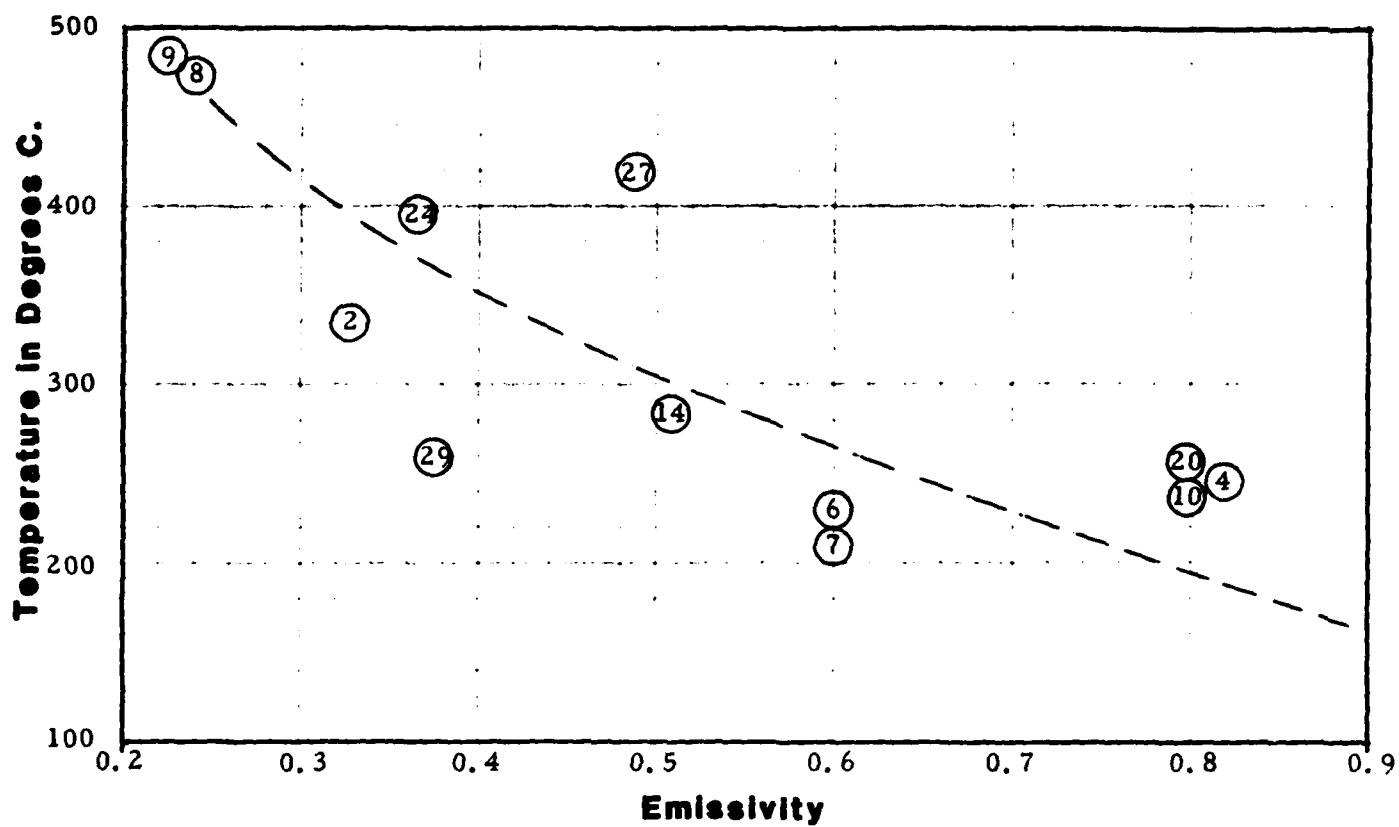


Figure 3. Calculated ignition temperatures vs. emissivity for the twelve burned samples in Table 2.

placed with the side of the tip against a thermocouple which was pressed into mechanical contact with the sample for a few moments and then removed. For each sample, the contact was maintained for increasing time intervals, with the thermocouple signal being noted at the end of each interval. Each time the heat source was removed, the board was inspected for a blemish. When one finally did appear, the indicated temperature at the end of the last heating interval was recorded. Typical contact durations were five to ten seconds.

It should be noted that the actual temperature of the thermocouple was somewhere between those of the soldering tip and the sample area being heated. The recorded temperature values, which are presented in Table 3, therefore do not indicate the actual softening temperatures of the materials, being somewhat higher than actual. However, they do serve as an index for the comparison of the various materials, and the variability is clearly seen. In particular, the data verify that the new, exotic materials (Samples 50, 51, 57 and 58) are indeed more heat-resistant than many of the others.

3.2 Damage Prevention on Laminates

The study of damage thresholds for substrate materials, which we have just described, was undertaken in order to assess the likelihood of accidental damage in case of inadvertent exposure to the laser beam. Such exposure could conceivably occur as the result of human or mechanical errors which resulted in a

TABLE 3. COMPARISON OF SOFTENING TEMPERATURES FOR SAMPLES.
(Thermocouple temperature in °C)

| <u>Sample No.</u> | <u>Temp.</u> | <u>Sample No.</u> | <u>Temp.</u> |
|-----------------------|--------------|-----------------------|--------------|
| 1 | 200 | 31 | 220 |
| 2 | 200 | 32 | 220 |
| 3 | 200 | 33 | 220 |
| 4 | 200 | | |
| 5 | 220 | 35 | 220 |
| 6 | 180 | 36 | 282* |
| 7 | 180 | 37 | 220 |
| 8 | 200 | 38 | 235 |
| 9 | 200 | 39 | 250 |
| 10 | 200 | 40 | 220 |
| 11 | 220 | 41 | 250 |
| 12 | 240 | 42 | 250 |
| 13 | 200 | 43 | 230 |
| 14 | 200 | 44 | 250* |
| | | 45 | 260* |
| 16 | 200 | 46 | 250* |
| 17 | 240 | 47 | 285* |
| 18 | 300 | 48 | 245* |
| 19 | 230 | 49 | 260* |
| 20 | 200 | 50 | 280* |
| 21 | 250 | 51 | 285* |
| 22 | 220 | 52 | 210 |
| 23 | 220 | 53 | 210 |
| 24 | 220 | 54 | 290* |
| 25 | 220 | 55 | 285* |
| 26 | 255 | 56 | 230* |
| 27 | 220 | 57 | 300* |
| 28 | 250 | 58 | 280* |
| 29 | 240 | 59 | 220 |
| 30 | 200 | 60 | 220 |

*Equilibrium temperature; sample did not melt.

part or all of the laser beam falling upon the laminate instead of on the more highly reflecting and more thermally resistant solder.

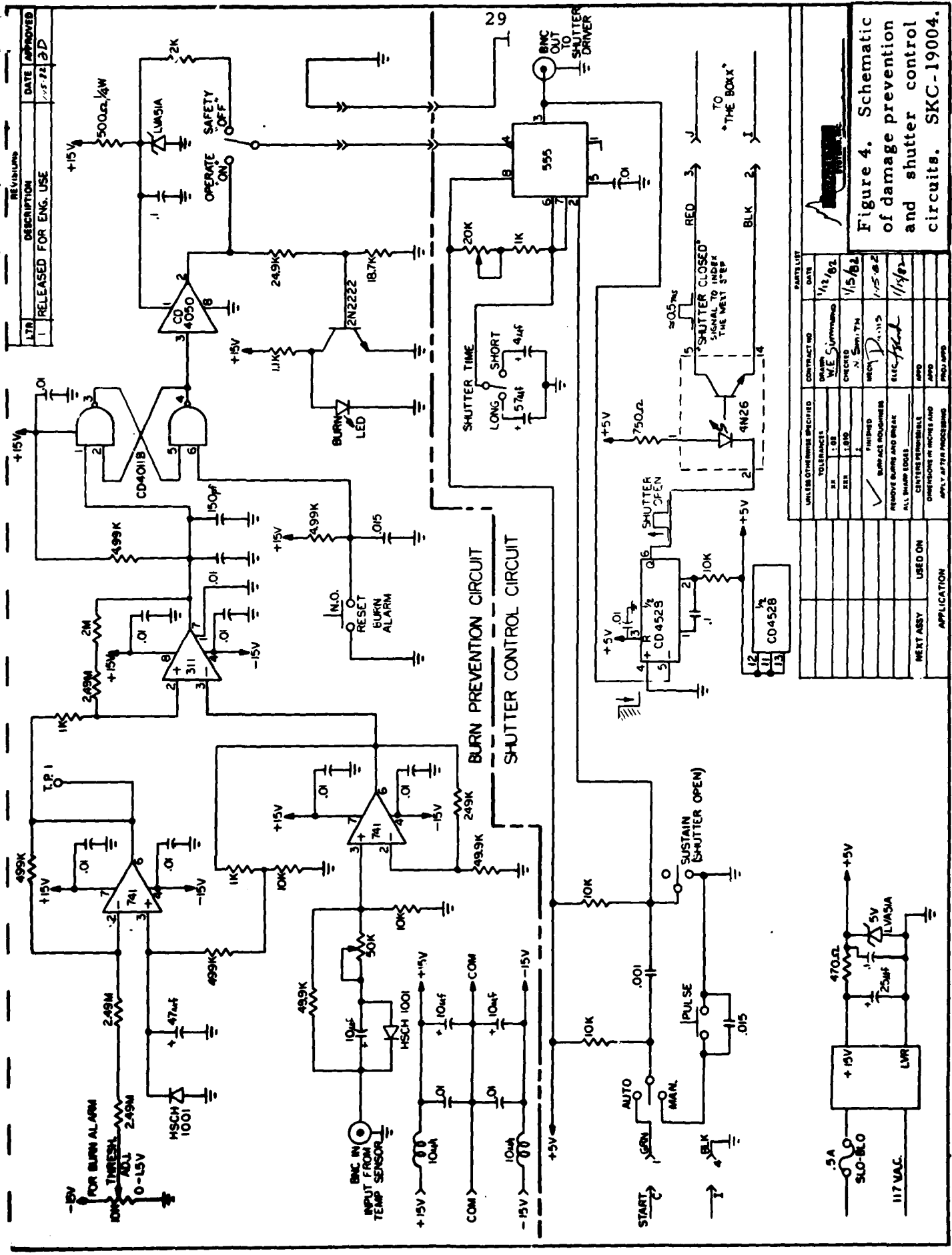
Apart from the question of damage susceptibility, there is the more pressing question of how such damage might be prevented. In a parallel effort, under this program, this question was considered and a practical solution to it has been implemented.

The solution takes the form of a "damage-prevention circuit". This circuit continuously monitors the output of the infrared detector as it follows the heating progress at a solder joint. Should a runaway heating condition be observed, the circuit calls for the immediate shutdown of the laser shutter, which action occurs within a few milliseconds.

The damage-prevention circuit and the shutter control circuit to which it is connected are depicted in Figure 4.

The laser shutter which was used in these tests is a Model 23L2A1X5 Uniblitz Electronic Shutter made by Vincent Associates of Rochester, New York. Its closing time is approximately 1.4 milliseconds. This interval includes 0.5 mSec of dwell time during which the electric field in the shutter solenoid collapses after the shutter receives a signal to close. This is followed by a 0.9 mSec transfer time in which the shutter springs pull the blades closed.

The circuit operates by monitoring the infrared detector signal which proceeds to the computer for solder joint quality assessment. During normal testing, the solder joints themselves are heated to somewhere between 100°F and 200°F, depending upon



| PART LIST | | DATE |
|--------------|--------------|---------|
| CONTRACT NO. | W.E. Symonds | 1/12/62 |
| DESIGN | W.E. Symonds | 1/15/62 |
| CHECKED | N. Smith | 1/15/62 |
| APPROVED | W.E. Symonds | 1/15/62 |
| DATE | 1/15/62 | |
| BY | W.E. Symonds | |
| FOR | ENGINEERING | |
| REVISIONS | | |
| 1 | CHANGED | |
| 2 | REMOVED | |
| 3 | ADDED | |
| 4 | CHANGED | |
| 5 | REMOVED | |
| 6 | ADDED | |
| 7 | CHANGED | |
| 8 | REMOVED | |
| 9 | ADDED | |
| 10 | CHANGED | |
| 11 | REMOVED | |
| 12 | ADDED | |
| 13 | CHANGED | |
| 14 | REMOVED | |
| 15 | ADDED | |
| 16 | CHANGED | |
| 17 | REMOVED | |
| 18 | ADDED | |
| 19 | CHANGED | |
| 20 | REMOVED | |
| 21 | ADDED | |
| 22 | CHANGED | |
| 23 | REMOVED | |
| 24 | ADDED | |
| 25 | CHANGED | |
| 26 | REMOVED | |
| 27 | ADDED | |
| 28 | CHANGED | |
| 29 | REMOVED | |
| 30 | ADDED | |
| 31 | CHANGED | |
| 32 | REMOVED | |
| 33 | ADDED | |
| 34 | CHANGED | |
| 35 | REMOVED | |
| 36 | ADDED | |
| 37 | CHANGED | |
| 38 | REMOVED | |
| 39 | ADDED | |
| 40 | CHANGED | |
| 41 | REMOVED | |
| 42 | ADDED | |
| 43 | CHANGED | |
| 44 | REMOVED | |
| 45 | ADDED | |
| 46 | CHANGED | |
| 47 | REMOVED | |
| 48 | ADDED | |
| 49 | CHANGED | |
| 50 | REMOVED | |
| 51 | ADDED | |
| 52 | CHANGED | |
| 53 | REMOVED | |
| 54 | ADDED | |
| 55 | CHANGED | |
| 56 | REMOVED | |
| 57 | ADDED | |
| 58 | CHANGED | |
| 59 | REMOVED | |
| 60 | ADDED | |
| 61 | CHANGED | |
| 62 | REMOVED | |
| 63 | ADDED | |
| 64 | CHANGED | |
| 65 | REMOVED | |
| 66 | ADDED | |
| 67 | CHANGED | |
| 68 | REMOVED | |
| 69 | ADDED | |
| 70 | CHANGED | |
| 71 | REMOVED | |
| 72 | ADDED | |
| 73 | CHANGED | |
| 74 | REMOVED | |
| 75 | ADDED | |
| 76 | CHANGED | |
| 77 | REMOVED | |
| 78 | ADDED | |
| 79 | CHANGED | |
| 80 | REMOVED | |
| 81 | ADDED | |
| 82 | CHANGED | |
| 83 | REMOVED | |
| 84 | ADDED | |
| 85 | CHANGED | |
| 86 | REMOVED | |
| 87 | ADDED | |
| 88 | CHANGED | |
| 89 | REMOVED | |
| 90 | ADDED | |
| 91 | CHANGED | |
| 92 | REMOVED | |
| 93 | ADDED | |
| 94 | CHANGED | |
| 95 | REMOVED | |
| 96 | ADDED | |
| 97 | CHANGED | |
| 98 | REMOVED | |
| 99 | ADDED | |
| 100 | CHANGED | |

the exposure conditions and upon the quality of the particular joint. The corresponding amplified detector signal may be somewhere between 0.1 and 0.5 volt, the higher of these being, of course, for a defective joint.

When a laminate material is heated by laser, its radiated thermal signal is generally higher than for a solder joint under the same conditions. This is most likely due to a higher emissivity than solder at the detector wavelength. The resulting range of amplified detector signals may be from a fraction of a volt to one volt or more, depending upon the absorptivity of the laminate at the laser wavelength.

In Figure 5 are shown two thermal signatures of a laser-heated laminate material. In both cases, relatively slow heating at low laser power was carried out. The horizontal time scale is five seconds per division, and one volt per division is represented vertically.

In the lefthand trace, we see a gradual warming at a decreasing heating rate and then a sudden rise in the thermal signal as ignition occurred. The laser shutter was closed shortly afterward, and normal cooling took place. Ignition is seen to occur at just above one volt of signal, and nearly six volts were recorded at the peak.

The righthand trace in Figure 5 was made with the damage-prevention circuit controlling the laser shutter. The circuit operates by continually comparing the detector signal with a fixed (but adjustable) threshold voltage which is stored in the

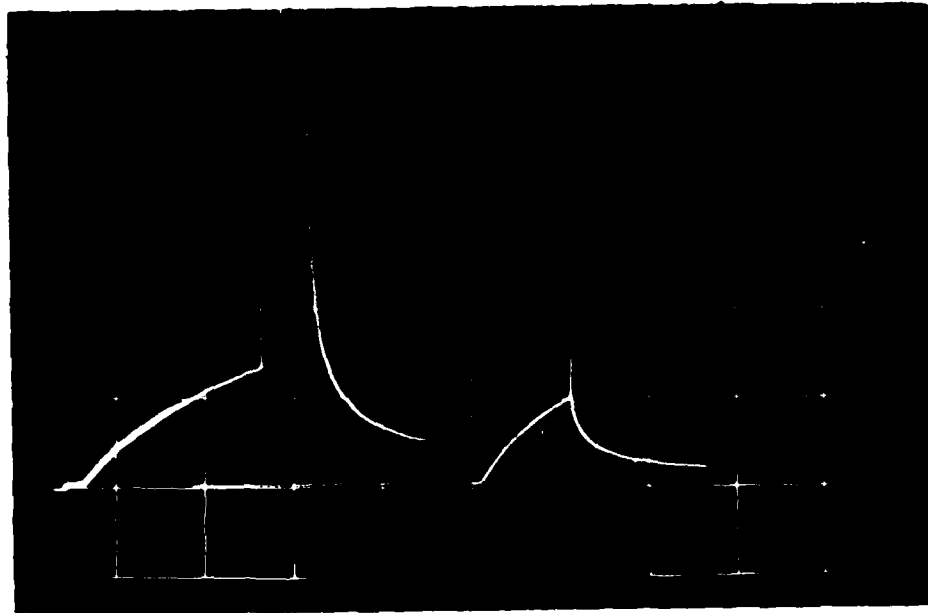


Figure 5. Left and right traces are without and with, respectively, the damage prevention circuit activated.

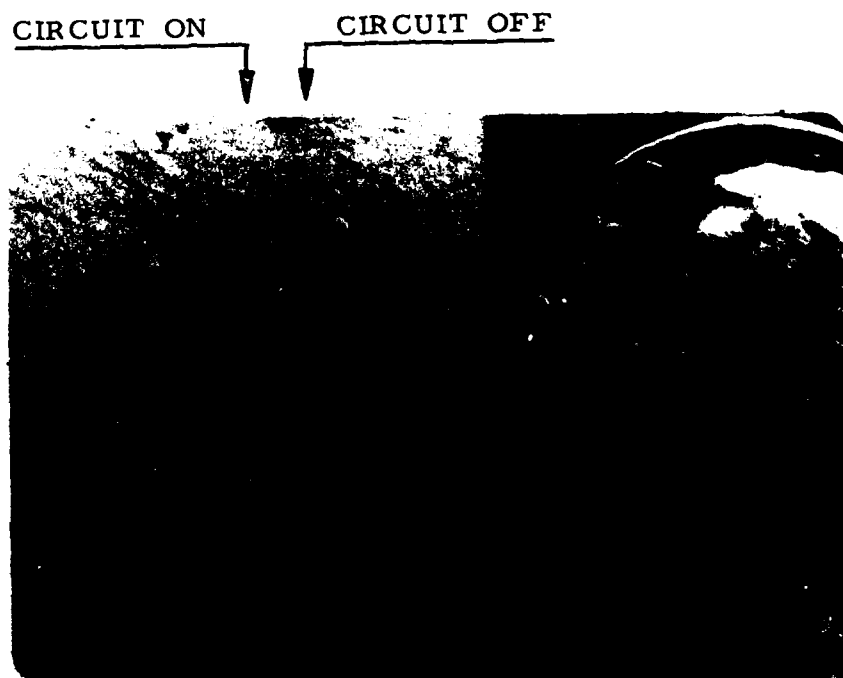


Figure 6. Circuit effectiveness is shown by the difference in burn severity in the two columns.

circuit. When the threshold is exceeded, the circuit delivers a shutdown signal to the shutter controller. In this case, the threshold level had been adjusted to a value close to one volt. The shutter was closed automatically just after this value was reached. A small vertical spike at the end of the heating curve replaces the larger one in the previous trace, but it reveals incipient combustion which indicates that the shutter should have been closed slightly earlier.

The matter of how early a shutdown command will be issued depends upon the setting of the adjustable threshold. In this case, the threshold was higher than necessary, for illustrative purposes. In Figure 7 we show a similar pair of comparison traces in which the threshold was lowered slightly, leaving a smaller ignition spike at the end of warming. The threshold was further lowered for Figure 8 which thus shows the absence of an ignition spike.

Returning to Figure 6, we see two columns of laminate burn marks, with one column being more readily visible than the other. In the lefthand column, the barely noticeable dots are incipient burns which resulted when the damage prevention circuit was active but with its threshold set as for Figure 5. For the righthand column, the circuit was inactivated and normal burn marks are the result. Had the threshold been adjusted as for Figures 7 and 8, either smaller burn marks or none at all would be seen in the lefthand column.

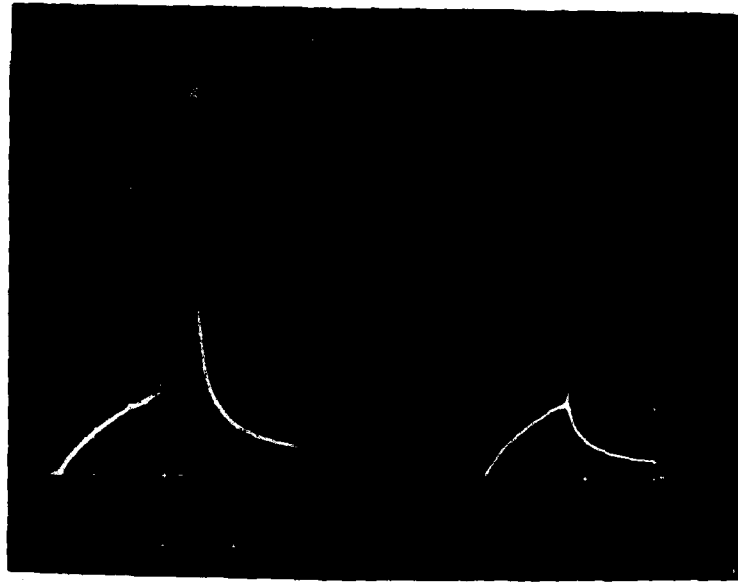


Figure 7. Tests similar to earlier one but with triggering threshold lowered.

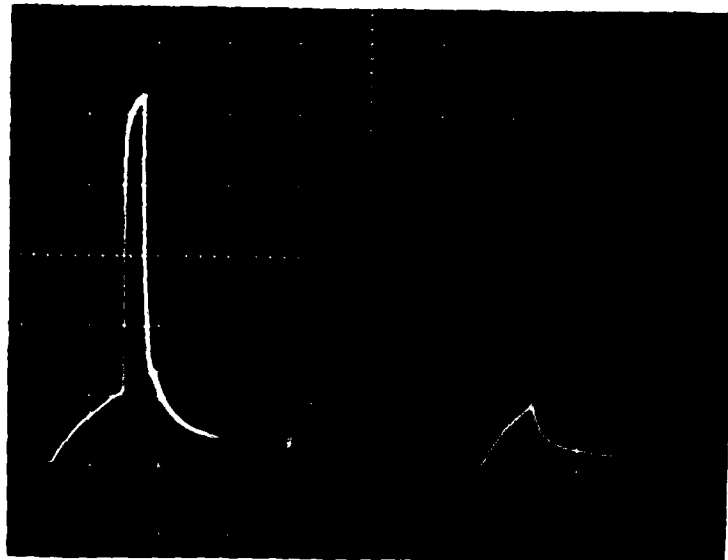


Figure 8. Similar to above but with still lower threshold.

The circuit incorporates an "anticipation feature" in which the threshold is automatically lowered as the heating rate increases. Thus, for dark colored samples which are easily burned, their higher absorption of laser power and consequent faster heating will cause a shutdown command sooner than otherwise.

Our present version of the damage prevention circuit, as depicted in the schematic diagram of Figure 4, uses a pair of flip-flops in order to become "latched" after triggering. The intent is that the laser/thermal system interrupt its operations until an operator can determine and correct the cause of the overheating. The system may then be manually reset and will resume operations by use of a pushbutton switch. An on-off switch allows the circuit to be inactivated for demonstration purposes.

Returning now to Table 2 on Page 21, we will discuss a typical one of several tests which we applied to the circuit in order to verify that it was operating as was intended. In our earlier discussion of Table 2, we had pointed out the columns marked "Shutdown Temperature" which pertained to testing of the damage-prevention circuit. The data in these columns were taken with the circuit activated and with the threshold adjusted so that no perceptible board damage occurred. In nearly all cases, the circuit was triggered very early during the laser exposure. This was especially true in the cases of the darker samples ($\epsilon = 0.6$ to 0.8) which became heated so rapidly that they brought into play the anticipation feature of the circuit. In all cases, the maximum temperatures at shutdown are seen to be safely lower than the corresponding values at which ignition took place.

Where no entries are shown in the shutdown temperature column, the samples were often high-reflecting materials (low emissivity) whose warming rates and maximum temperatures were so low as not to induce triggering, for which there was, of course, no need. In all such cases, the materials did not show combustion even with the circuit inactivated and with the maximum 4.8 watts of available laser power in use.

One question which will be answered at a later time concerns the effectiveness of the damage prevention circuit at higher laser-beam powers than the one which was available at the time of these tests. Conceivably, heating of the substrate might occur so rapidly that the 1.4-mSec shutter-closing time will not be short enough to prevent damage. In that regard, we point out that solder-joint testing in the final laser/thermal system will most likely be conducted with beam powers of less than ten watts. Too high a beam power can raise the surface temperature of the solder close to the fusion point before the surface heat has had time to dissipate into the interior. (In separate tests, we have shown that a seven-watt beam concentrated onto a 0.050"-diameter through-hole joint can reflow the surface solder within one second.)

Thus, the damage prevention circuit will have to be shown still to be effective at beam powers about double of that at which it was tested, and we are confident that this will be the case. Some leeway is available in lowering the threshold and in increasing the sensitivity of the anticipation feature. Should there still be a problem, faster shuttering methods are available, such as electro-optical instead of mechanical ones.

3.3 Laser/thermal Testing Through Conformal Coatings

One of the objectives of Phase 2.2, as outlined in the USAF Engineering Specification for the program, was to perform comparative laser/thermal tests on solder joints and on substrates in the presence of and in the absence of conformal coatings. It was suggested that our tests be confined to two of the several available coating types.

The purpose of these tests was to determine whether, on circuit boards which had been returned from the field for repair, the coating would have to be removed before laser/thermal testing could be carried out.

The appropriate military specification on conformal coatings was reviewed (MIL-I-46058C and its Amendment 5) and five general types of coating were identified under "1.2 Classification". Of these, two were selected on the basis of the recommendations in Section 3.13 of the cited Engineering Specification. One of these was to be a relatively thick and soft coating, and for this purpose the selection was made of Dow-Corning R-4-3117 Conformal Coating. This is an elastoplastic silicone resin which is recommended for coating thicknesses of about 0.005 inch. The other coating, which was to be thin and hard, was an epoxy resin material to be applied in a 0.002-inch thickness. For this purpose, we chose Techform TC-3285, a two-part composition to be mixed in equal parts and which polymerizes overnight after being sprayed, brushed or dipped.

We shall first summarize the findings of this study and will then proceed to the test details and results:

1. There was no laser damage to the conformal coatings at the exposure levels which are sufficient for solder-joint testing;
2. Thermal signals are higher on coated solder joints than on uncoated ones;
3. Thermal signals are lower on coated substrates than on uncoated ones.

In preparation for the tests, coatings of the proper thickness were applied by flowing the material onto the sample and by drip-draining it until the recommended thickness remained. The technique for doing so was developed through trial and error until the proper thickness resulted. Coating thicknesses were checked with a micrometer caliper after the film was hard.

The first coating to be tested was the silicone resin. This was applied to a section of sample board which contained a row of eight through-hole joints which alternated between good and bad. The "bad" ones comprised cold solder joints. The eight samples can be seen in Figure 9 where the alternating qualities of successive joints are easily seen, with the odd-numbered ones being shiny and the even ones dull.

Figure 10 is a set of thermal signatures of these joints in their uncoated state. On the same vertical scale, Figure 11 shows the signatures after the joints had received an approximately 0.005"-thick coating of the resin.

The signal amplitudes are approximately doubled by the coating and the characteristics of the signatures are preserved, if not enhanced. The alternating sequence of low and high peaks is more easily seen in the lower photo.



Figure 9. Alternating sequence of "good" and "cold solder" joints from No. 1 through No. 8.



Figure 10. Thermal signatures of uncoated joints.

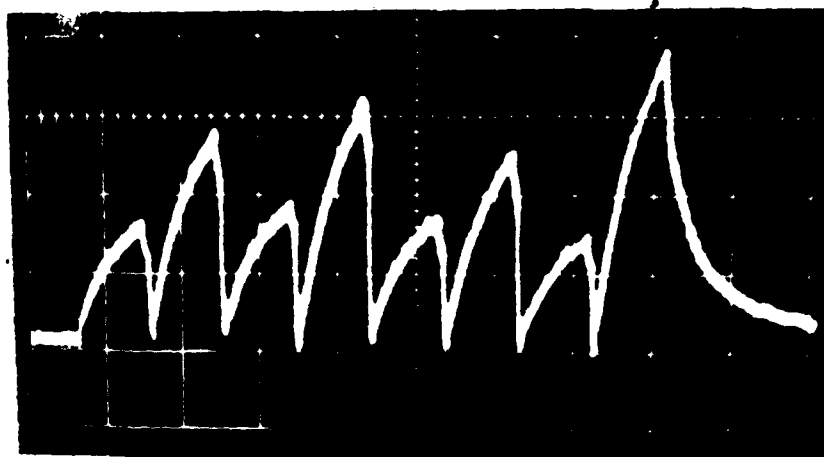


Figure 11. Thermal signatures of same joints with 0.005" thickness of Dow-Corning R-4-3117 Conformal Coating.

From these and similar test results, we speculate that the greater heating due to the coating results from a combination of two effects:

1. The "greenhouse effect" in which the 1.06- μ m radiation is converted to heat within the solder and is then trapped by the coating material, which may be assumed to be opaque to the greater-wavelength thermal radiation. The heat within the solder is thus prevented from escaping normally by radiation and convection and thus the heat buildup is greater.
2. Some of this heat is conducted to the coating layer, which is a better thermal emitter than the solder and so provides a higher infrared signal to the detector.

The silicone resin was then removed from this section of board (by use of D-Sol F-13, a solvent used for the cleaning of printed circuit boards) and the proper thickness of the epoxy coating was applied.

Figure 12 is a comparison pair of oscillograms showing the thermal signatures before and after the new coating was applied. These compare favorably with those shown in Figures 10 and 11.

The "before" and "after" oscillograms of Figure 12 were prepared one day apart, to allow the coating to "air dry" overnight. In order to test for any optical or electronic drift in the laser/thermal system during this time, our intention was to avoid coating the first two pins which are presented in the oscillograms so that they would be in the same condition on both days. Although the Pin 1 signatures agree well from one day to the next, a small amount of coating bled onto the edge of Pin 2, accounting for a slightly higher peak in the second photograph.

The peaks for Pins 3 through 8 are seen to be about twice as high when coated as otherwise, agreeing with the earlier results even though the epoxy coating is thinner.

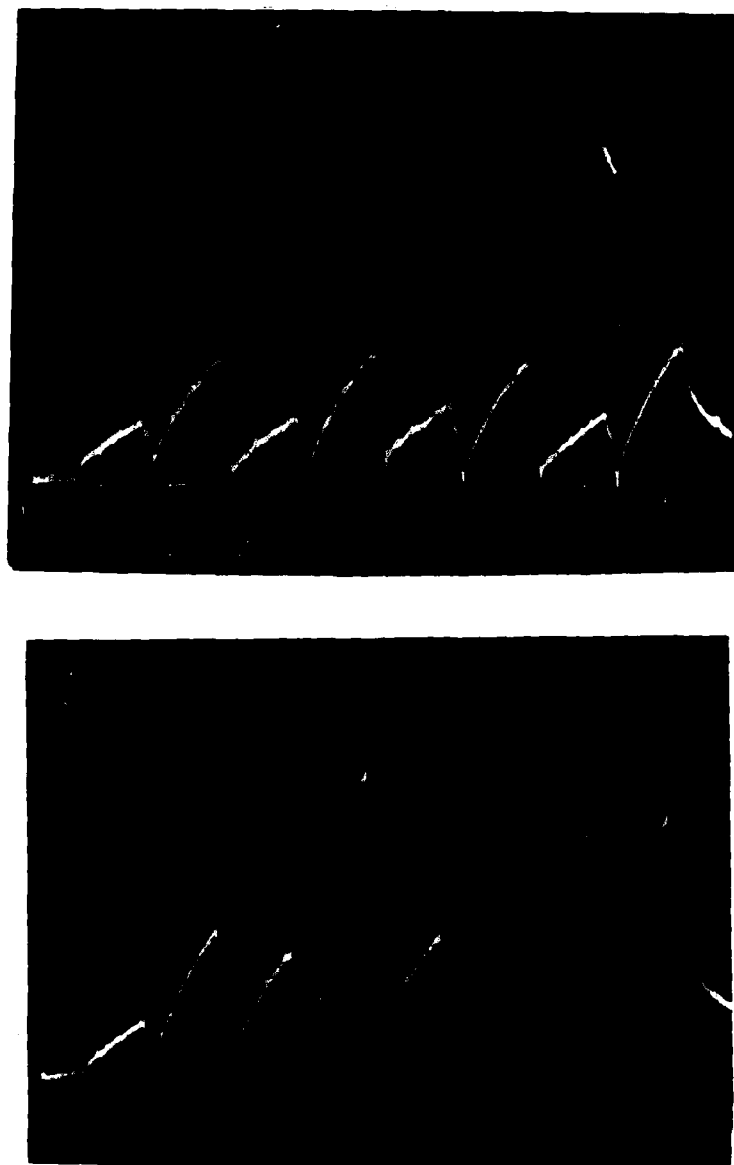


Figure 12. Thermal signatures of uncoated joints (upper photo) and of the same joints coated with a 0.002" thickness of Techform TC-3285 epoxy resin. Exposure and display conditions are the same in both cases. First joint in lower photo was left uncoated for control purposes. The thermal signatures, from left to right, are for Pins Nos. 1 through 8 in Figure 9.

In no case in our testing was any damage observed when the coating was exposed to the laser beam.

Having tested the effects of the coatings on solder, we proceeded to repeat the coating tests while using various substrate materials as targets. The first of these tests was conducted by the use of the silicone material. From the laminate materials which we had used earlier for damage-susceptibility tests (see Table 2, Page 21), we selected the first ten numbered samples, applying a patch of coating to a part of each one. Most of the samples were subjected to a one-second exposure on the coated and uncoated parts; the others, which were more highly absorbing, were exposed for only 0.015 second. The laser beam power was less than one watt.

By use of the oscilloscope, the peak thermal signals were recorded and are tabulated below, with Samples 4, 5, 6 and 10 having received the shorter exposures:

WARMING RATES ON SAMPLE LAMINATES

| <u>Sample No.</u> | <u>With Silicone Coating</u> <u>mV/Sec</u> | <u>Without Coating</u> <u>mV/Sec</u> |
|-------------------|---|---|
| 1 | 180 | 240 |
| 2 | 180 | 250 |
| 3 | 300 | 510 |
| 4 | 260 mV/0.015 Sec | 600 mV/0.015 Sec |
| 5 | 80 | 120 |
| 6 | 35 mV/0.015 Sec | 110 mV/0.015 Sec |
| 7 | 35 mV/0.015 Sec | 80 mV/0.015 Sec |
| 8 | 500 | 700 |
| 9 | 450 | 650 |
| 10 | 450 mV/0.015 Sec | 1000 mV/0.015 Sec |

We observe that the coating suppressed the heating rate in all cases. Figures 13 and 14 show examples of the comparative heating rates on two of the samples.

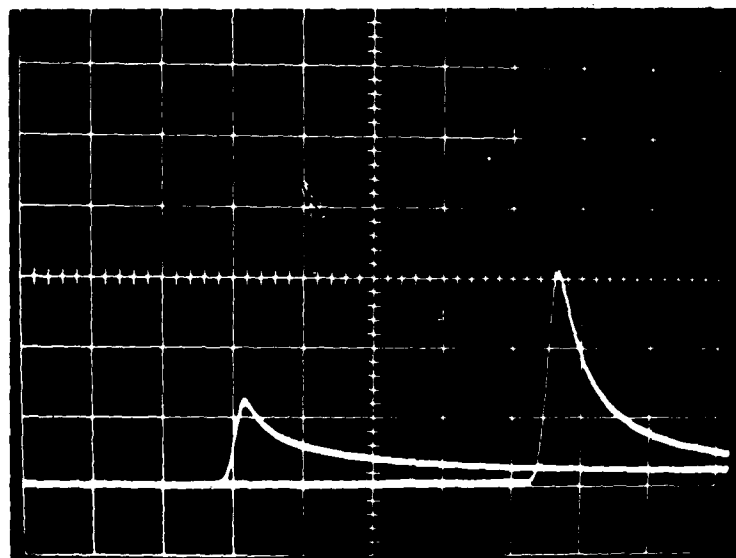


Figure 13. Relative heating rates on Laminate Sample No. 4 (FR-4, black) with (left) and without silicone coating.

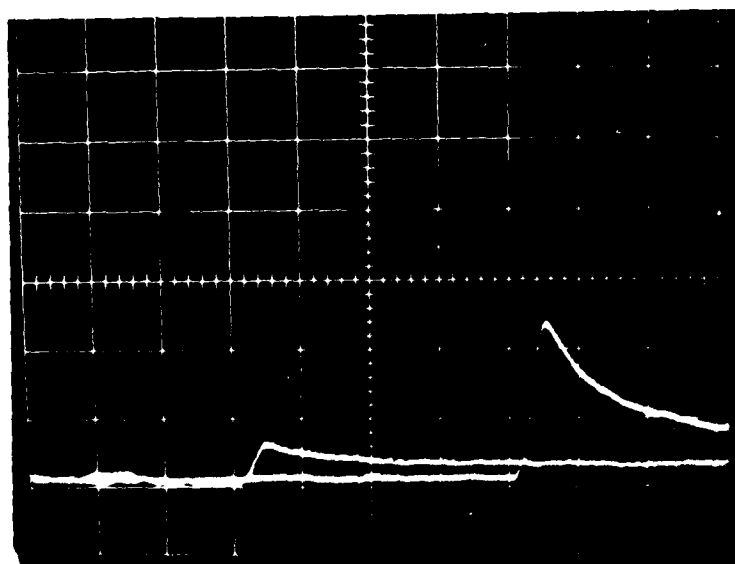


Figure 14. Same but on Sample No. 6 (FR-4, dark green).

In the final test series on conformal coatings, substrate materials were again tested, this time by use of the epoxy resin formulation. The same sample boards and procedure were used as before, with the following results:

WARMING RATES ON SAMPLE LAMINATES

| <u>Sample No.</u> | <u>With Epoxy Coating mV/Sec</u> | <u>Without Coating mV/Sec</u> |
|-------------------|--------------------------------------|-----------------------------------|
| 1 | 190 | 200 |
| 2 | 190 | 200 |
| 3 | 360 | 380 |
| 4 | 75 mV/0.015 Sec | 95 mV/0.015 Sec |
| 5 | 90 | 110 |
| 6 | 20 mV/0.015 Sec | 30 mV/0.015 Sec |
| 7 | 20 mV/0.015 Sec | 30 mV/0.015 Sec |
| 8 | 440 | 460 |
| 9 | 385 | 430 |
| 10 | 145 mV/0.015 Sec | 170 mV/0.015 Sec. |

In comparing these results with those shown in the preceding tabulation, we note a similarity except in the cases of Samples Nos. 4 and 10. For these two samples, the warming rates are noticeably lower in the epoxy case than with the silicone. Both samples are black but are supplied by different sources. Sufficient information is not available to permit an explanation of this occurrence.

As we have done in the case of the coated and uncoated solder joints, we can speculate again about the effect which the conformal coating has on a laminate material during laser heating.

It is apparent that the coating has opposite effects on the heating rates in the target materials, serving to enhance the infrared signal from the solder and to suppress it from the laminate. We have indicated our belief that the coating serves both as a heat-trap and as an emissivity-enhancer for the solder. In the case of the laminate, we feel that the coating plays a small or no part in emissivity enhancement because the thermal emissivity of most laminate materials is inherently high. Regarding the role of heat-trapping, we believe that any such effect is far overwhelmed by the cooling effect which the coating has upon the surface of the substrate. Because the substrate is more easily heated by a laser beam than is a solder surface, it tends to reach a much higher temperature. Such temperatures are readily susceptible to the cooling effect of the adjacent conformal coating because of the greater temperature difference between the substrate and the coating.

Experimental verification of these speculations is left to a later time. In summary of this section, we point out again that:

1. No laser-beam damage has been observed on the coatings which we have used while they were being tested at power levels which are suitable for testing solder joints, and
2. The presence of the coating actually enhances the thermal signals from the solder while reducing the possibility of accidental overheating of the substrate.

3.4 Testing of Solder Joints

We turn our attention now to the major portion of the program, which was the laser/thermal testing of a statistically

significant number of solder joints. Earlier phases of the present program had verified the usefulness of this method with a smaller number of samples.

In Section 3.4, we shall discuss the preparation of samples, the testing conditions and scoring procedures, and we will present the test results.

3.4.1 Preparation of Samples

Approximately one thousand solder-joint samples were prepared, comprising a mixture of good joints with those having various types of defects. Most of them were prepared to our specifications by an outside supplier, and the remainder were prepared by us. They included both feed-through ("through-hole" or "pin in hole") joints on DIPs and lap joints on flat-pack ICs.

The joints were prepared on nine separate sections of standard board materials. The first eight of these are shown in Figure 15 and the eighth and ninth ones are shown in more detail in Figure 16. The ninth board has been designated as No. 8B.

In general, each board contained a mixture of good joints with defects of one or two types, identified as follows:

Feed-through joints at plated-through-holes

- | | | |
|--------------|---|------------|
| Board No. 1: | Generally good joints, made with large preforms on solder side | 128 joints |
| Board No. 2: | Insufficient solder and shallow fillets, made with small preforms on solder side | 126 joints |
| Board No. 3: | Cold solder joints on solder side, made without flux and with solder containing no rosin core | 124 joints |

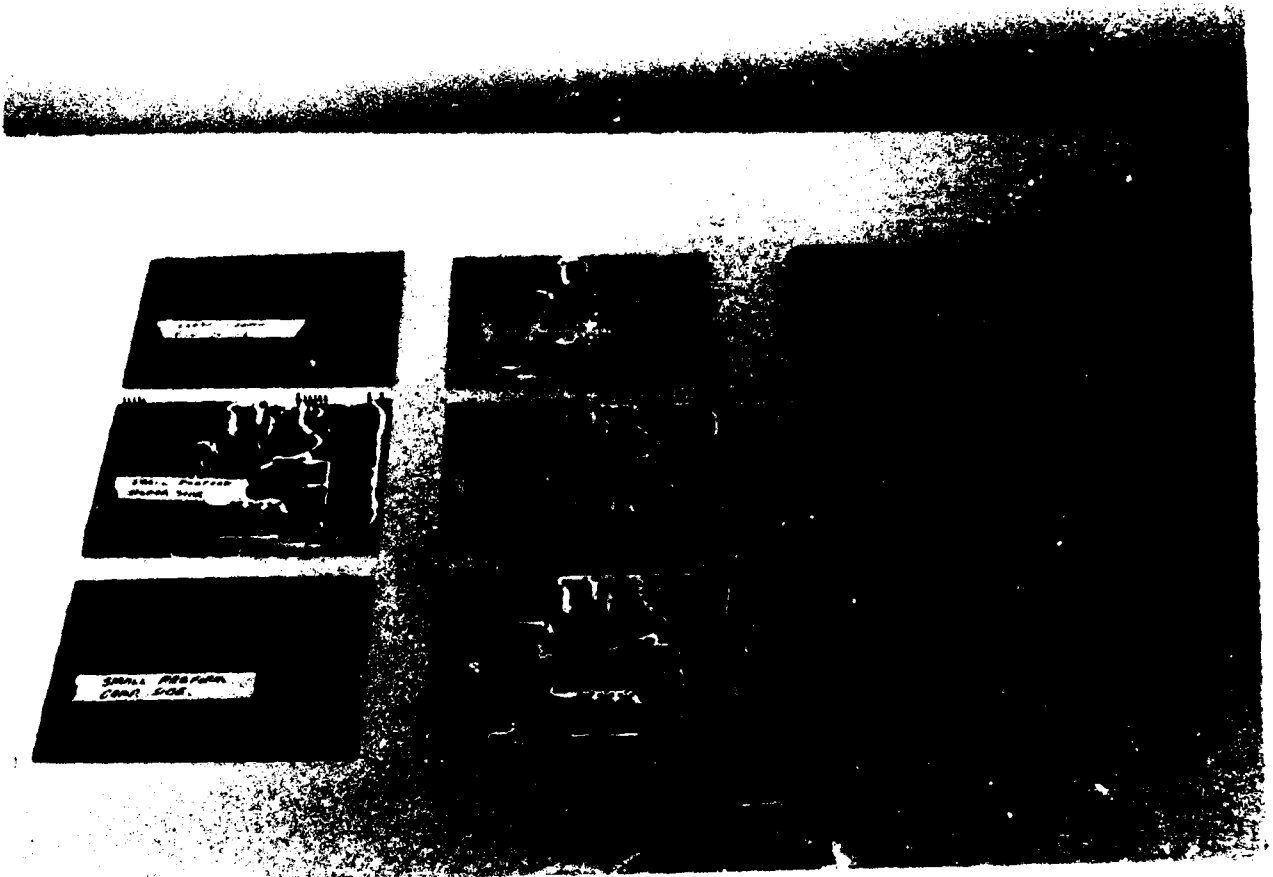


Figure 15. Component-side view of 926 solder-joint samples prepared for statistical testing. In the first two rows of boards, the dummy ICs containing the samples are at the righthand edges of the boards.

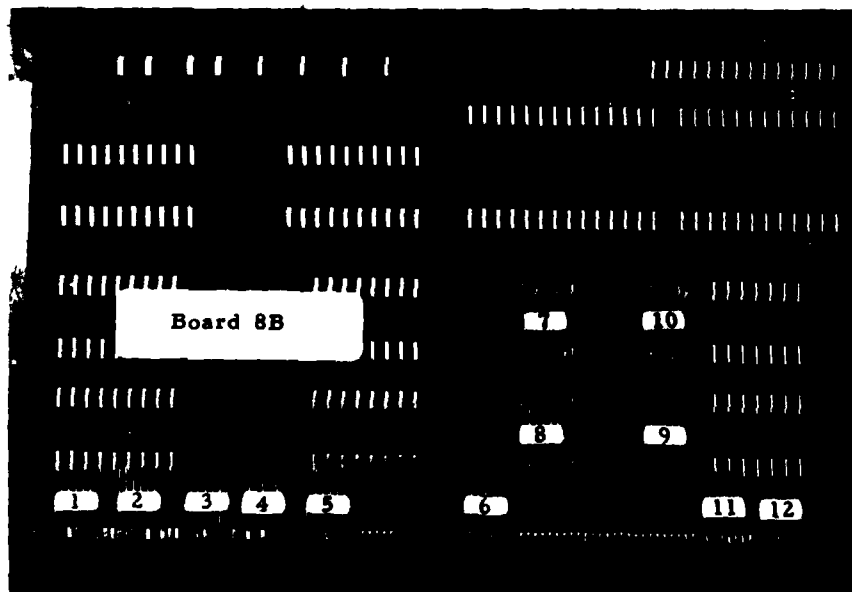
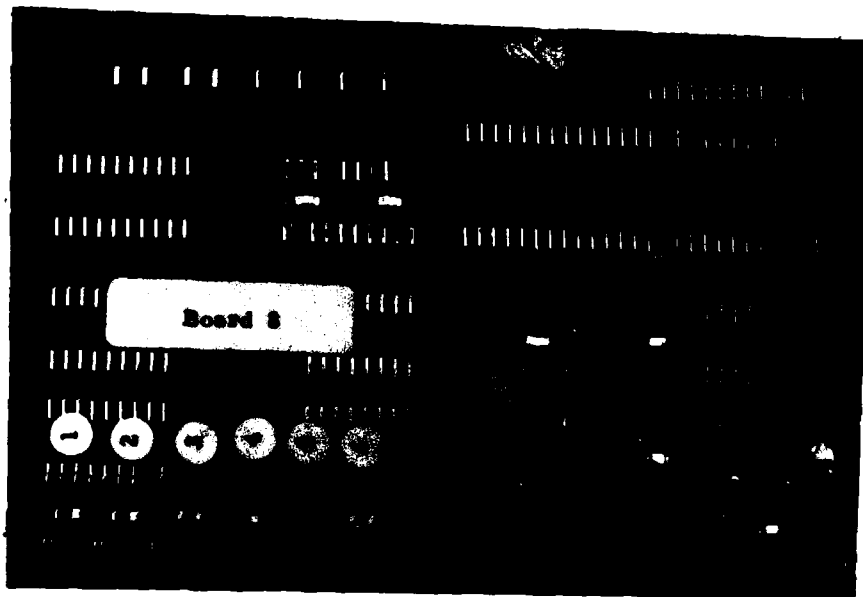


Figure 16. Boards 8 and 8B containing 238 hand-fabricated lap joints.

- Board No. 4: Voids and shallow fillets, made with small preforms on solder side 118 joints
- Board No. 5: Generally good joints with some shallow fillets, made with large preforms on the solder side 128 joints
- Board No. 6: Overheated joints, mostly in the surrounding board, made by brute-force heating with over-size soldering iron 128 joints
- Board No. 7: Internal voids, made by inserting either epoxy resin or wire-insulation shavings before soldering 38 joints

Lap joints at flat-pack ICs

- Board No. 8: Assorted defects including solder-mass variations, cracks, cold joints, etc. 126 joints
- Board No. 8b: Similar to Board No. 8 112 joints
- A total of 1,028 joints is included in the above.

3.4.2 Testing Conditions

All laser/thermal testing in Phase 2.2 was performed with the use of the laboratory system depicted in Figure 6 of Appendix A. Some of the pertinent features of this system are:

Heating laser: GTE Sylvania Model 607 Nd:YAG. Six-watt multimode (continuous) maximum rated beam power. Various beam power levels were used throughout the tests, in the range from about one to six watts.

Pointing laser: Spectra Physics Model 155 helium neon (HeNe). 0.0005 watt continuous. Brought into coincidence with YAG beam by use of folding mirrors.

Infrared detector: Indium antimonide (InSb). Judson Infrared Series J-10, liquid-nitrogen cooled to 77°K, active area 0.004" square, $D^*(500,900,1) = 2.3 \times 10^{-10} \text{ cm Hz}^{1/2} \text{ watt}^{-1}$ or greater, photovoltaic mode, time constant = 1 microsecond or less. Provided with germanium filter for daylight suppression. Peak wavelength: 5 micrometers. The detector signal is amplified via low-noise amplifiers including a current-to-voltage converter.

Detector optics: Eight-inch diameter f/l imaging mirror with flat folding mirrors, aluminized and overcoated. Resulting detector sensitivity to target-temperature change = approximately 1°C for blackbody target, this signal change being comparable to the detector noise level. (Sensitivity can be improved by use of electronic filtering and longer integration times.)

In terms of the amplified detector signal, a calibration curve for the detector/optics combination was presented as Figure 2.

Heating-laser beam geometry: The 4-mm diameter multimode YAG laser beam is focused upon the target area by use of a 50-mm focal length lens. The rated 10-mrad beam divergence angle (between $1/e^2$ points) provides a nominal spot diameter of 0.020" with such a lens. Round beam spots were used in most of the tests. In a few tests, the spot was elongated by use of a cylindrical lens when lap joints were being tested. This was done in order to determine whether improved sensitivity to defects might be achieved by use of a spot shape which more closely matched the configuration of the flat-pack lead. (See Section 3.4.6.3.)

In the testing of lap joints, spot diameters of 0.020" to 0.025" were used in order to span the widths of the nominally 0.015"-wide leads which were located irregularly on the somewhat wider solder pads. During testing on feed-through joints, which are nominally 0.050" in diameter, the beam spot was enlarged by defocusing in order to better match the target dimension.

The multimode beam spot is known to be most intense at the center and to diminish in intensity radially in an irregular manner.

Positioning table: The XY table was furnished to our specification by Automation Unlimited Inc. of Woburn, Mass. The table provides 12" x 12" of travel and is "open-loop" controlled by a controller to be described. The design provides for lightweight parts to minimize inertia in order to achieve our required table speed of 0.050" in 0.050 second between lap joints. This duration, plus the anticipated laser-beam exposure while the table was stationary, was intended in order that we might achieve the desired eight-joints-per-second inspection rate.

The table resolution is 0.001" and the repeatability is 0.0005". The table operates on Thomson-type recirculating ball bushings and round rails and is driven by five-pitch lead screws which are energized via SLO-SYN MO61-FD08 stepping motors.

Table controller: Automation Unlimited Model C52-401-111 two-axis CNC control with front-panel programming controls including jog controls and with a digital magnetic recording capability for the storage of programs.

Exposure conditions: Solder joints were tested with the heating-laser beam impinging nearly vertically on the target and with the infrared sensor axis vertical. Lap joints were face-up on the positioning table as were the solder sides of feed-through joints (except for one case to be noted in Section 3.4.5). Various exposure durations were used at different times in order to match the thermal masses of the targets and to meet our needs for various testing rates, on the one hand, and for various thermal signal maxima on the other. Exposure durations ranged from approximately 50 mSec to one second or more during investigative procedures. One exposure per solder joint was used except in a test series in which several lap joints were irradiated at a progression of points, as will be described in Section 3.4.6.

Maximum solder temperatures: During the various tests, exposure durations were selected on the basis of being sufficient to provide easily discernible thermal signatures between test joints of varying qualities. Exposure durations greater than this would decrease the inspection rate and would pose the risk of reflowing the solder joints and thus altering their quality.

In the detector calibration curve of Figure 2, we note that many millivolts of amplified detector signal will result from a target-temperature change of a few Centigrade degrees. The calibration curve is based upon blackbody radiation conditions; thus, it represents actual temperatures when the target is a perfect radiator. This condition is approached only in the case of highly defective joints, such as burned ones, joints contaminated with residual flux or other foreign matter or, in the case of feed-through joints, deep surface voids or the absence of solder. For normal joints, which are poor emitters, the actual surface temperature will be several times higher than that which is indicated by the chart. For a joint whose thermal emissivity is known (such as 0.5, for example), the observed signal voltage must be increased -- that is to say -- it must be divided by the emissivity value in order for the actual temperature to be deduced from the chart. Thus, the observed signal would have to be doubled (i.e., divided by 0.5) in order to provide the correct reading for a sample having an emissivity of 0.5.

Typically, amplified detector signals of a few hundred millivolts were used. Assuming emissivity values of the order of 0.2 for a clean, highly reflective solder joint, this value might have to be increased to about one volt or slightly more in order to provide an actual temperature reading. From Figure 2 we deduce, in such a case, that solder surface temperatures in the vicinity of 100°C might thus be achieved in such cases. This is safely below the approximately 182°C minimum melting temperature of various lead-tin solder mixtures.

In no case has any unexpected reflowing of a test joint been observed. In separate tests, we have determined that seven

watts of laser-beam power are required for approximately one second if a clean, shiny solder joint is to be reflowed intentionally.

Data format: Thermal signals were monitored visually, as they occurred, by use of a storage-type oscilloscope. Those data which were of interest were recorded photographically by use of a Polaroid oscilloscope camera. For long data runs, chart recordings were prepared by use of a Sanborn recorder having a 1.2-volt full-scale deflection and with a variety of chart speeds. The raw thermal data to be presented in this report will consist of reproductions of either of the two data formats.

3.4.3 System Repeatability

In preparation for the testing of solder joints, preliminary tests were carried out in order for us to determine how much variability there might be in the laser/thermal system when the same target was tested repeatedly. Such variability could be conceived of as arising from several sources such as table vibration, positioning errors, detector noise and so forth.

In one such test, the intent was to discover how much thermal-signal variability might be expected from a number of supposedly identical solder joints. Because all of our available samples had been prepared by hand instead of by machine, they could not be used for tests on "identical" solder joints. In their place, we elected to use a group of "machine made" solder pads on Board No. 8B. Twenty-two such pads were used as targets; they appear at the lower right in Figure 16, between ICs Nos. 6 and 11.

Two identical passes were made over the pads, and both sets of thermal signatures are seen in Figure 17. Unexpectedly, we observed large variations in the thermal peaks within each



Figure 17. Two identical thermal passes over a row of 22 unused solder pads. The pads are similar except for minor scratches and blemishes due to handling, causing differences in the thermal peaks. Note the repeatability from one set to the other.



Figure 18. Twenty-four exposures on the same part of one solder joint with the XY table being moved and returned between exposures. Maximum height variation of thermal peaks is +3%.

pass over the group. A microscopic examination then revealed that the pads were not as identical as was expected. Instead, they contained various scratches and blemishes, apparently from normal handling because this board had been in use for some time.

More importantly, the two sets of signatures in Figure 17 resemble each other quite closely, indicating that the laser/thermal system is fairly repeatable.

In a more critical test, a single solder joint was used as the target. This was exposed to the laser beam, allowed to cool while the table was moved to a different position, and then the target was automatically re-positioned and re-exposed. The results of 24 such exposures are shown in Figure 18. Here the thermal peaks are more nearly alike, although a variation of about $\pm 3\%$ about the mean can be observed. The question was then raised as to whether the variation was due to laser/thermal system variability or to table re-positioning errors.

In order to eliminate the latter possibility, the table was left in position while the same part of the same joint was exposed repeatedly. The results are shown in Figure 19 as three sections of one continuous chart trace, and almost the same variability as before can be seen. This implies that little or no variability is due to the table motion.

The key to the variability is seen in the lower part of each trace where the target is cooling. The ripples are familiar to us as detection-system electrical noise, which arises most often in the detector itself and is amplified. Such noise is common to all detectors if their signals are amplified highly enough,

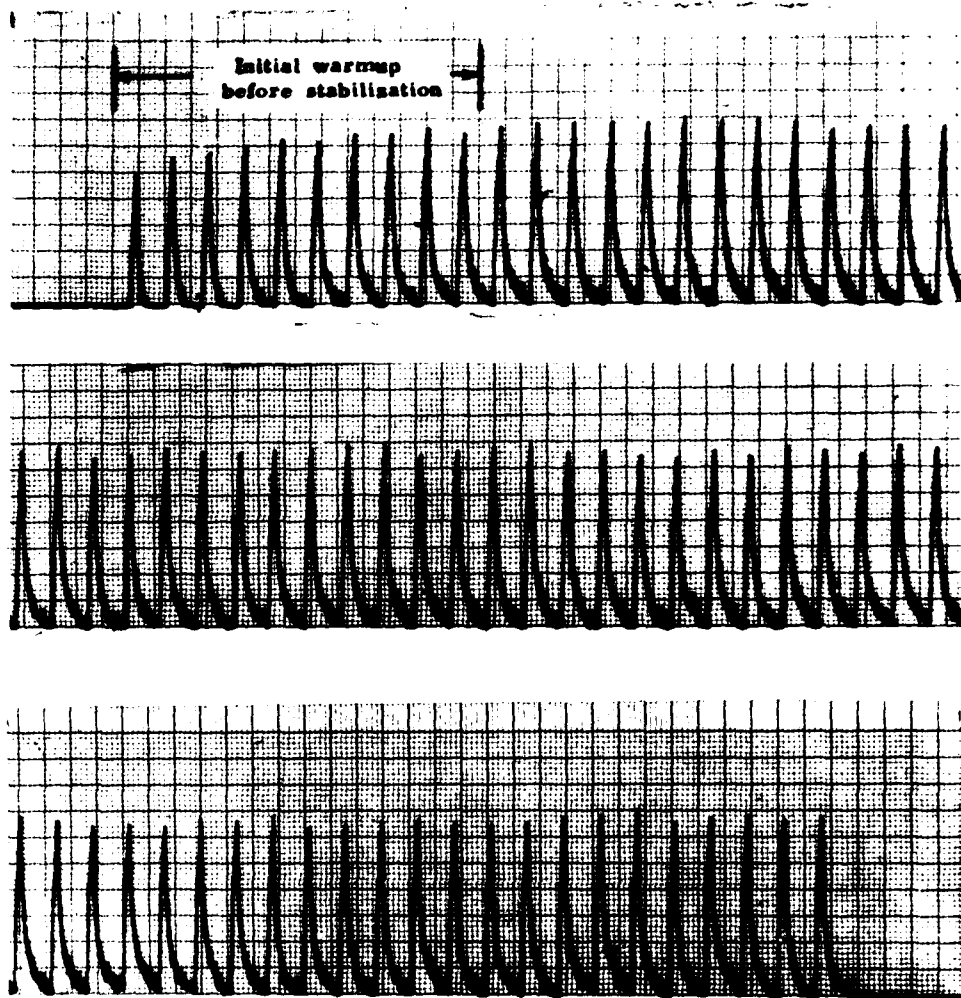


Figure 19. Repeated thermal signatures at the same location on one solder joint at seven-second intervals to allow cooling. Table was not moved between exposures. Peak-height variation is about $\pm 2.5\%$ and is due to detector noise.

and it limits the smallest change in temperature which the detector can measure reliably. The noise is especially noticeable when high signal amplification must be used in order to measure small changes in target temperature. When larger changes are to be observed, less amplifier gain need be used, and the noise becomes less noticeable.

From our knowledge of the infrared system performance, we can equate the noise amplitude to an uncertainty of about one Centigrade degree in the temperature measurement. (This uncertainty would be reduced if the detector signal were electronically filtered, with some sacrifice of response speed.) An inspection of Figure 19 reveals that the thermal signal amplitude at the peak of each signature is approximately ten times the value of the noise amplitude. This indicates that the highest blackbody target temperature reached is about ten Centigrade degrees above room temperature, and this is in accordance with our earlier experience with laser/thermal testing of solder joints.

We conclude, then, that the temperature uncertainty of the present laser/thermal system is about one Centigrade degree and that this shows up as height variations in the peak thermal signals. This is because each peak occurs randomly at some point during a noise pulse which might be a maximum point or a minimum point.

An important fact to be noted is that if more intense laser exposures are made (in order to achieve higher target temperatures), the temperature uncertainty, which is fixed, becomes a smaller part of the target temperature. That is, a one-degree

uncertainty in a twenty or thirty degree temperature change is clearly more desirable than in a ten degree change.

This will be an important consideration in the design of the final system.

The value of the tests which we have just described is in pointing out that the remaining data to be presented in this report are repeatable to within a few percent in the positive and negative directions. If two thermal peaks are seen to differ by a greater amount than this, then the difference can be assumed to be real instead of being due to system noise.

3.4.4 Method of Scoring

The solder joints which were prepared for the tests were intentionally of varying quality over the range from "normal" ones to rejects. They thus included many joints between "good" and "bad" which might be considered as acceptable by some inspectors and as rejectable by others. This "questionable" category was included because it represents a real-world situation and it highlights an important point about the operation of the final laser/thermal system. That point is that the questionable joints will lead to thermal peaks which fall somewhere between those of the acceptable and the rejectable joints. Therefore, the matter of where the dividing line should be placed in order to separate the good from the bad joints must be a human decision, and this may vary from one operator to another. Preferably, instead of a dividing line, a band would be used which encompassed all of the

questionable joints. The computer would therefore identify three levels of joint quality:

Definitely good
Definitely bad
Questionable.

In practice, the operator would inspect all joints in the questionable category. He may wish, also, to verify those which were indicated as definitely bad, at least during initial use of the system. Later, these could be automatically marked for repair by an ink jet or other means under computer control.

Considering that, in a normal PC board, only a small percentage of rejects occurs, the relative number of questionable joints which had to be inspected would be very small.

The solder joints which were tested included all of those on the nine test boards which had been prepared during the course of Phase 2.2. When a group of joints was selected for testing, it was first examined via a stereomicroscope in detail. The quality of each joint was hand-recorded on the basis of its visible characteristics.

The group was then subjected to laser/thermal testing and the recording was examined. Arbitrarily, a line was placed somewhere just above the thermal peaks corresponding to the known good joints, leaving some leeway for normal variations such as those due to harmless cosmetic blemishes. This line serves as the lower limit of a "questionable" band which we established on the chart. The upper limit of this band was placed somewhere below the higher peaks on the chart which corresponded to known defective joints.

This was followed by a procedure in which we scored the results by observing whether:

1. All known good joints were represented by thermal peaks below the questionable category; and
2. All known defects (including hidden ones) showed peaks above the questionable category; and
3. All others fell within the questionable category.

If all of these conditions were met by a group of samples, then the score was 100%. If it was not, as was sometimes the case, then the failure was due to one or more of several causes:

1. An improper human judgment as to joint quality during visual inspection;
2. The presence of a minute blemish which raised the thermal signature of a joint of acceptable quality;
3. The presence of a localized defect which caused an unacceptable visual rating but which was not located closely enough to the center of the target area to be detected by our system. (This might occur because of the nature of the laser beam spot with its uneven power distribution and the central "hotspot", a matter which was remedied in a separate effort by passing the beam through an optical fiber in order to homogenize it.)
4. The presence of an unsuspected hidden defect -- that is, one which occurred without our knowledge during sample preparation and whose presence could be verified by mechanical sectioning.

Most of the tests were conducted at laser-beam powers of one or two watts, requiring exposure durations of a large part of a second or more in order to bring out the differences in thermal signatures. In some of the tests, the exposure durations were increased beyond the required minimum but, as was expected, without any particular benefit to the discrimination capability.

3.4.5 Component-side Testing

As we have indicated, all feed-through joints with one exception were tested from the solder side. The exception involved a group of test joints on one IC which had been prepared such that the solder did not "wick up" fully into the holes. The result was a series of voids, visible from the component side, where the leads entered the holes. These are seen as dark crescents in Figure 20 which shows a few of eight such joints on one side of a 16-pin IC.

The depth of solder penetration was not known to us and we attempted to detect the presence of the voids by laser/thermal testing from the solder side. As we shall illustrate in a later section, such voids are detectable when they are large enough or close enough to the test surface to reduce appreciably the amount of thermal mass beneath the test surface. As it happened, the voids in this case were not detectable from the solder side and we concluded that they were too shallow to be revealed by such testing.

We then considered the idea that it may be advantageous to test a board from both sides, consecutively, when certain defects might be found more easily from the component side. We recognize that there are instances where the component sides of the joints are obscured by overhanging parts of the components themselves. However, statistically speaking, we believed that enough such joints on an average board might be accessible, and so we proceeded to verify that such testing would be feasible.

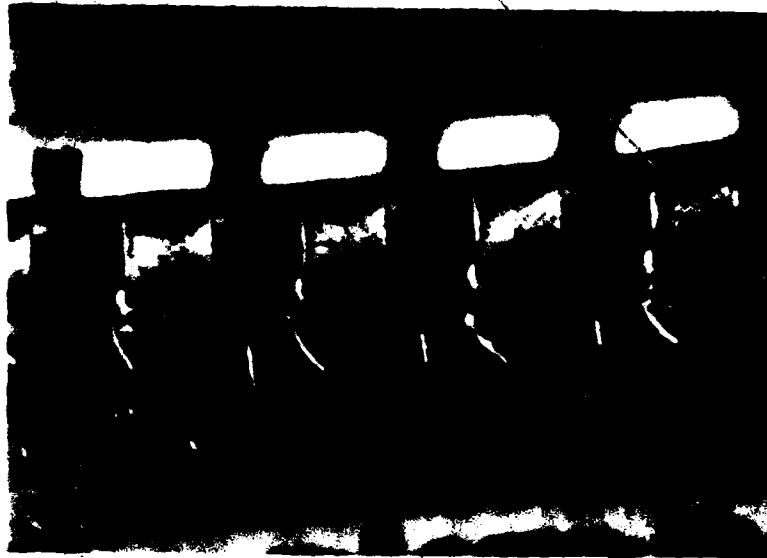


Figure 20. Close-up view of solder voids on component side of board giving rise to high peaks in Figure 21. Voids appear as dark crescents where the pins enter the holes.

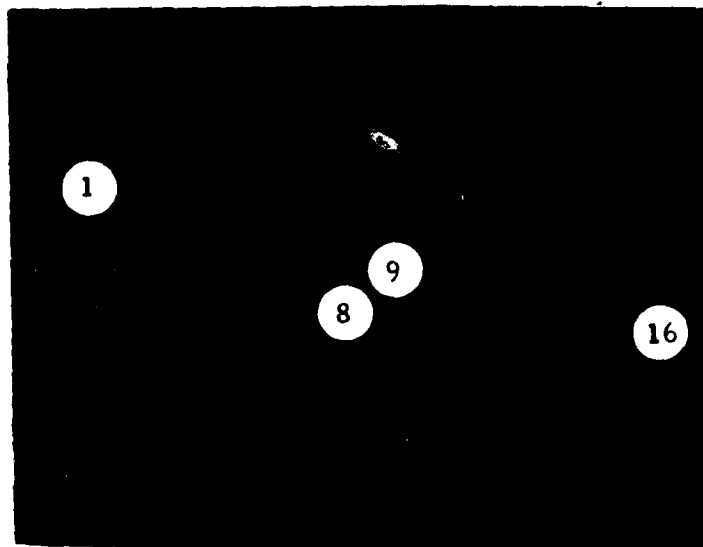


Figure 21. Eight component-side voids and eight good joints for reference. Testing was from the component side of the board. Void No. 8 was not visible and gave low thermal peak. Numbers signify end-pins in the two rows.

Thermal signatures were obtained for the eight defects in question, followed by a series of eight signatures for normal joints, all from the component side. The sixteen signatures are shown in Figure 21 where the thermal peaks numbered 1 through 8 identify the defects. Nos. 1 through 7 are higher than the other peaks, as was expected. The eighth defect was not revealed because the lead was in close contact with the outer edge of the hole and the dark crescent was not visible at the laser-beam angle.

We notice that Peak No. 9, the first of the normal series, is higher than the others. This was due to a speck of burned, residual solder flux which could be seen only by microscope.

These signatures were prepared with 2.4 watts of laser beam power and with 0.96-second exposures per joint. The vertical scale in the oscillogram is 50 mV/division and the horizontal scale is two seconds per division.

All other tests on feed-through joints were conducted from the solder sides of the boards.

3.4.6 Test Results on Lap Joints

The lap joints which were tested in this program were prepared on Boards Nos. 8 and 8B and, chronologically, were tested before the feed-through joints. We shall therefore discuss lap joints first, and in Section 3.4.7 we will consider the test results on Boards Nos. 1 through 7 which have feed-through joints.

Section 3.4.8 will present a summary of the data on all boards tested, along with a commentary on the test results.

Some exploratory tests preceded the actual testing of the lap joints in order that we might optimize our testing parameters and refine our testing and scoring procedures.

3.4.6.1 Exploratory Tests

A randomly chosen group of 29 lap joints was selected for these tests, having been hand-fabricated so as to include various degrees of quality ranging from "good" to "bad".

Figure 22 presents some early test data on the 29 joints which included good ones, one lifted lead, joints having light solder although fully attached, and joints being soldered only at their tips.

Figure 23 is an overall pictorial view of the joints. Below the photograph, we present our assessment of joint quality as based on visual inspection through a microscope.

Figures 24 and 25 are photomicrographic views of small groups of the 29 joints.

The oscillogram of Figure 22 shows the 29 thermal signatures, their most obvious feature being the wide variation in the heights of the thermal peaks. The purpose of the test, of course, was to be able to correlate high peaks with bad joints, and so forth. The principal question to be answered, as one examines the oscillogram, is where to locate a horizontal threshold which will separate the peaks into "high" ones for bad joints and "low" ones for good joints.

When this is done, the next question is whether all of the good signatures will fall below the threshold, with the bad ones above it.

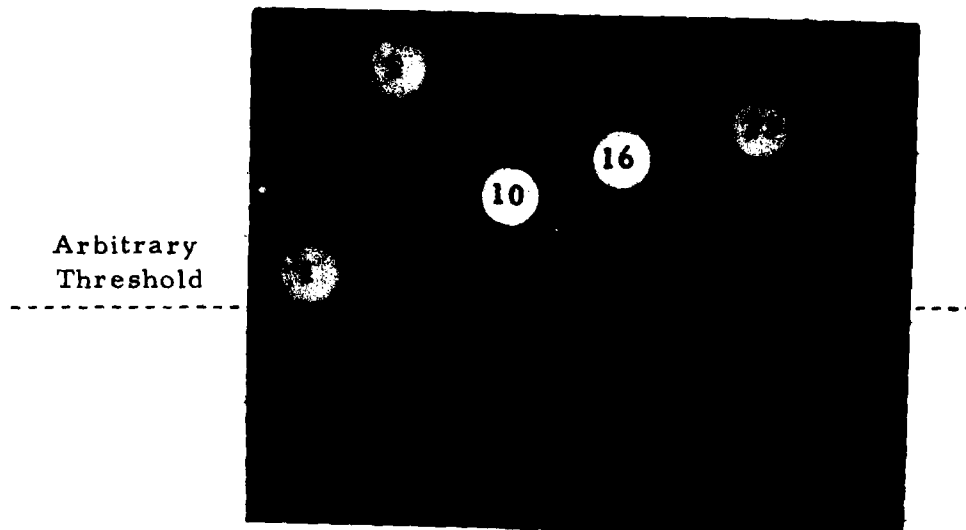
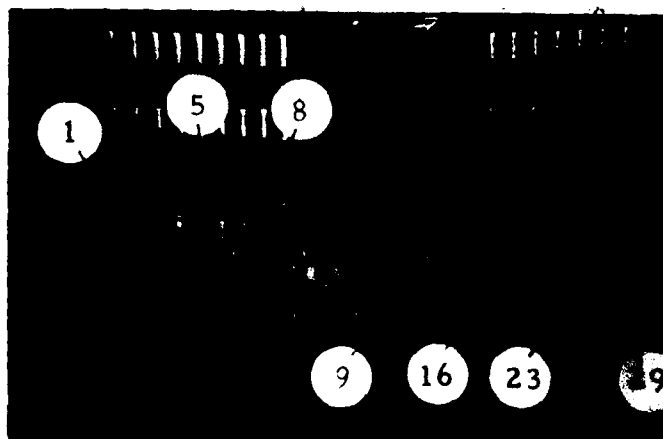


Figure 22. Thermal signatures of 29 test joints of various qualities.



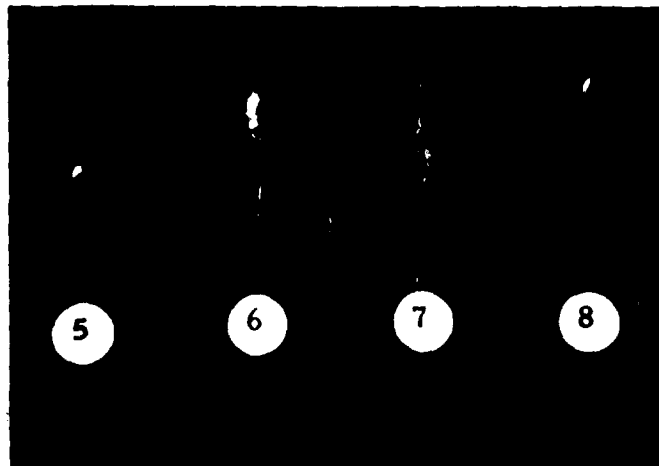
| <u>Sample No.</u> | <u>Condition of Joint</u> |
|-------------------|---------------------------|
| 1-4 | Good |
| 5 | Lifted lead |
| 6-9 | Good |
| 10 | Light solder |
| 11 | Good |
| 12 | Light solder |
| 13 | Good |
| 14 | Light solder |
| 15 | Good |
| 16-29 | Solder only at tip |

Figure 23. Numbering and quality assessment of the 29 samples.

Samples 1 through 4



Samples 5 through 8



Close-up of lifted lead
Sample No. 5

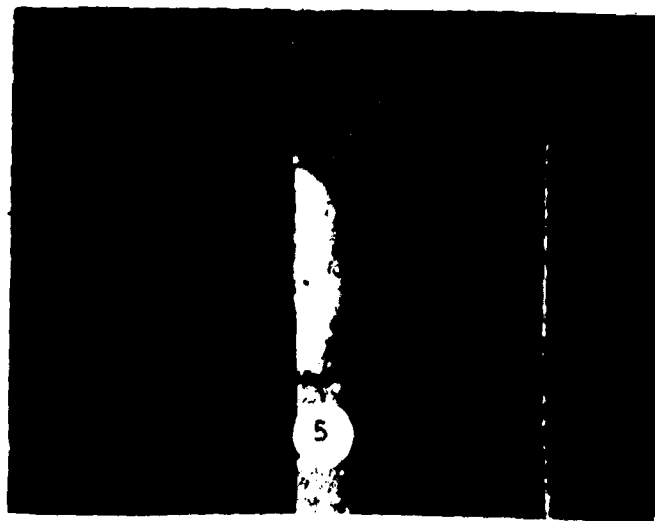
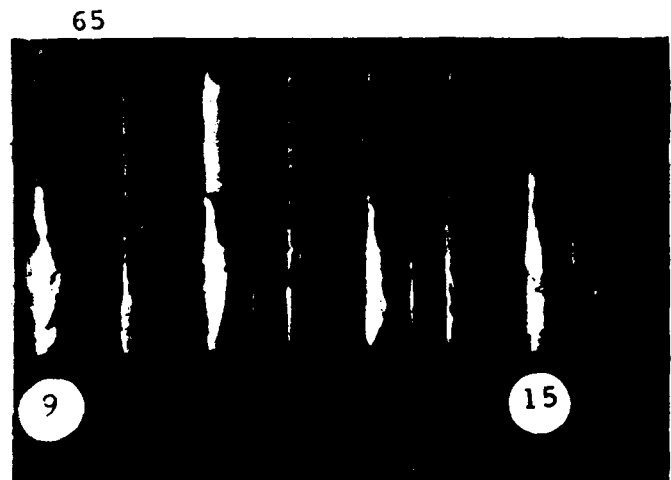
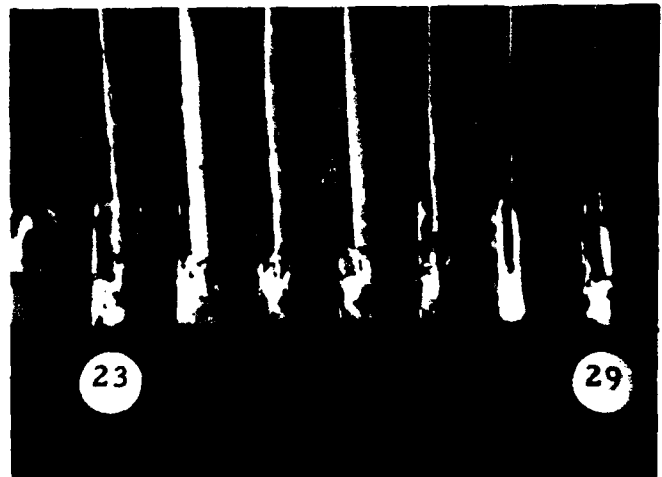


Figure 24. Micrographs
of Samples 1 through 8.

Samples 9 through 15



Samples 16 through 22



Samples 23 through 29

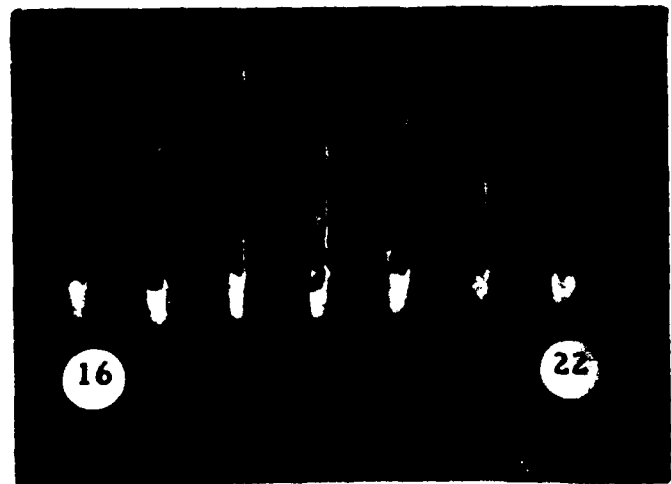


Figure 25. Micrographs
of Samples 9 through 29.

As it happens, in this oscillogram, it is not possible to pick a threshold value which will clearly separate all of the good and bad joints according to the way that we have defined them by visual inspection. For instance, we have declared Joint No. 15 to be "good" whereas its thermal peak is actually higher than the one for Joint No. 12 which we have said to be "bad". The disagreement results either from an error by our testing method or a faulty definition of what visually appears as "good" or "bad".

A clue as to why the signature for No. 15 was high is seen in Figure 26. This is a higher-magnification view than is shown at the top of Figure 25, and with a different lighting arrangement. The central area of the solder is pitted and rough, compared with the smoothness of Nos. 11 and 13. In the tests, the laser beam was directed at the centers of the joints, and this would explain the high peak for No. 15. Thus, the disagreement between the data and our visual assessment of the joint might be resolved by either:

1. Declaring the joint to be faulty because of the blemish, thus agreeing with the test result, or
2. Declaring the joint to be good, despite the blemish, and expanding and elongating the beam spot in order to average out the effect of the blemish.

Regarding the other thermal signatures in Figure 22, if we place a threshold at an arbitrary height as shown in the figure, then there is a fairly clear separation between bad and good joints on the basis of high and low thermal peaks. In some cases, the peaks are close to the dividing line because not all

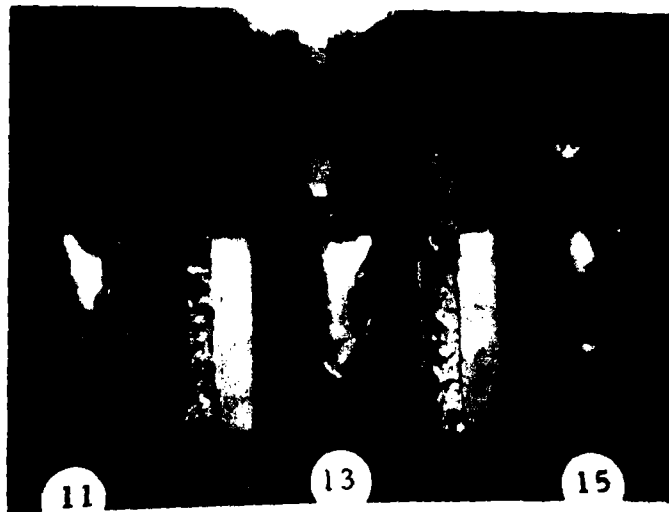


Figure 26. Blemish at center of Sample No. 15 is held responsible for high thermal peak in Figure 22.

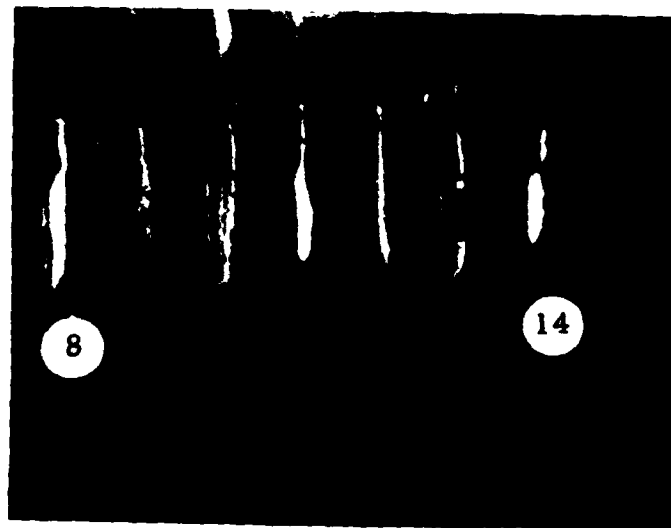


Figure 27. Solder joints at Pins 8-14 of IC No. 9, Board No. 8. The first, middle and last joints are normal; the others consist of tinned, lifted leads.

real-world solder joints are "clearly good" or "clearly bad". There is a band about the threshold which indicates joints of questionable quality which should be checked by an inspector.

Commenting further on the thermal signatures of Figure 22, we note that those for Samples 16 through 29 are high, as they should be, for the leads are attached only at the tips and are separated by a thin air space elsewhere. We also point out that, except at the joint, the highly reflecting gold plating is exposed, tending to suppress the thermal signatures. The laser-beam spot fell partly on the gold and partly on the solder tip. The low, overall thermal mass of the soldered tip plus the unsupported lead drove the thermal signals upward, despite the high reflectance of the gold. We expect that, had the leads been tinned along a greater length, the thermal signals would have been much higher.

3.4.6.2 Tests Using Elongated Beam Spot

We refer, now, to the third flat-pack IC shown in Figure 23, which was omitted in the preceding tests. In the photo, the handwritten numerals 7 through 10 refer to our arbitrary numbering of the ICs on Board No. 8, and we turn our attention to IC No. 9. Its pins Nos. 8 through 14 are shown in Figure 27 where the first, middle and last joints are well formed. The other four consist of lifted leads which have been tinned and are either raised from the pad or are lying loosely on it but without good thermal contact.

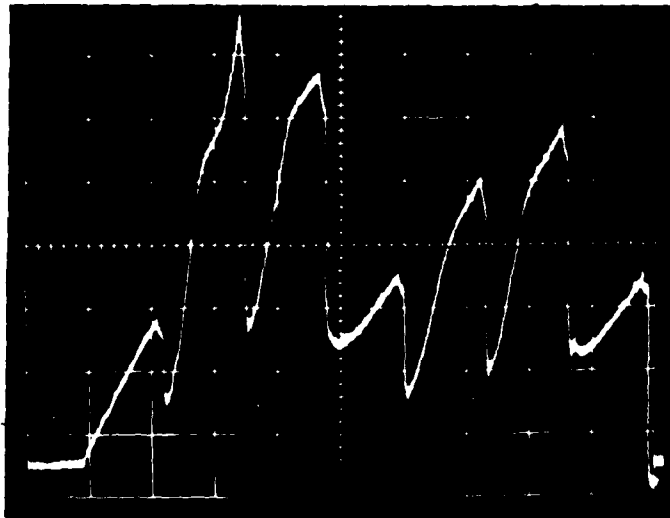
This set of samples is of interest to the system-parameter optimization study (see Section 3.5), with special reference to the possible elongation of the laser-beam spot. The question has arisen in earlier phases of this effort as to whether such a spot shape could provide better data for lap joints by averaging the thermal properties over the length of the joint instead of sampling largely at the center. Limited effort was applied to this question earlier, and we have renewed the effort in the present study.

Our procedure was to test IC No. 9 with and without a cylindrical lens applied to the existing objective lens in order to lengthen the spot. To that end, we have prepared the oscillograms of Figure 28 in the hope of drawing some preliminary conclusions.

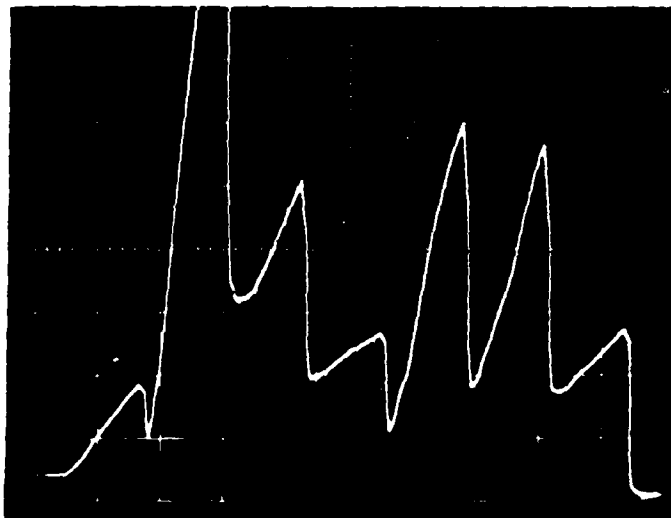
In both cases, we note the pattern in which the first, middle and last peaks are the lowest. In the lower photo, however, we note an off-scale thermal peak for the second signature, indicating a possible localized defect on the lead. The more uniformly high peaks in the upper photo seem to indicate better averaging of local properties along the lead, as we would expect.

We point out that the vertical gain in the lower photo is one-fourth of that in the upper. The round beam spot coincides more nearly with the infrared-sensitive area than does the elongated one, thus providing a much greater signal. For most effective detection with elongated laser-beam spots, the detector spot should be lengthened correspondingly.

It was not practical to elongate both spots simultaneously with the present system configuration. The laser-beam and



With cylindrical lens



Without cylindrical lens

Figure 28. Thermal signatures at Pins 8 through 14 of Figure 27 with and without laser-beam spot elongation.

detector axes are not coincident but converge upon the target area with a small angle between them. Because of the required proximity of the cylindrical lens to the target (in order to achieve effective spot elongation), two such lenses could not be used without there being mechanical interference.

The lens which was used was a section of 2-mm diameter (0.080") sapphire rod which was positioned a few millimeters above the target area. Various other placements were tested in the hope that a single such element could elongate both spots. However, because of the non-colinear axes, it was not possible to achieve two elongated spots which coincided.

Sapphire had been selected because of its transparency to both the laser beam and to the longer-wave thermal radiation used by the detector.

In Section 3.5 on system optimization, we shall discuss a design concept in which the laser and detector axes are brought into coincidence and then impinge vertically upon the target. In such a system design, simultaneous spot elongation would be easily achieved.

3.4.6.3 Focus Considerations

We have pointed out, on earlier occasions, that the state of focus of the laser-beam spot is an important consideration in providing high quality thermal signatures. It is a feature of most laser beams that they contain a "hotspot" at the center, which is not easily eliminated. If the beam is focused sharply the hotspot becomes sensitive to small, local

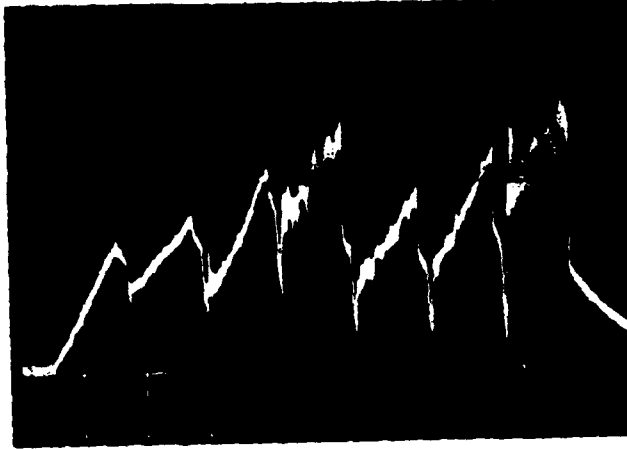
irregularities which are not important in quality-assessment of the joint. One solution is to defocus the beam, and thus the hotspot, but not to such an extent that the edge of the beam spot spills over to the substrate. This would add spurious thermal signals because of its high sensitivity to the beam.

To demonstrate the effects of focusing, we selected a set of seven joints on flat-pack Board No. 8 (IC No. 3, Pins 8-14) which were intentionally good and quite uniform, but containing a few tiny blemishes. A round instead of elongated beam spot was used. Figure 29 presents three oscillograms with the two-inch focal length lens in various states of focus, starting with the in-focus position and being moved away from the target in 0.200" increments.

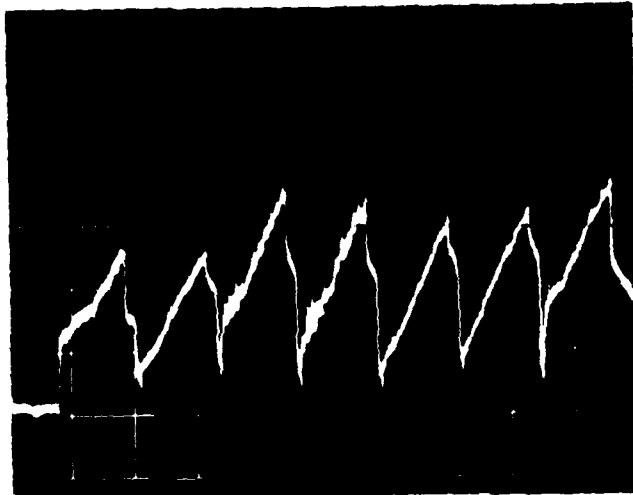
The uniform condition of these joints indicates that a uniform set of thermal signatures would best characterize them. The in-focus signatures are relatively erratic and contain oscillations which we recognize as due to intense local heating of a small blemish. This is the effect which we referred to as "anomalous heating" in an earlier phase of this program, before learning that it was due to normal table vibrations causing the hotspot to oscillate about the blemish.

The successive oscillograms show that a more uniform set of signatures is obtained farther from focus.

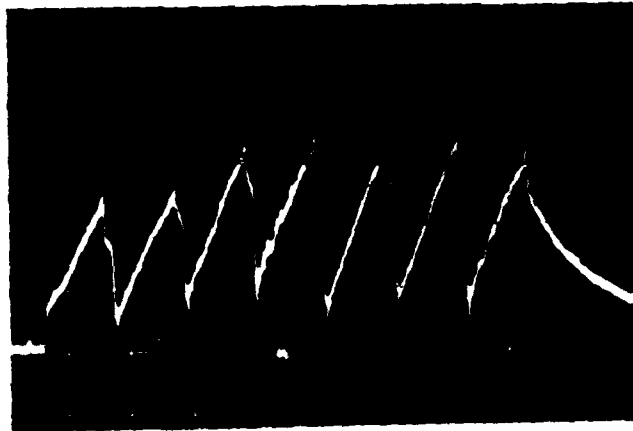
The experiment was repeated on Pins 8 through 14 of IC No. 9 on the same board. These joints, which were shown in Figure 27, consist of good joints and lifted leads with the first, fourth and seventh being the good ones. Again, the quality of the thermal signatures was improved by defocusing, as is seen in Figure 30.



In focus

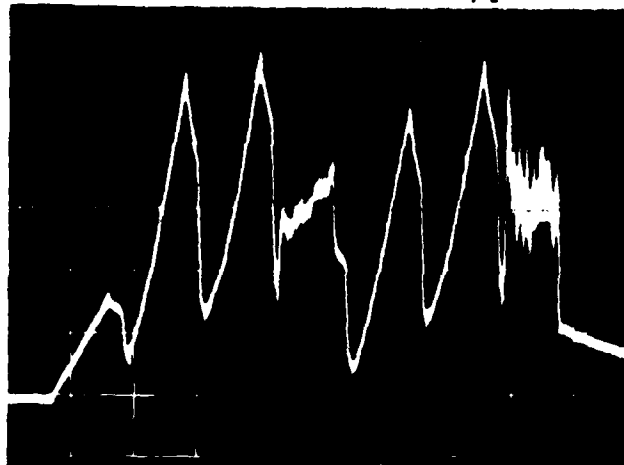


0.200" back
from focus

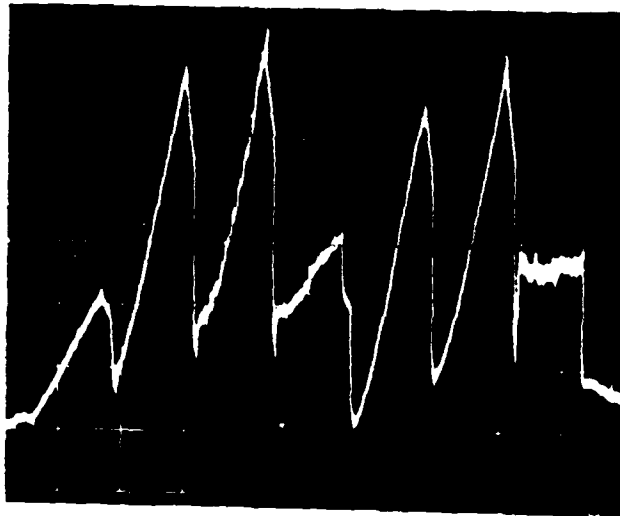


0.400" back
from focus

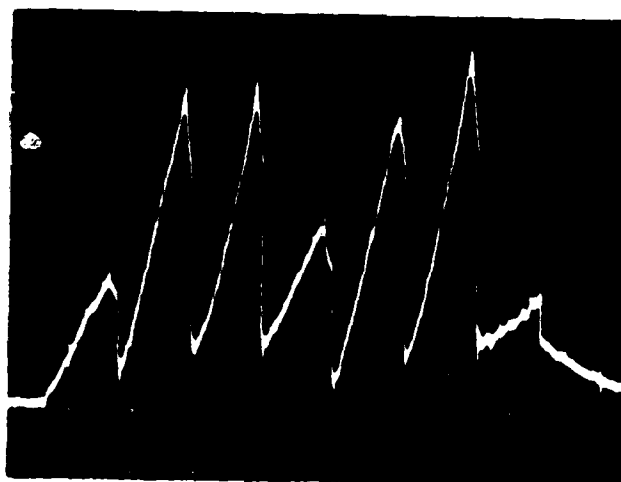
Figure 29. Effect of defocusing a two-inch focal length laser-beam objective lens to achieve uniform thermal signatures from good joints.



In focus



0.200" back
from focus



0.400" back
from focus

Figure 30. Repeat of Figure 29 test on a different set of samples. Sequence of joints is "normal, lifted, lifted, normal, lifted, lifted, normal".

3.4.6.4 Point by Point Testing Along the Lead Length

A flat-pack lead was selected which was joined to the pad at its tip but lifted elsewhere along its length (Figure 31). This typified an extreme case of a cracked joint, being about 80% detached. The joint was examined in detail for thermal signatures along its length. The method was to start with an exposure at the tip, allow the target to cool, and move in 0.002" increments toward the heel while repeating the process. Figure 32 shows the gradual increase in thermal peaks as the target area is moved farther from the heat-sinking effects of the joined tip.

Figure 33 shows the thermal signatures at the tip and heel only, so that they may be compared. A continuous scan along the center of the row of joints shown in Figure 31 reveals the thermal peak of the lifted lead as standing out against the others. This is the last peak in Figure 34. The second peak in this series arises from a joint at which the pad is not bonded to the laminate surface.

The results are pertinent to the question of how a lap joint should be scanned if one is looking for cracks. If the crack is at the tip or heel only, then several exposures are called for. The question arises as to whether three exposures may be sufficient or whether more are necessary. Each additional exposure slows the inspection rate that much more.

In order to explore this matter further, we examined some leads having shorter separations than the above one. Two of these appear in Figure 35. The first one is lifted at the toe for a distance of about one-third of the length of the joint. The other, Pin No. 5, is lifted at the heel for about 40% of the joint.



Figure 31. An extreme case of a "cracked joint".

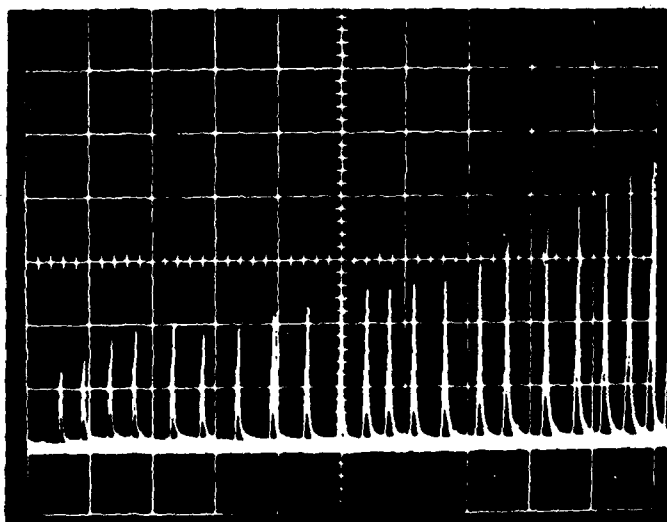


Figure 32. Sequence of increasing thermal signal amplitudes from toe to heel of above lead.

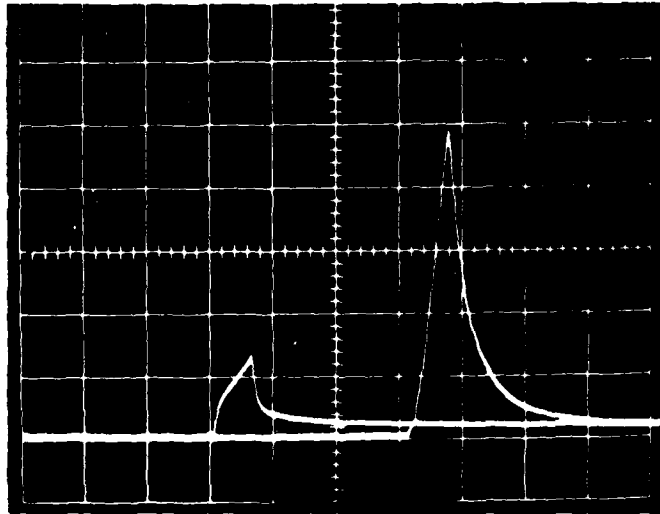


Figure 33. Thermal signatures at the tip (left) and heel of the lead shown in Figure 31.

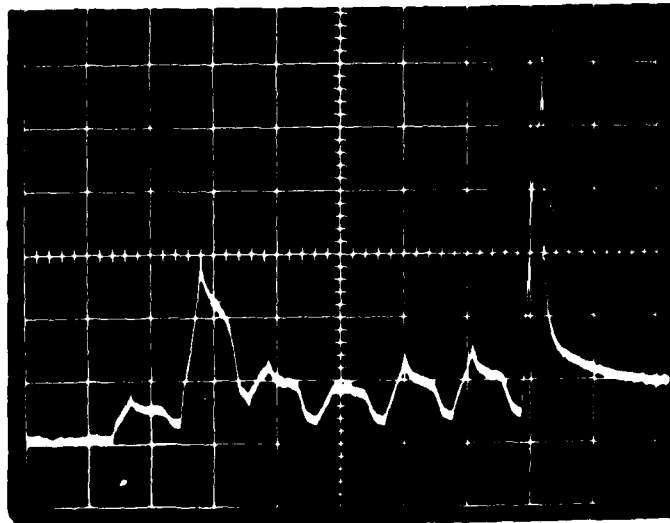


Figure 34. A scan across the centers of the joints shown in Figure 31, starting at the left.

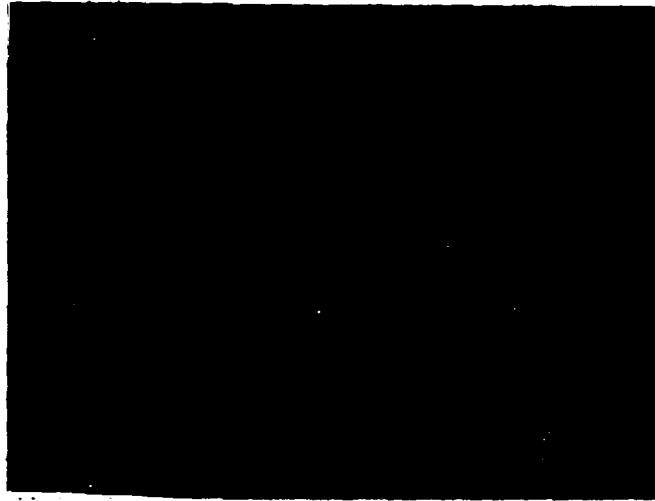
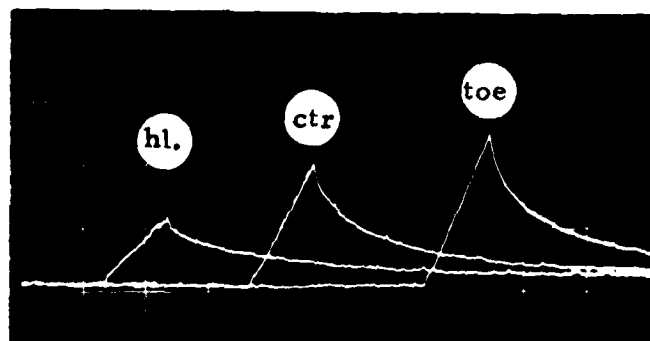
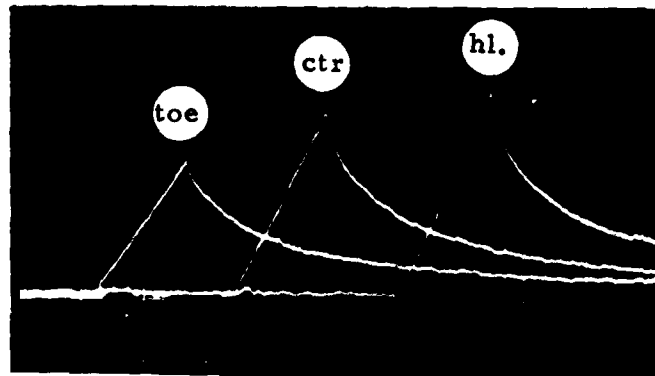


Figure 35. Test Board No. 8B, IC No. 1, Pins 1 through 6. Pin 1 was prepared with a lifted toe and Pin 5 with a lifted heel.



Pin 1, lifted toe



Pin 5, lifted heel

Figure 36. Thermal signatures at three points along two types of defective joint.

Figure 36 shows the thermograms obtained when each lead was exposed at three different points. These points were centered in the outer, middle and inner thirds of the joint length. On both leads, the height of the middle thermal peak, obtained where the lead is partly in and partly out of the solder, is intermediate to the other two peaks for that lead.

We point out, first, that for both samples the signal difference between the high and the low peaks is sufficient for automatic recognition by the computer. That is, the detachment, whether at the toe or heel, would be automatically detectable by probing the joint only twice, once near each end; the exposure at the center is not necessary.

On the other hand, the central peak in both thermograms is sufficiently higher than the normal peak (for the attached part of the lead) as to be computer-detectable without the need for the exposures near the ends. Thus, we can think of the normal peak in each thermogram as being the reference peak which is stored in the computer for that particular joint. A detachment of the nature shown by these samples would yield the thermal signal shown by the central peaks in the oscillograms. Such a signal would indicate a defect regardless of whether it were at the toe or heel and even though the lead is partly submerged in solder at the testing point.

As a matter of interest, Figure 37 depicts a specially prepared defect in which both the toe and heel are separated from the pad. As expected, this defect gave rise to the series of thermal signals seen in Figure 38. One might be concerned that

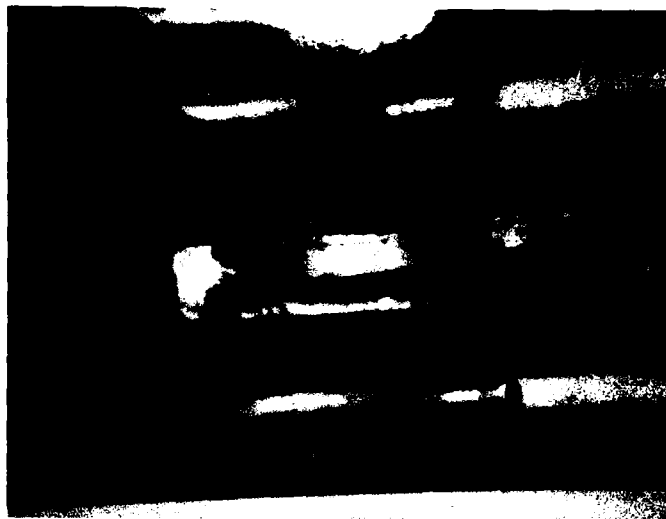


Figure 37. A lead with the toe and heel bent up, adjoined by two normal joints.

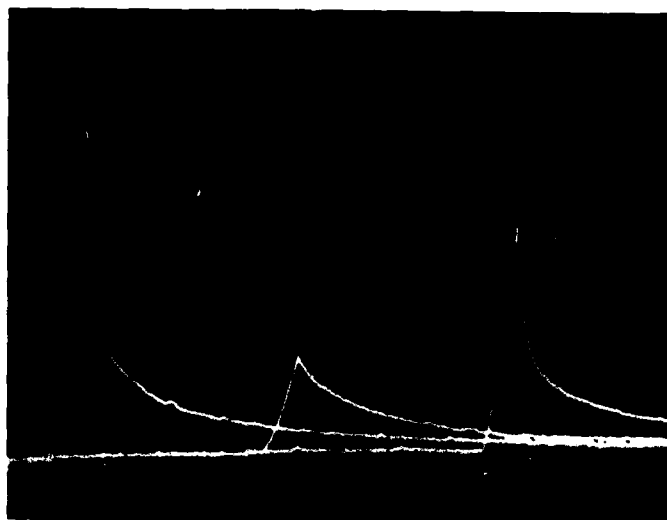


Figure 38. Thermal signatures of the toe, center and heel of the above lead.

this type of defect may not be detectable by a single exposure at the center of the lead where it is well attached. As it happens, there is less solder at the attachment than at the centers of the two adjacent joints. Figure 39 shows a thermal scan across a row of seven joints, the middle three being those shown in Figure 37. The central peak in Figure 39 represents the lead under discussion and it is clearly higher than its neighbors.

A straight-on view of the seven joints is seen in Figure 40.

Had this joint contained more solder at the center, the defect would have been missed.

We conclude, from these tests, that leads which are lifted by at least one-third of their lengths from the underlying pads are highly likely to be detectable with at least two, and no more than three, exposures. If shorter detachments than this must be detected, one has the option of using a greater number of exposures, but at the expense of inspection rate.

3.4.6.5 Statistical Testing of Lap Joints

We come now to the matter of the systematic testing of a relatively large number of lap joints, as opposed to the detailed testing of a few at a time, as in the foregoing discussions. The 238 joints which had been shown in Figure 16 were the subjects of these tests, most of them having been intentionally prepared as defective, with a few good ones included for reference purposes.

In the following four sections, we will discuss these tests in some detail at first so as to familiarize the reader with our testing procedure and with our method of assessing the resulting

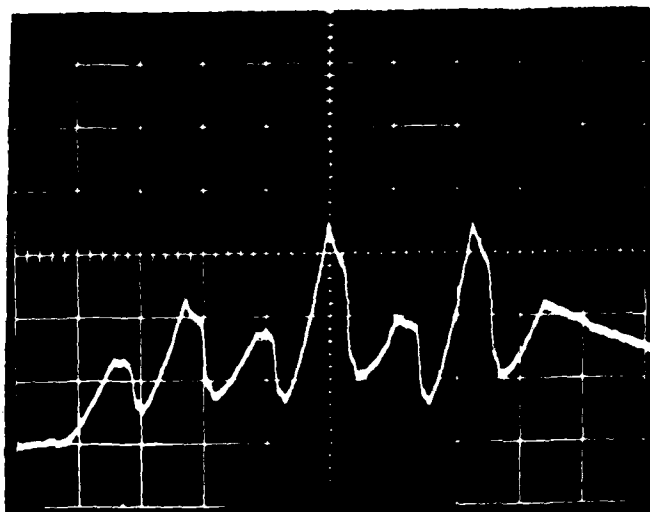


Figure 39. A thermal scan across seven joints (Board 8, IC 5, Pins 8 through 14). The three middle peaks are for the three joints shown in Figure 37.

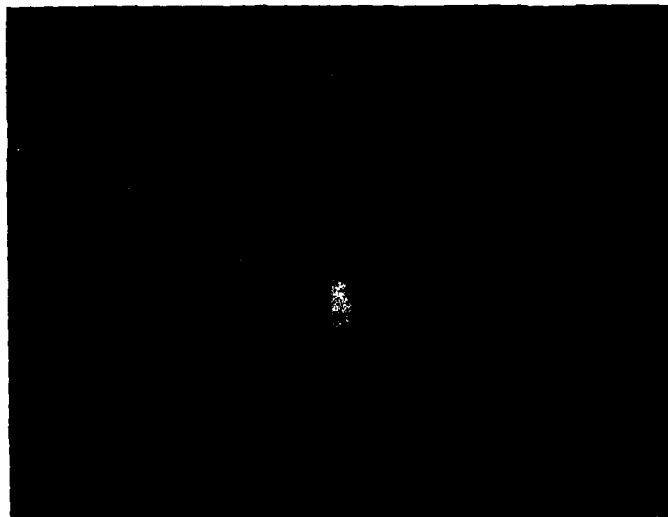


Figure 40. A view of the seven joints represented in the above thermogram.

data. As the discussion progresses, there will be less need for particulars and we will proceed more rapidly.

The results of all of the statistical testing, including those on feed-through joints, will be summarized and reviewed later in this report under Section 3.4.8.

3.4.6.6 Board 8B, IC 1

Figure 41 is a close-up view of the first three ICs on Board 8B while Figure 42 is a still closer view of Pins 12 through 14 on IC No. 1. Pin 12 is an example of a 50%-lifted heel and Pin 14 is a 50%-lifted toe. Thermal data regarding these joints will be discussed shortly.

In order to illustrate our testing procedure, we will use the ICs of Figure 41 as examples and will discuss our visual assessments of their solder-joint qualities, the thermal data from several tests, and the accuracy of our test results. In later parts of this report, the data resulting from the other tests will be presented in more abbreviated form.

In the photos, the pin numbering of each IC starts at the upper right and progresses counterclockwise. In Figure 41, only the lower rows of pins are soldered; these are Nos. 8 through 14 on each IC. We use a two-part designation to identify each solder joint, first by IC-number, then by pin-number.

Our visual assessment of these 21 joints is:

(Board 8B)

- 1-8 Heavy solder, toe lifted 30%
- 1-9 Normal, shiny
- 1-10 Light solder, dull (cold joint)

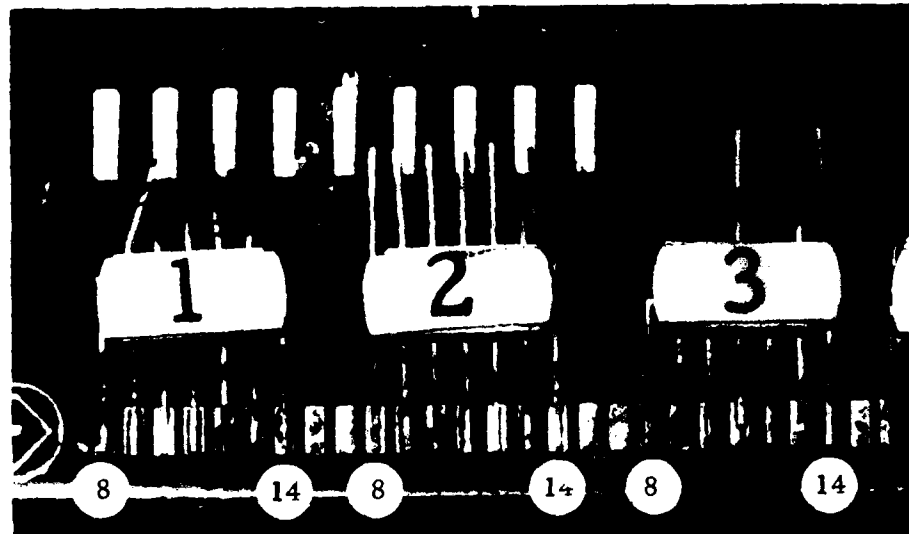


Figure 41. ICs 1 through 3 on Board 8B.



Figure 42. Close-up view of IC 1 Pin 12 (lifted heel) and Pin 14 (lifted toe).

NO-A112 703

VANZETTI SYSTEMS INC. STOUGHTON MA
INFRARED DETECTION OF FAULTY SOLDER JOINTS. PHASE 2.2.(U)
MAR 82 A C TRAUB

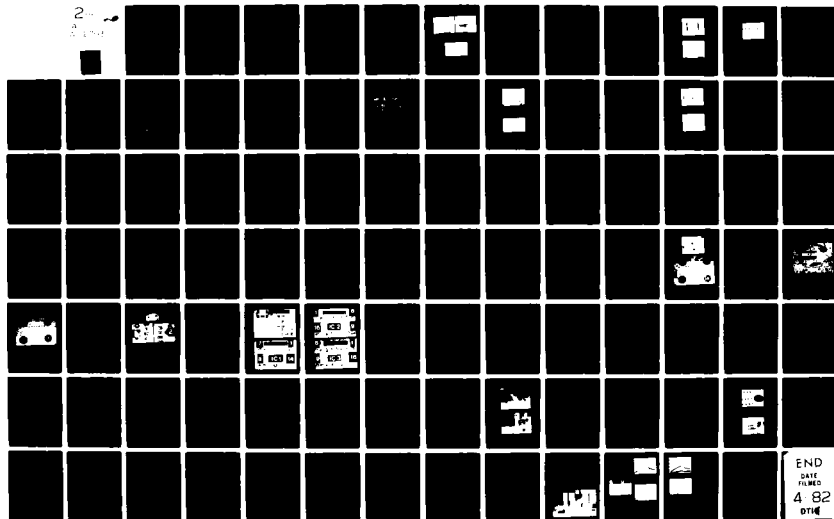
F/G 14/5

F04606-80-C-1338

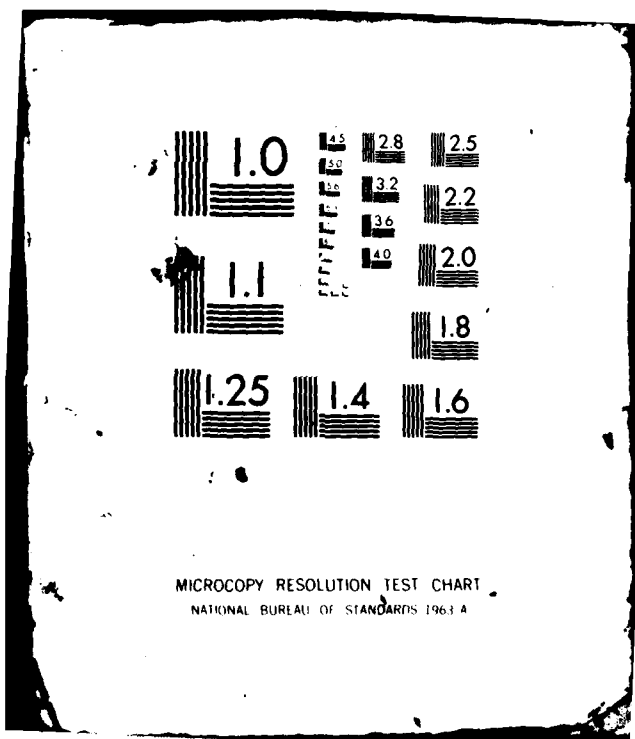
NL

UNCLASSIFIED

2-
1-1



END
DATE
FILMED
4 82
DTIC



- 1-11 Normal but less shiny, dull at tip
- 1-12 Heel lifted 50%
- 1-13 Normal, shiny
- 1-14 Toe lifted 40%

- 2-8 Heel lifted 75%; insufficient solder, weak toe
- 2-9 Normal but rough
- 2-10 Heel lifted 50%; toe-half intact
- 2-11 Normal but dull
- 2-12 Light solder and dull
- 2-13 Normal; very shiny
- 2-14 Insufficient solder; attached at center 1/3 only; heel and toe are off pad

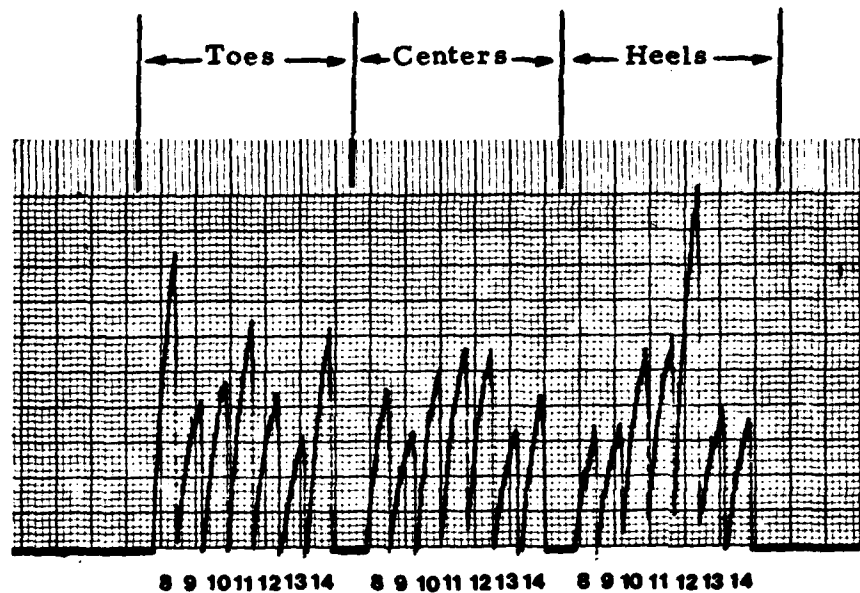
- 3-8 Normal
- 3-9 Heel lifted 25%
- 3-10 Normal but rough
- 3-11 Toe lifted 40%
- 3-12 Excess solder; dull
- 3-13 Heel lifted 30%
- 3-14 Normal.

For the moment, we confine our attention to IC 1. In Figure 43 we see a series of scans along three axes perpendicular to the lead lengths on this IC. These axes are, respectively, in the toe-side one-third of the lead length, across the centers of the leads, and in the heel-side one third. Figure 43 also reviews the visible descriptions of the joints as seen via microscope.

In these descriptions, we notice that Pins 9 and 13 are the only normal ones. We notice, also, that in each group of seven thermal signatures, Nos. 9 and 13 are among the lowest.

The central peak in each group, No. 11, is from a joint which was intended to be good but which turned out to be streaky and rough. The height of its peak is somewhat variable from group to group.

In the three sets of data, the peaks for dull joint No. 10 fall between those of Nos. 9 and 11 although we had expected them to be higher.



| Pin No. | Visual Properties |
|---------|---------------------------------|
| 8 | Heavy solder, toe lifted 30% |
| 9 | Normal, shiny |
| 10 | Light solder, dull |
| 11 | Normal, less shiny, dull at tip |
| 12 | Heel lifted 50% |
| 13 | Normal, shiny |
| 14 | Toe lifted 40%. |

Figure 43. Scans across the toes, centers and heels of Pins 8 through 14 on IC 1 of Board 8B.

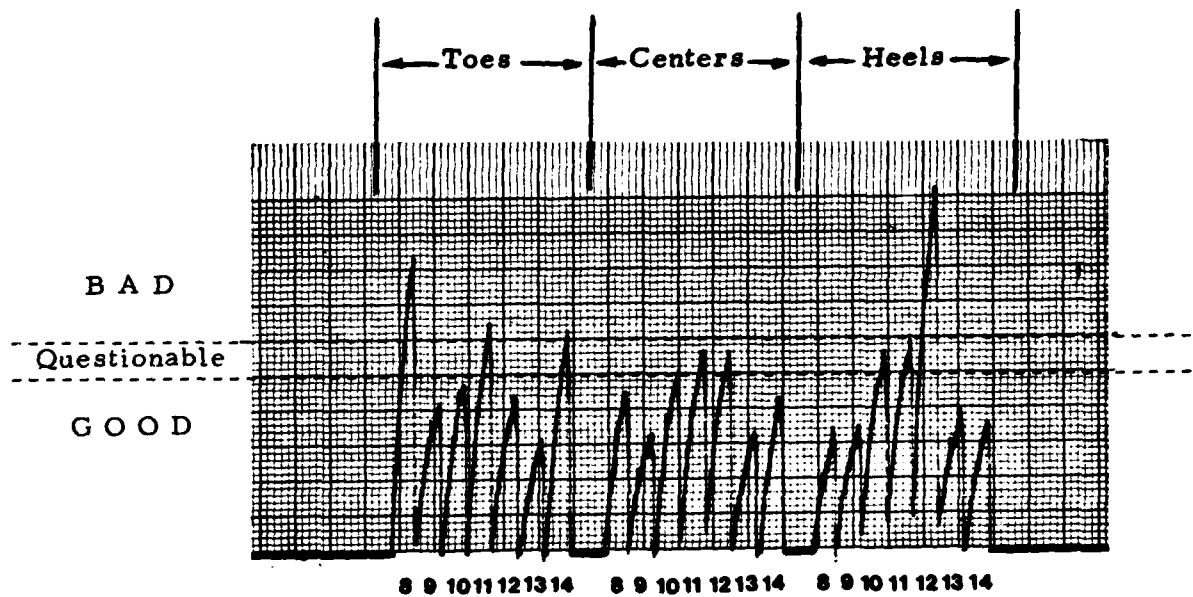
In the scan across the toes, the lifted toes Nos. 8 and 14 are clearly in evidence. In the scan across the heels, the presence of lifted heel No. 12 is obvious.

We conclude, from these tests, that the characteristics of the thermal signatures are very close to what would be expected on the basis of the visual examination of the targets.

The next question concerns the matter of where to place the threshold so that a computer might automatically separate the good and bad joints.

What we recommend, in this regard, is that the good and bad joints be separated by a band which is designated "questionable" so that the human inspector may use his own judgment about their quality. Therefore, we have added such a band to Figure 43 and this is shown in Figure 44. Because of the triple scan, in this case, we may think of each joint as being divided into three areas such that each area, of itself, may be either good or bad. In Figure 44, we see that Joint No. 8 has one bad area and two good ones; No. 11 is questionable in all three areas, and so forth. In the scan across the centers, three of the central areas are questionable and four of them are good. All lifted heels and toes are either questionable or bad.

In this particular test series, we conclude that we have separated the good joint areas from the bad or doubtful ones with 100% accuracy.



| Pin No. | Visual Properties |
|---------|---------------------------------|
| 8 | Heavy solder, toe lifted 30% |
| 9 | Normal, shiny |
| 10 | Light solder, dull |
| 11 | Normal, less shiny, dull at tip |
| 12 | Heel lifted 50% |
| 13 | Normal, shiny |
| 14 | Toe lifted 40%. |

Figure 44. A "questionable" band entered on the trace of Figure 43 separates various solder-joint sections into various levels of quality.

3.4.6.7 Board 8B, ICs 2, 3 and 4

We have discussed in some detail the results on IC 1 of this board, and we will proceed more quickly through the next three ICs. Thereafter, we will present the data of other tests in more abbreviated form.

We stress the fact that solder joint defects come in a variety of sizes, shapes and natures. In some cases, two inspectors will not agree as to whether a certain joint needs to be "touched up" or not and, as we have learned in our tests, there are times when the laser/thermal system does not "agree" with a human judgment.

An interesting example of this is given by the joints shown in Figures 45 and 46. Both are examples of heel cracks, and we expected to find high thermal peaks when both were probed at the heel section. Although the first one, No. 2-8, did behave as expected, we were unable to obtain any unusual signature for No. 2-10 on repeated attempts. This included targeting the center of the lifted heel and "walking" the beam spot in various directions in 0.002" increments to eliminate any possible aiming errors.

Typical data are shown in Figure 47, where the first and third peaks show the "high" and "low" values which were obtained.

Here we have a case where the laser/thermal system firmly refuses to reject a joint which looks questionable to the eye. After much deliberation, we had to agree that the toe-half is well immersed in solder which is smooth and shiny and that there is a good thermal pathway from the lifted heel to the solid part of the joint. Therefore, we must bow to the judgment of the automatic



Figure 45. Board 8B, IC 2, Pin 8. A severely cracked joint, poorly attached toe, insufficient solder.



Figure 46. Same but Pin 10. Heel crack but well attached toe and ample solder.

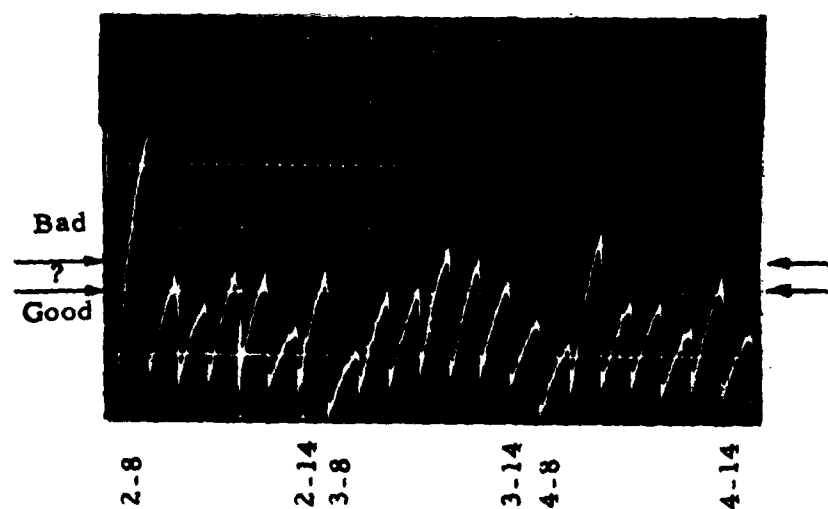


Figure 47. Pins 8 through 14 on ICs 2, 3 and 4. Scan was across central areas of pins, slightly toward toe half.

system and must concede that human judgment was in error in declaring this joint to be defective. Impartial inspectors would possibly agree that the 50% heel detachment is of little consequence in this case.

Regarding the other joints represented in Figure 47, the question, as always, is where to place a dividing line or band in order to separate the "good" and "bad" thermal peaks with full reliability. The success with which this can be done depends upon the effectiveness of human judgment in deciding, by use of visual inspection, which joints are good and which are bad.

We point out that the scan of Figure 47 was carried out across the center regions of the joints, somewhat toward the toe side. A round laser beam spot was used and, as will be discussed shortly, such a scan is not effective in detecting defects which are limited to the heel or toe regions. This will be taken into account as we assess the accuracy of the test results.

Our visual assessments of the first two sets of Figure 47 targets, for ICs 2 and 3, have been given in the preceding section. For IC 4 we observe:

- 4-8 Normal
- 4-9 Insufficient solder, dull
- 4-10 Normal
- 4-11 Heel lifted 25%; insufficient solder, dull
- 4-12 Normal
- 4-13 Toe lifted 30%
- 4-14 Normal.

In glancing at the oscillogram, we note that all peaks for "normal" joints fall within, or not far above, the two lowest divisions on the scale. These are Joints Nos.: 2-9, 11, 13
 3-8, 10, 14
 4-8, 10, 12, 14.

There is some height variation among them because of surface quality variations, being largely a matter of shininess vs. slight cloudiness.

If we establish a threshold at the level shown by the upper arrows in Figure 47, there are four peaks which rise above it.

They correspond to

- 2-8 75% heel crack
- 3-11 Toe lifted 40%
- 3-12 Dull appearance
- 4-9 Cold joint with insufficient solder.

These joints can definitely be classified as defective.

We can also set a lower threshold, shown by the lower arrows in the figure, so that a "questionable" band is established between the thresholds. The joints falling into this band are:

- 2-9 Normal but rough
- 2-11 Normal but dull
- 2-12 Light solder, dull
- 2-14 Solder at center only; heel and toe lifted
- 3-10 Normal but rough
- 3-13 Heel lifted 30%
- 4-13 Toe lifted 30%.

Of these, there are three that we would have preferred to fall into the "defective" category. These are 2-14, 3-13 and 4-13. The reason that they were not rejected is that our present testing method confines itself to the center of the joint and is not sensitive to heels and toes which are one-third detached. As we shall see later in Figure 49, these defects can indeed be found if each joint is scanned in three sections.

The other four joints in the questionable category have non-shiny areas, including joints which otherwise appear normal, and these should be checked by an inspector.

Up to this point, we must claim that laser/thermal testing has identified truly defective joints and has pointed out joints having suspicious properties. The key to this success, of course, lies in our knowing where to set the thresholds, as in Figure 47.

We come now, however, to the first "error" which the system has made, and we attribute it to a positioning error during programming rather than to a faulty threshold selection. The error concerns Joint No. 4-11 which we had visually classified as being dull with insufficient solder and having a heel crack. It is adjoined by good joints but, in Figure 47, its thermal peak was not higher than its neighbors.

This joint and its neighbors are seen in Figure 48, which includes an oscillogram showing the results of a repeated trial on the three samples. This time, with more careful positioning, the faulty joint is clearly identifiable by its higher thermal peak.

We can offer no explanation as to the cause or nature of the positioning error in the earlier trial.

Returning to an earlier matter, we will discuss Joints 2-14, 3-13 and 4-13 which tested as "questionable" at their centers while having lifted heels and/or toes. Figure 49 presents both an oscillographed scan and a separate chart-recorded scan of the three joints in question, along with three normal joints. The two scans were made under slightly different aiming conditions. For each defective joint, its normal neighbor was used for reference.

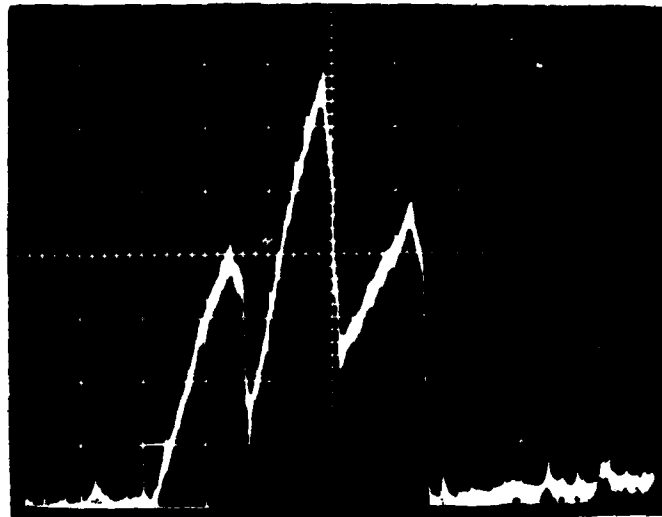


Figure 48. A defective lap joint (center) adjoined by two good ones. (Left to right: Joints 4-10, 11 and 12 on Board 8B.)

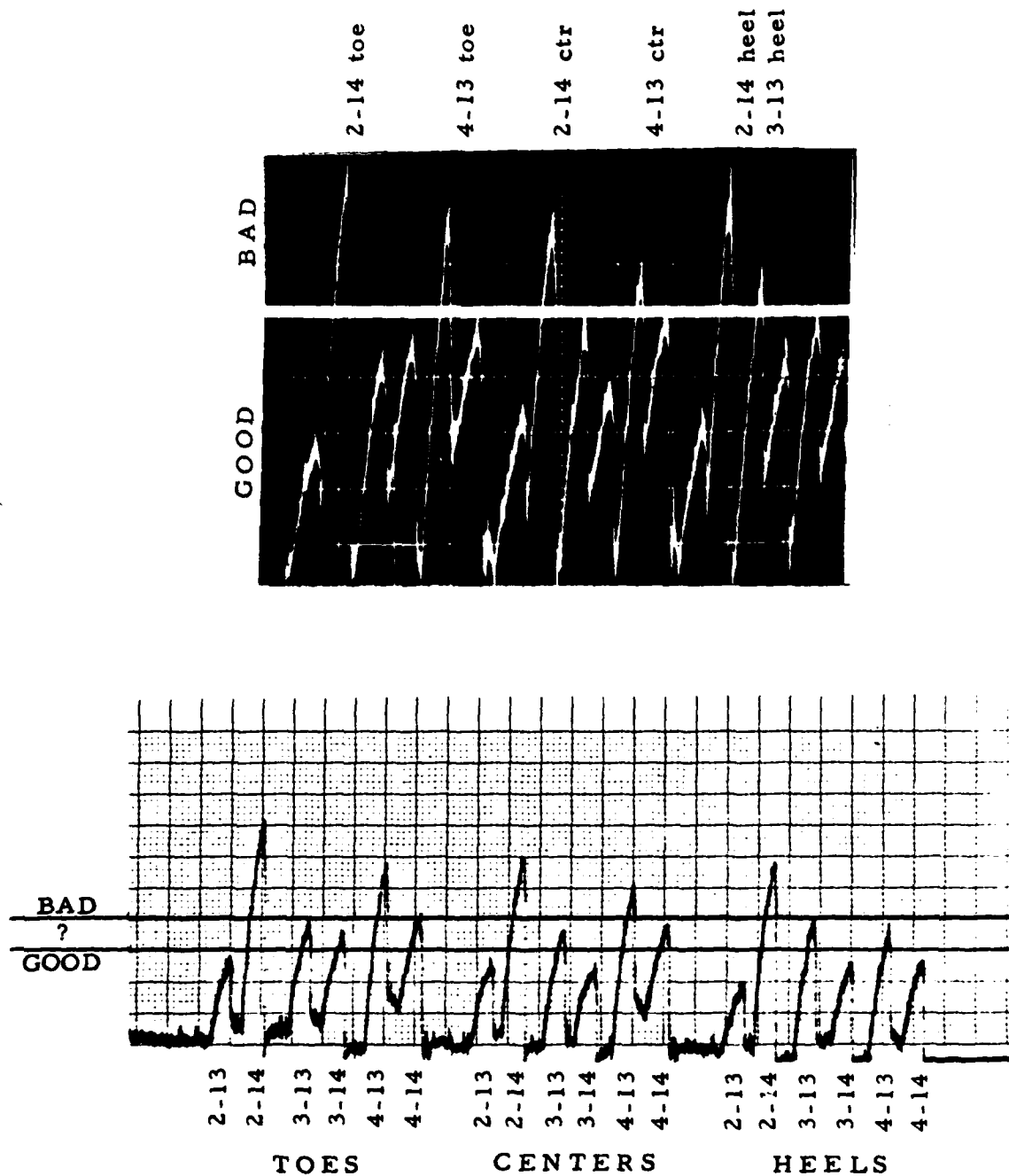


Figure 49. Two different scans of three sections on each of six joints.

In both scans, the sequence of joints was:

2-13 Normal
2-14 Heel and toe lifted
3-13 Heel lifted
3-14 Normal
4-13 Toe lifted
4-14 Normal.

In each trace, the first six signatures represent a scan across the toes. The second and third groups of six result from scans across the centers and heels, respectively.

On the oscillogram, we have placed a white bar which separates the "bad" from the "good" thermal peaks with perfect effectiveness. In this case, not only do the heel and toe of 2-14 show up as defects but the center does as well. The lifted heel of 3-13 is apparent although, being somewhat shiny, its peak is only slightly above the divider. The lifted toe of 4-13 is prominent and even its center is designated as defective. All peaks below these are associated with normal sections of joints, although there is considerable variability because of local irregularities in surface quality.

Arbitrarily, instead of a single dividing line, we have placed a "questionable" band on the strip chart of Figure 49. This time, because of slightly different aiming, only five of the above six peaks show up as rejects and the one for the lifted heel of 3-13 is in the "questionable" band. Also in this band are several of the irregular parts of the normal joints.

In this case, the failure of 3-13 to be classified as defective is a matter of where the upper threshold was arbitrarily placed. Had it been lower, 3-13 would become rejected rather

than questionable, but so also would several supposedly good joints which contained blemishes of one sort or another.

The question must now be raised as to whether such blemishes are grounds for rejection of an otherwise good joint. If not, then their rejection during laser/thermal testing must be recognized as a deficiency of the method, which most likely arises from the non-uniformity of the laser beam. We have indicated frequently that the central hot spot makes the method highly sensitive to tiny defects. In a separate effort late in Phase 2.2, we have succeeded in homogenizing the beam and we are confident that this will eliminate such problems in future testing.

In summary of our test results so far in this report, we can state the following: regarding ICs 1 through 4, if we overlook any problems which arise from the laser-beam hot spot, then the only error made in the tests was the failure to identify Joint 4-11 as faulty on the first try.

3.4.6.8 Board 8B, ICs 5 and 6

The only significant features among the joints on these ICs are:

- 5-10 Tarnish
- 5-11 Light solder
- 6-11 Lifted toe.

No. 6-9 was intended to have a lifted center, but the center was plugged with solder and behaved as a normal joint. Nos. 5-9, 5-13 and 6-13 were prepared as "heel only" joints, with the toe halves missing, but these did not show any unusual signatures. All other joints on these ICs were standard, with normal variations

among them in surface texture, solder mass and so forth.

The data for these and the earlier ICs are shown as chart recordings in Figure 50. Each group of seven peaks represents Joints Nos. 8 through 14 on a particular IC. On ICs 5 and 6, the peaks for the first two joints listed above stand out clearly above their neighbors. In the toe scan, the lifted toe of 6-11 is evident.

Some of the "peaks" are so low as to be indiscernible; hence, some ICs appear to have only five or six joints.

3.4.6.9 Board 8B, ICs 7 through 12

Of these ICs, the first four were prepared with 14 solder joints and the last two with seven. All of the joints in the group are characterized by much rougher and duller surfaces than in the previous groups and so the thermal peaks are much higher, including the "normal" ones which are often dull or tarnished.

In the interest of brevity, we will not deal at length with the individual defects and their thermal signatures but will discuss them generally.

Most of the joints in this group are intentionally defective; very few good ones are included. As an example, we will list the 14 joints for IC No. 7:

- 7-1: heel lifted 40%, light solder
- 7-2: tarnished tip-half
- 7-3: heel lifted 50%, light solder
- 7-4: light solder, burned
- 7-5: light solder
- 7-6: residual solder flux
- 7-7: lifted, residual flux

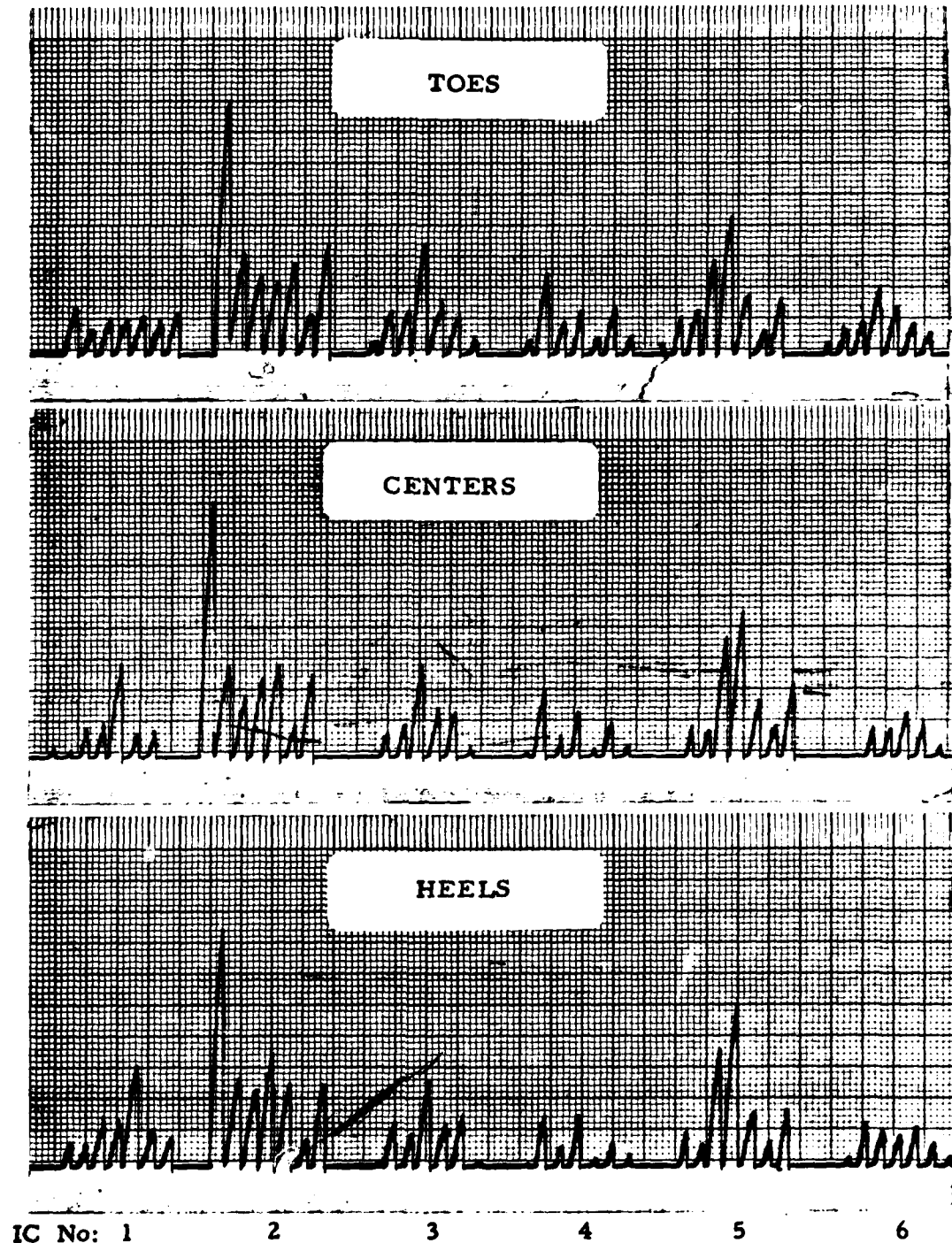


Figure 50. Thermal scans across the toes, centers and heels of ICs 1 through 6 on Board 8B.

7-8: burned
7-9: lead twisted and burned
7-10: burned
7-11: heel lifted 50%
7-12: heel lifted 40%
7-13: toe lifted 25%
7-14: light solder.

We note that IC 7 contains no joints which are classified as acceptable. In fact, the only good joints on this section of the board are:

8-2
8-5
9-2
11-11.

In addition, 9-11 has a 20% lifted toe but is otherwise normal and so we treat it as a good joint.

The joints were scanned at their centers with the round laser beam spot, and so we will evaluate our results based only on the conditions of the joints at the centers. That is, short lifted heels and toes are excluded from consideration, although longer ones (50% or more) are not.

Figure 51 presents the thermal data on these 70 samples. We have indicated a dividing line which separates the five good joints from the bad and questionable ones, and we point out the effectiveness with which laser/thermal testing has distinguished between them. One might arbitrarily add another line three or four major divisions higher than the first one in order to separate definite rejects from questionable joints. The exact location of this line would depend upon an individualistic judgment as to which joints qualified for rework.

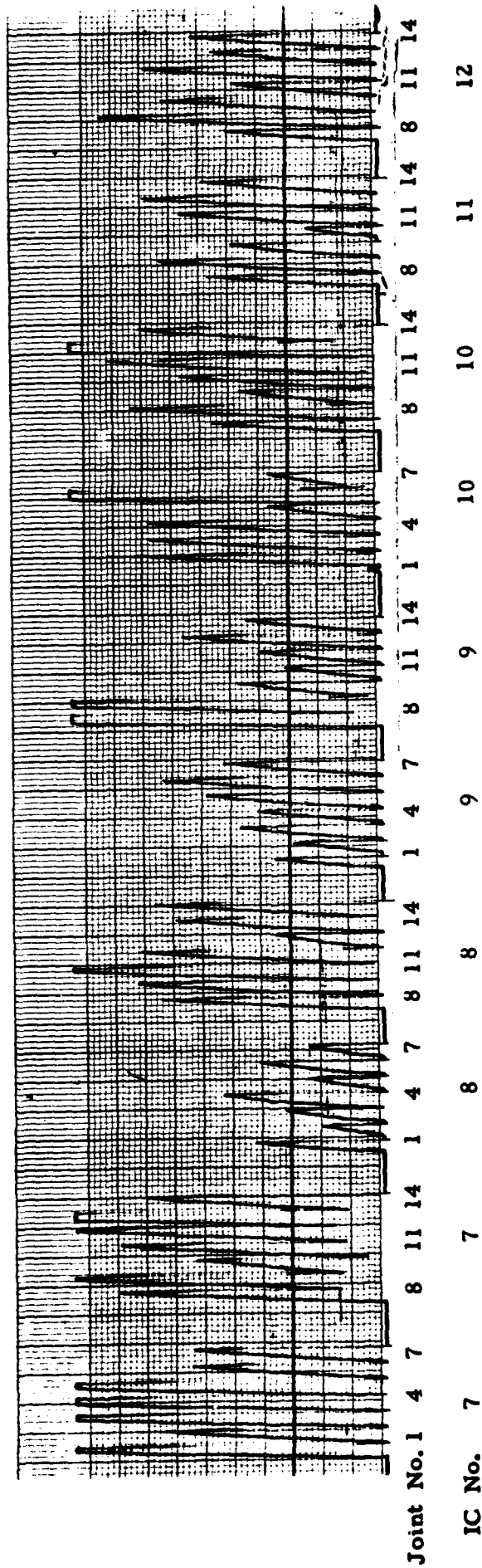


Figure 51. Thermal scans across the centers of Joints 7-1 through 12-14 on Board 8B. Dividing line separates good joints from questionable and bad ones.

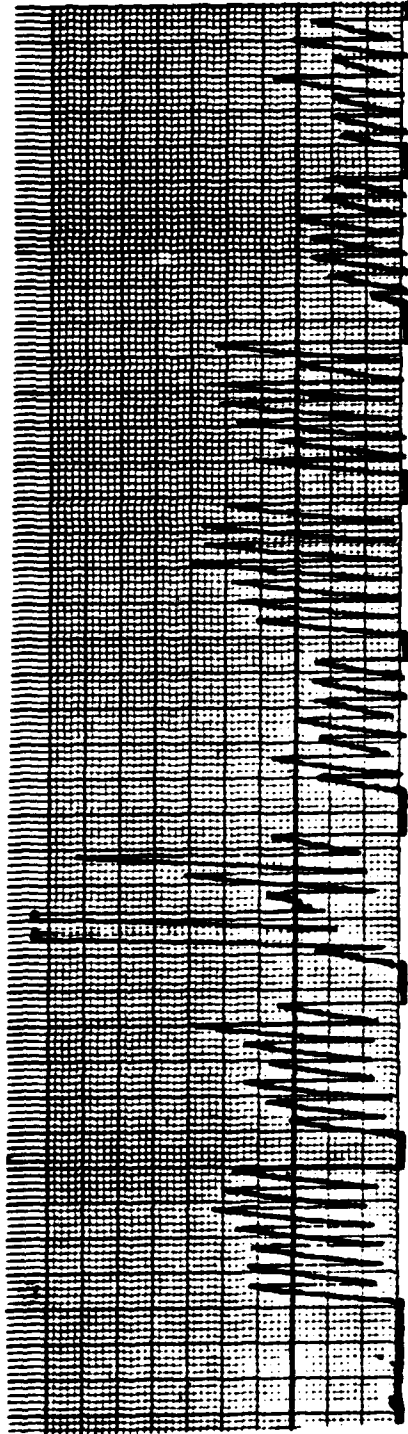
Our attention is called to the very small peak for Joint 10-1. This is an "exposed gold" or "yellow flat top" lead with solder only at the tip one-third. Another dividing line could be placed just above it to mark it as a defect by separating it from the good joints. However, this is one of a few joints which not only had exposed gold but which were attached only at the tips and not in the centers. It should, therefore, have been rejected by having too high a thermal peak instead of too low. We therefore have to consider this a shortcoming of the laser/thermal method; that is, the reliability of detection of a crack or lifted lead is diminished when the target area is predominantly of exposed gold. (Later, we shall point out the low probability of two types of defect occurring on the same lead.)

On the other hand, the other lifted, exposed-gold leads in this series (Nos. 8-4 and 9-7) were indeed characterized by high thermal peaks. In one case this was due to tarnish on the gold. In the other, it may have been due to laser-beam "spillover" onto a nearby solder area.

3.4.6.10 Board 8

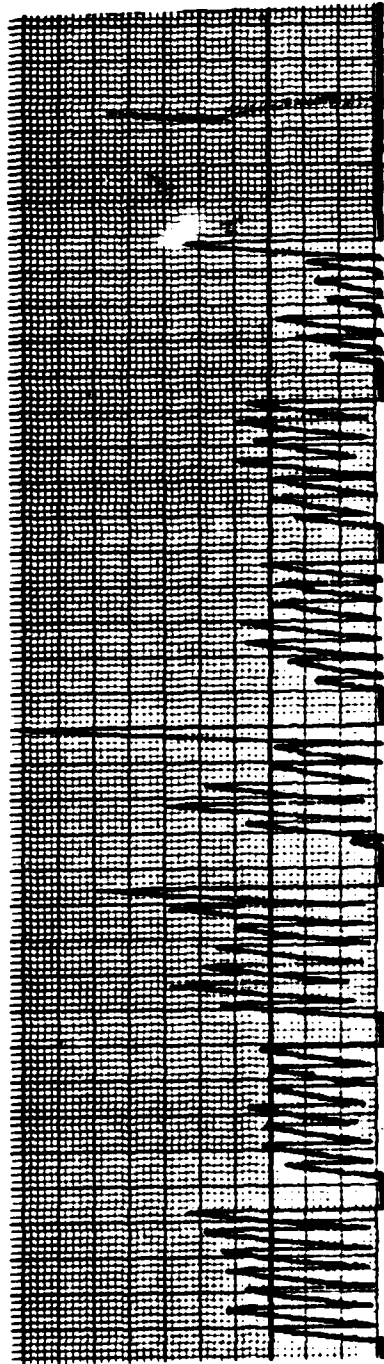
This board holds 11 ICs, seven of which have seven solder joints each and four of which have 14, for a total of 105 samples. By comparison with Board 8B, this board contains a higher proportion of good samples.

Figure 52 presents thermal data on the centers of the 105 joints, again ignoring their conditions at the tips or heels.



Joint No: 8 14 8 14 8 14 8 14 8 14 8 14 1 7 8 14

| | | | | | | | | | |
|--|--------|---|---|---|---|---|---|---|---|
| | IC No: | 1 | 2 | 3 | 4 | 5 | 6 | 7 | 7 |
|--|--------|---|---|---|---|---|---|---|---|



| | | | | | | | |
|-------------|-----|------|-----|------|-----|------|----|
| Joint No. 1 | 7 8 | 14 1 | 7 8 | 14 1 | 7 8 | 14 8 | 14 |
|-------------|-----|------|-----|------|-----|------|----|

| IC No: | 8 | 8 | 9 | 9 | 10 | 11 |
|--------|---|---|---|---|----|----|
| | | | | | | |

Figure 52. Thermal signatures of Joints 1-8 through 11-14 on Board 8.

As before, we have arbitrarily entered a dividing line at the top of the third major division. Our procedure, then, was to examine all joints via microscope in order to find if it was generally true that the signatures of the good ones fell below the line, and so forth.

If we were to place a second line on the chart, three divisions down from the top, we would observe five thermal peaks to stand out above the rest:

3-9
3-10
3-11
9-7
9-14,

all leads of which are completely separated from their pads. Figure 53 shows the row which contains the first three of the above joints. We notice that 3-12 appears detached also, and this was verified by stereomicroscope. Its thermal peak falls short of the others because the lifted lead is shinier, but the peak is nonetheless above the lower line and in what we can call the questionable region.

We then visually examined the joints whose peaks fell in the "good" zone of the chart, starting with 3-8. There were 42 such joints and our visual assessment of their qualities agreed with the test data in 38 cases and disagreed in four cases, the latter being:

4-11 and 4-13: These have light solder and are dull. Their peaks should have been higher. The leads are off center and the shiny pad beneath may have been in the target area.

7-9: Light solder but shiny.

11-8: Heel lifted 80% but shiny.

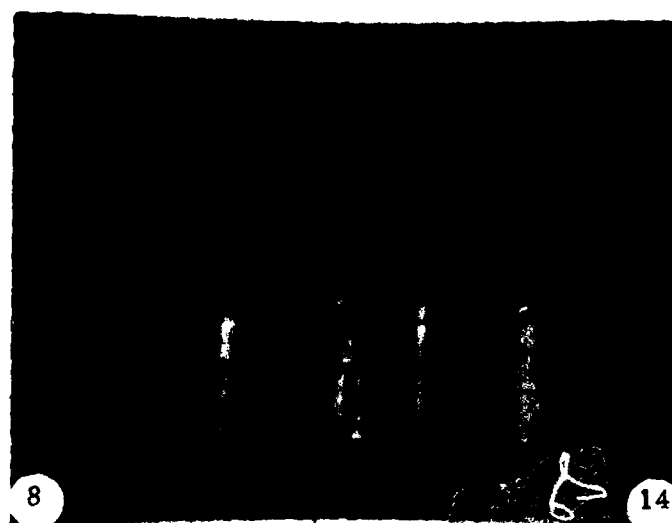


Figure 53. Joints 3-8 through 14 on Board 8.

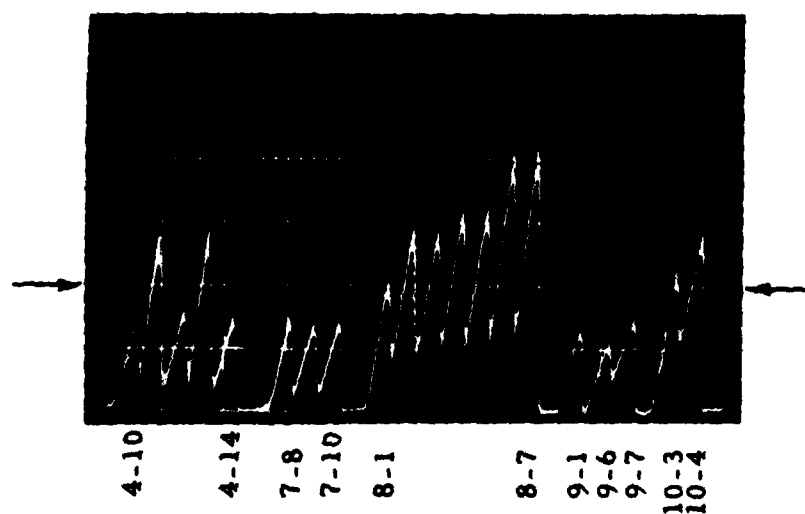


Figure 54. A second pass over some of the joints represented in Figure 52.

As will be shown shortly, the first two "errors" were due to faulty positioning and were corrected on a repeated pass. The second two are admittedly due to a shortcoming of the laser/thermal method, of the same type which we have seen previously at a lifted lead with exposed gold. Although light solder and lifted leads are ordinarily detected easily via their high signatures, any unusual shininess tends to "pull" the signatures down to where the defect evades detection.

What is important is the question of how often the system might make such an error in actual practice. This is difficult to predict but, at least, there is some available information which might help us guess as to a reasonable answer.

A major computer manufacturer with whom we are collaborating indicates that in manufactured PCBs, one solder joint out of a thousand, on the average, is defective. The defect may be any of several types such as a cold joint, insufficient solder, and so forth. Let us say that we are interested in PCBs with lap joints, and that the defect may take the form of a heel crack, a lifted lead, insufficient solder being unusually shiny, and perhaps three other types, all occurring with equal frequency. This means that one joint per thousand may have some kind of defect and, out of these, only one in six may be a lifted lead, indicating an occurrence rate of one per six thousand for a lifted lead.

Using these same probabilities, we might predict that one joint in 6,000 will have a tinned, shiny appearance due to insufficient solder.

The probability that both of these defects would occur at the same joint is the product of the individual probabilities, that is, one chance in 36 million.

These statistics are, of course, speculative and their actual values must await the outcome of broad field experience with the system, after millions of joints have been tested. However, even if the chance of a system error-detection failure is as high as one in five million or one in one million, this is still competitive with the human operator, who is also known to miss an occasional defect, according to another major computer manufacturer with whom we communicate.

Considering the fact that laser/thermal testing can reveal hidden defects which the human inspector has no chance of identifying, then this should more than compensate for an occasional detection-failure which might occur with laser/thermal testing.

Regarding the two "light solder" defects which were missed on the chart recording, these were easily revealed when they were positioned more exactly in the target area. They are the first two high peaks seen in Figure 54, rising above their neighboring peaks which are for good joints. Figure 55 is a view of the two defective joints and their three good neighbors. The fact that the defects were not apparent at first is laid to the use of too small a laser-beam spot.

In Figure 54, the second set of thermal signatures shows another attempt at revealing Joint 7-9 which was mentioned above as having light solder but being shiny. The attempt was not

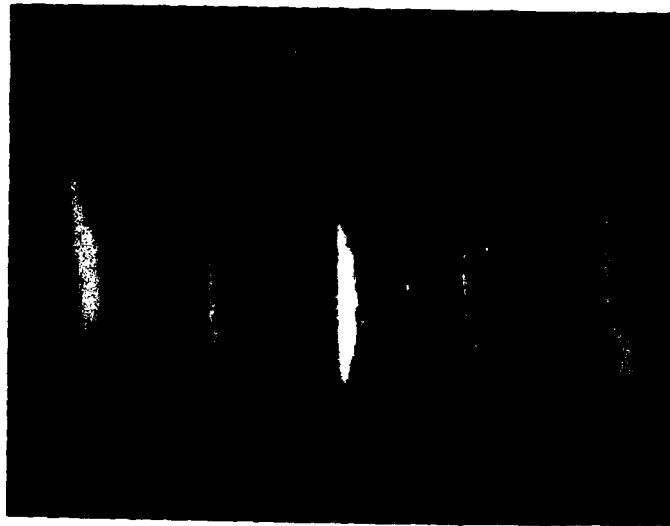


Figure 55. Joints 4-10 through 4-14 on Board 8.

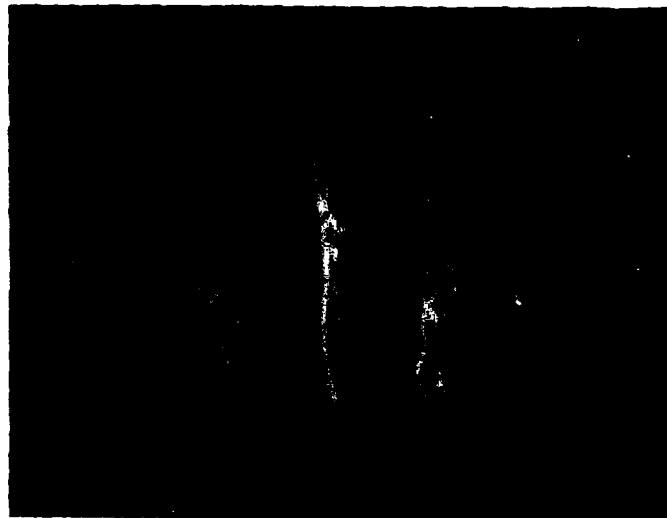


Figure 56. Joints 11-8 through 11-14 on Board 8.

successful and verifies the difficulty of defect detection when highly reflective surfaces are present.

The other peaks in Figure 54 will be discussed presently.

Having evaluated the peaks below the line in Figure 52, we turned our attention to those above the line, our hope being to verify that these were all either bad or questionable.

In most cases this was true, but there were a few exceptions. Nos. 3-11 and 3-14 were intended as good joints but contained small blemishes which placed their peaks just above the dividing line. This is not regarded as an error by our testing method, for these joints should at least be checked by an operator.

The next unexpected result, which turned out not to be an error after all, concerned IC No. 8. Its joints 1 through 7 were intended to be identically good, but the first thermal peak was at the dividing line and the others were above. The third set of signatures in Figure 54 shows the result of another pass over 8-1 through 8-7. In this figure, if we placed the dividing line at the second line above the baseline, it is seen that the seven signatures are nearly identical to their counterparts in Figure 52. This perplexing result brought about a closer microscopic examination of these joints, whereupon it was revealed that this IC had been used in earlier tests on conformal coatings. The coating, in this case, had not been completely removed, thus enhancing all thermal peaks. A faint trace of the residual coating on the other side of this IC is responsible for the somewhat high peaks for the 8-8 through 8-14, which were also intended as good joints.

Proceeding to IC No. 10 which adjoins No. 8, this was likewise intended as an "all good" set of joints. Again, in Figure 52, some of its peaks are above the divider, and traces of residual coating in the IC No. 10 area are held responsible for this.

On IC No. 9, Joints 1 through 7 are all intentionally defective, having lifted leads which are attached at the toes only. All of these show up as defective in Figure 52. Nos. 9-1, 9-6 and 9-7, however, are yellow flat tops as well as being lifted; their peaks were not expected to be as high. We conclude that some laser beam spillover onto the pad helped to raise the peaks above the divider. A more tightly focused, carefully positioned beam spot produces the low signatures expected of yellow flat tops. They are seen as the next to the last set of peaks in Figure 54 where they are below the divider. Because the leads are detached, the peaks are higher than for ordinary exposed-gold joints.

The last two peaks in Figure 54 verify the enhanced signatures of 10-3 and 10-4 due to residual conformal coating.

To summarize our results on Board No. 8, we found three types of lap-joint defect which were not revealed by laser/thermal testing:

- Lifted leads which are shiny
- Insufficient solder but shiny
- Insufficient solder but decentered.

The last type of error can perhaps be corrected by use of a larger and homogeneous beam spot, possibly elongated to provide more complete coverage of the pad area.

The total number of "missed defects" in Figure 52 is four out of 105. We attach no significance to this number as an actual score. The number resulted by chance as being the number of undetectable-defect samples which we happened to prepare on Board 8. Had there been more or fewer, our "score" would have been poorer or better. What is important is the question of how often such defects occur in the field.

We emphasize that, except for the effects of residual conformal coatings on "good" joints, all peaks above the divider in Figure 52 did indeed represent defective or questionable joints. These included lifted leads or sections of leads, insufficient solder, granular and uneven surfaces and tarnish due to overheating.

The leftmost joint in Figure 56, No. 11-8, holds the 80% lifted heel which was missed, its shininess being the reason. At the far right, No. 11-14 is a similar joint but with "cold solder", giving a relatively high peak (the last one in Figure 52). In between is an assortment of joints which gave low thermal peaks, including the second and the next to last joints which are well attached for about half their lengths.

3.4.7 Test Results on Through-hole Joints

We have dealt in considerable detail with the tests on lap joints, comprising only two of the nine boards that were tested. Our purpose was to give the reader some insight into our testing procedure and into the way we evaluated our test results. Hopefully having made these points clear, we can proceed more quickly

through the remaining data, in which we will give the results with a minimum of explanation.

The feed-through-joint data were recorded on strip charts. In some cases, several passes were made over the same board, with slightly different beam-spot positioning. The charts, which are normally rolled up, were then laid out flat and secured on mounting boards for ready evaluation. Several square feet of chart area resulted, with a small portion of it being shown in Figure 57.

In the figure, the three lower traces represent three passes over Board 1, which is comprised mostly of good joints, while the upper trace is from Board 2, having some defects. Straight lines have been drawn under some of the traces on the charts. These represent the "baseline" for each group of thermal peaks and are used to accommodate some drift in the detector reference level which shifts with slight changes in room temperature. (In the final system, the drift will be compensated for electronically.)

When the heights of various thermal peaks are to be compared with each other, the height measurement is made from the baseline, rather than from the bottom of the chart.

Each numbered group of eight joints represents one column on the board. On some boards, columns having fewer joints appear because smaller ICs were used.

We point out that the different boards were tested on different days. Over a period of time, there is a gradual decline in laser beam power until the lamps are replaced.

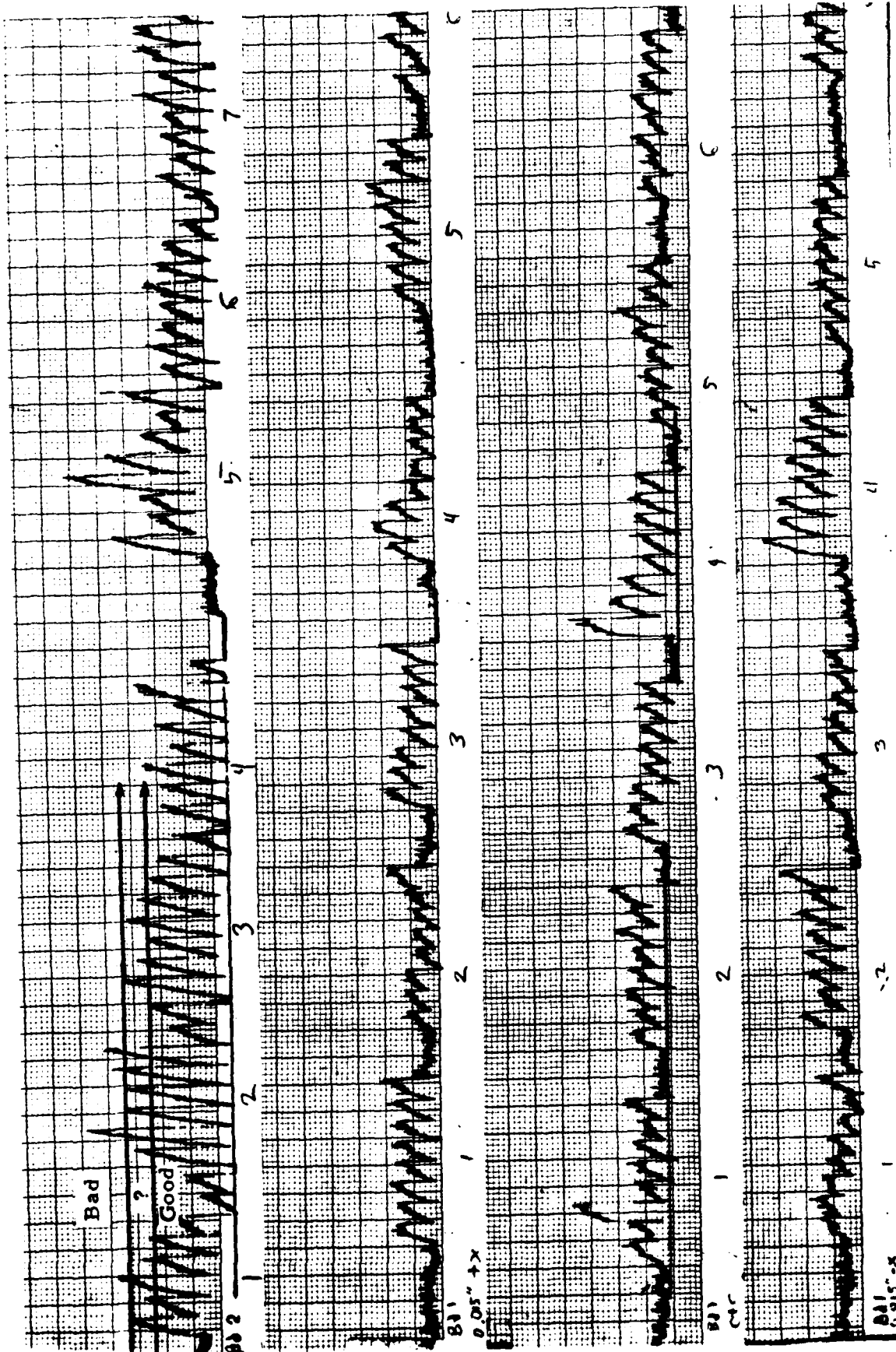


Figure 57. Appearance of the recorded data during testing of feed-through joints. Lower three strips represent relatively good joints on Board No. 1. Upper trace is from joints of mixed quality on Board No. 2.

The final system will be equipped with a beam power monitor so that the computer may take account of power fluctuations. We do not yet have such a system in operation and so this is done "manually".

The consequence of the power fluctuations is that good joints on a given board will have different thermal peak heights from those tested on another day. Therefore, a normal threshold cannot be established for all boards. Instead, it is established board by board, and this is done by correlating the heights of the lower peaks with the visible qualities of the better joints on that board.

3.4.7.1 Board 1

Board 1 contains 16 columns of eight joints each and is intended as a reference board having all good joints. Being hand made, the joints were subject to some variability in the form of scattered pinholes, depressions, residual solder flux and so forth.

Three passes were made over the 128 joints. In the first pass, the beam spot was at the geometrical center of each joint. In the other passes, the beam spot was 0.015" to one side or the other of center in such a direction as to place it closer to or farther from the emerging pin. The pins in alternate columns were clinched in opposite directions, and the laser beam was directed toward the joint from such a direction that the clinching angle did not matter.

Chart data for the first six columns (three ICs) appear in the lower three traces of Figure 57. If we place a dividing line at 2.0 divisions above the thermal baseline (which varies from one IC to another), then a few thermal peaks rise above it and, by microscope, these have all been verified as representing unintentional blemishes. These include scratches, foreign matter, cavities, residual solder flux, and so forth, which are distributed over the eight ICs on the board.

Among the higher peaks in the "good" category are represented joints with less solder than others but otherwise good.

On Board 1, we score our tests as 100% effective in separating what we judge, visually, to be good joints from those which should be questioned.

3.4.7.2 Board 2

This board was tested with somewhat higher laser beam power and the resulting thermal peaks are higher, on the average, than those for Board 1, as is seen in Figure 57. To some extent, the higher proportion of defects on Board 2 contributes to the higher average.

Board 2 contains a selection of normal joints and a variety of defects of varying severity. These include shallow fillets or concavities, some having deep pits, foreign matter or dull surfaces. Those defects which are of average severity comprise a group which we must label as "questionable" because opinions might differ as to whether re-work is in order. An example

would be a well-mounded, smooth solder mass which appeared normal but which had a slight cloudiness and was not as shiny as other normal joints. Another would be a shiny normal joint having a slight tool-mark from the soldering iron.

Optimal differentiation into "good", "questionable" and "bad" categories is best done by placing dividers at three and at four major divisions, respectively, above the thermal baseline on the chart, as is indicated in Figure 57.

We can then tabulate the joints, listing them by column number and pin number and can then decide whether the laser/thermal information agrees with the visual assessment of the joint.

Table 4 illustrates how this was done for the first ten columns on Board 2. The scores indicate the state of agreement between the human judgment and the thermal data, using the thresholds that were selected.

Of the 78 joints tested, there were 69 "correct answers", seven cases where thermal testing was more critical than human judgment, and two cases where it was less critical by designating as questionable a joint which the human found to be bad. In no case did the system identify a "bad" joint as "good".

In the case of the two "X's" in Table 4, the first of these occurred when a small, deep cavity was obstructed by a pin which was inadvertently clinched in the wrong direction. The cavity was deep enough to qualify the joint as bad, and the detection failure should probably be regarded as an operator error rather than a system error.

TABLE 4. METHOD OF SCORING THE DATA ON BOARD 2, COLUMNS 1 - 10.

| Joint No. | Visual Assessment | Laser/thermal Assessment | Score | Joint No. | Visual Assessment | Laser/thermal Assessment | Score |
|-----------|-------------------|--------------------------|-------|-----------|-------------------|--------------------------|-------|
| 1-1 | Quest. | Quest. | C | 6-1 | Good | Good | C |
| 2 | Good | Quest. | S | 2 | Good | Good | C |
| 3 | Bad | Bad | C | 3 | Good | Good | C |
| 4 | Quest. | Quest. | C | 4 | Good | Good | C |
| 5 | Quest. | Quest. | C | 5 | Good | Good | C |
| 6 | Good | Good | C | 6 | Good | Good | C |
| 7 | Good | Good | C | 7 | Good | Good | C |
| 8 | Good | Good | C | 8 | Good | Good | C |
| 2-1 | Bad | Quest. | X | 7-1 | No pin | Not tested | C |
| 2 | Bad | Bad | C | 2 | Good | Good | C |
| 3 | Quest. | Quest. | C | 3 | Good | Good | C |
| 4 | Quest. | Quest. | C | 4 | Good | Good | C |
| 5 | Bad | Bad | C | 5 | Good | Good | C |
| 6 | Bad | Bad | C | 6 | Good | Good | C |
| 7 | Good | Good | C | 7 | Good | Good | C |
| 8 | Good | Good | C | 8 | Good | Good | C |
| 3-1 | Bad | Quest. | X | 8-1 | No pin | Not tested | - |
| 2 | Quest. | Quest. | C | 2 | Good | Good | C |
| 3 | Good | Good | C | 3 | Good | Good | C |
| 4 | Quest. | Quest. | C | 4 | Good | Good | C |
| 5 | Quest. | Quest. | C | 5 | Good | Good | C |
| 6 | Good | Good | C | 6 | Good | Good | C |
| 7 | Good | Good | C | 7 | Good | Good | C |
| 8 | Good | Good | C | 8 | Good | Good | C |
| 4-1 | Good | Good | C | 9-1 | Good | Good | C |
| 2 | Good | Good | C | 2 | Good | Good | C |
| 3 | Good | Quest. | S | 3 | Quest. | Bad | S |
| 4 | Good | Good | C | 4 | Good | Good | C |
| 5 | Good | Good | C | 5 | Good | Quest. | S |
| 6 | Good | Good | C | 6 | Bad | Bad | C |
| 7 | Good | Quest. | S | 7 | Good | Good | C |
| 8 | Good | Good | C | 8 | Good | Good | C |
| 5-1 | Quest. | Quest. | C | 10-1 | Good | Good | C |
| 2 | Good | Good | C | 2 | Good | Good | C |
| 3 | Good | Good | C | 3 | Good | Good | C |
| 4 | Bad | Bad | C | 4 | Good | Good | C |
| 5 | Bad | Bad | C | 5 | Bad | Bad | C |
| 6 | Good | Good | C | 6 | Good | Good | C |
| 7 | Good | Good | C | 7 | Good | Quest. | S |
| 8 | Good | Quest. | S | 8 | Good | Good | C |

Scoring Code: C = Correct
 S = System disagrees on safe side
 X = System disagrees in unsafe direction

In the second case, a large, deep cavity was present which, through chance, showed a high-reflecting, smooth surface which prevented the usual light-trapping action and almost escaped human detection as well.

In any case, both defects would have been discovered in the human inspection which was called for when the system placed them in the "questionable" category. Moreover, a slight lowering of the upper threshold in Figure 57 would have placed both joints into the "bad" category, as it would have done with other questionable joints as well.

Alternatively, one might eliminate the upper threshold and the "bad" category and simply call for human inspection of all samples with peaks above the lower line.

Thus far we have dealt with the first ten of 16 columns on Board 2. For the remaining six columns our tabulation resulted in the following scores:

| | |
|---|----|
| System agrees with human judgment . . . | 32 |
| System disagrees on safe side | 13 |
| System disagrees in unsafe direction . | 3. |

The last three disagreements are regarded as true system errors and are most likely due to the fact that the laser beam spot is not yet homogenized. It is thus more sensitive to small defects near the center of the sample than toward the edges. The three defects in question were small, deep pits located off center. Human judgment called these joints "questionable" (not "bad") while they tested as "good". Hopefully, this problem will be eliminated in a later phase of our work.

3.4.7.3 Board 3

This board had a high proportion of cold joints, irregular surfaces, loose leads and various cavities. Relatively few good joints were present, and the overall thermal peak height was greater than for the previous boards.

Departing from the previous procedure of having three categories of joint quality, we will use only two for Board 3. One is called "good" and the other may be called "bad", "questionable", "rejected", or by any suitable name.

In evaluating the thermal data, we used the same 2.5-division threshold as before in order to separate good samples from the others.

There were 124 joints which were tested on this board. As before, they were graded visually and the laser/thermal test results were compared with the visual ratings and were scored. The scoring results are:

| | |
|--------------------------------|-----|
| System agreement | 118 |
| Safe-side disagreement | 4 |
| Unsafe-side disagreement . . . | 2. |

The last two disagreements occurred at joints which were not considered to be well wetted but whose upper surfaces happened to be smooth and shiny, causing low thermal peaks. The manner in which these joints were fabricated is not considered representative of "real world" joints and so these "errors" may be fictitious.

3.4.7.4 Board 4

There are no good joints on this board, merely a handful of questionable ones and the rest bad.

This board was prepared by applying undersized preforms on the component sides of the holes in order to simulate missing or insufficient solder on the solder side. As a result, most of the "joints" appear as bare leads emerging from black cavities which provide very high thermal signals.

At the few questionable joints, some solder did emerge through the hole but was punctuated by pits, cracks, dullness, or marks. We rate all of these as questionable because human inspection would be in order, although the result of that inspection might be to classify some of the joints as acceptable.

Board 4 holds 118 joints, for which the scores were:

System agreement 114

Safe-side disagreement 1

Unsafe-side disagreement . . . 3

Our comments about the last three disagreements are:

| <u>Joint No.</u> | <u>Human rating</u> | <u>System rating</u> | <u>Comments</u> |
|------------------|---------------------|----------------------|--|
| 1-2 | Bad | Good | Operator error. Pin not clinched. Shiny tip deflected laser beam, giving very low thermal peak, same as exposed gold. This type of defect might be detectable if all signatures below bottom threshold are rejected. |

| <u>Joint No.</u> | <u>Human rating</u> | <u>System rating</u> | <u>Comments</u> |
|------------------|---------------------|----------------------|--|
| 2-3 | Bad | Questionable | Same situation as above, but giving a higher signal. |
| 12-7 | Bad | Questionable | This joint is truly borderline. The solder wetting is good but the fillet is depressed and contains a small pit at the center. The human's judgment may be too conservative. |

3.4.7.5 Board 5

This board was fabricated by applying large preforms to the component side and letting the reflowed solder run through to the other side. The defect types were pits, cavities and crevices, among others.

Although 128 joints were prepared, the last one was connected to a massive, heat-sinking land and so its thermal signature could not be compared with the others. Therefore, 127 joints were scored:

System agreement 113

Safe-side disagreement . . . 10

Unsafe-side disagreement . . 4.

Of the safe-side disagreements, two of them involved the system calling a good joint questionable. These could be called "false alarms", in the sense that an operator might unnecessarily be called upon to check them. The other eight were cases of questionable joints being called bad. These should best be checked by the inspector in any event, and so no inconvenience is involved.

Regarding the "false alarm rate" on this particular board, it is not as high as it first appears. Of the 127 joints, 73 were judged by the operator as being either bad or questionable, and two others were called questionable by the system. Thus, of 75 joints which would have to be checked by the inspector, two of them would be checked unnecessarily, or 2.7 percent of those checked. Considering our earlier estimate of one joint per thousand being defective in actual practice, or 0.1 percent, then $2.7\% \times 0.1\%$ or 0.0027% of the total joint population would be false alarms, based on the Board 5 results.

Regarding the four unsafe-side disagreements, all were of a similar nature in which the system rated a joint as good when the human observer called it bad or questionable because of a small pit or crack. The detection failure is again explained as being due to the laser-beam inhomogeneity, with the hot spot falling elsewhere than on the defect.

3.4.7.6 Board 6

This board contains examples of overheated or burned joints where enough heat was applied as to burn the flux or the laminate, causing scattered deposits of charred material to be randomly distributed over the solder surfaces. The result was an assortment of good, questionable, and bad surfaces.

Our scoring of this board resulted in no unsafe-side disagreements. Seven safe-side disagreements occurred, including two in which the good joints, as judged by eye, were called questionable or bad by the system. The disagreements are explained

by the speculation that the laser beam and the eye were not "looking at" exactly the same parts of the solder joints.

The number of joints tested here was 128, so that agreement as to joint quality occurred in 121 cases.

3.4.7.7 Board 7

This board was prepared in the hope that we could provide USAF with results on the statistical testing of subsurface voids. This type of defect had not been specifically listed in the work statement, but we had done some exploratory work early in this program which had been encouraging.

Unfortunately, the preparation of a large number of voids on this board was accompanied by considerable variation in surface quality from one joint to another. The surface variations led to large thermal signature variations which masked most of the effects due to internal structure.

We therefore decided to evaluate the test results on the basis of the visible features of the joints. In so doing, we did discover several sequences of uniformly shiny, well-mounded joints which gave excessively high thermal signatures and these are attributed to known internal voids. Among the other joints (both with and without internal voids), typical surface defects included dull and rough surfaces, various blemishes, solder peaks, and a few crevices which simulated cracks between the solder and the barrel. All of these were detected by laser/thermal testing.

Of 98 joints present on this board, the thermal data yielded

96 agreements and two safe-side disagreements. In both latter cases, the solder joints each contained a small blemish but, being otherwise well formed, they had to be rated as good by visual inspection. However, the blemishes caused "questionable" ratings by the system.

Other work on subsurface voids is discussed in Section 3.4.9.

3.4.8 Summary and Discussion of Test Results

In reporting our test results, we stress again that there is a certain amount of arbitrariness in them because human judgment was involved in selecting the decision thresholds which separated the thermal signatures into various categories.

Human selection of these thresholds will be required in the computerized version of the laser/thermal testing system also, which places a responsibility upon the operator. Too low a threshold can ensure that no bad joints are missed but will result in a certain number of "false alarms" in which some of the good joints are rejected. Too high a threshold will reduce the number of false alarms but can increase the number of detection failures for bad joints.

In Figure 58, we illustrate this matter by an example. An actual sequence of thermal signatures is shown. In order to represent a hypothetical but practical case, we have added above the chart several fictitious but realistic descriptions of the types of joint which might yield the thermal peaks of the heights shown. Notice that the shiny heel crack (Peak No. 9) has a lower peak than some of the cosmetic blemishes.

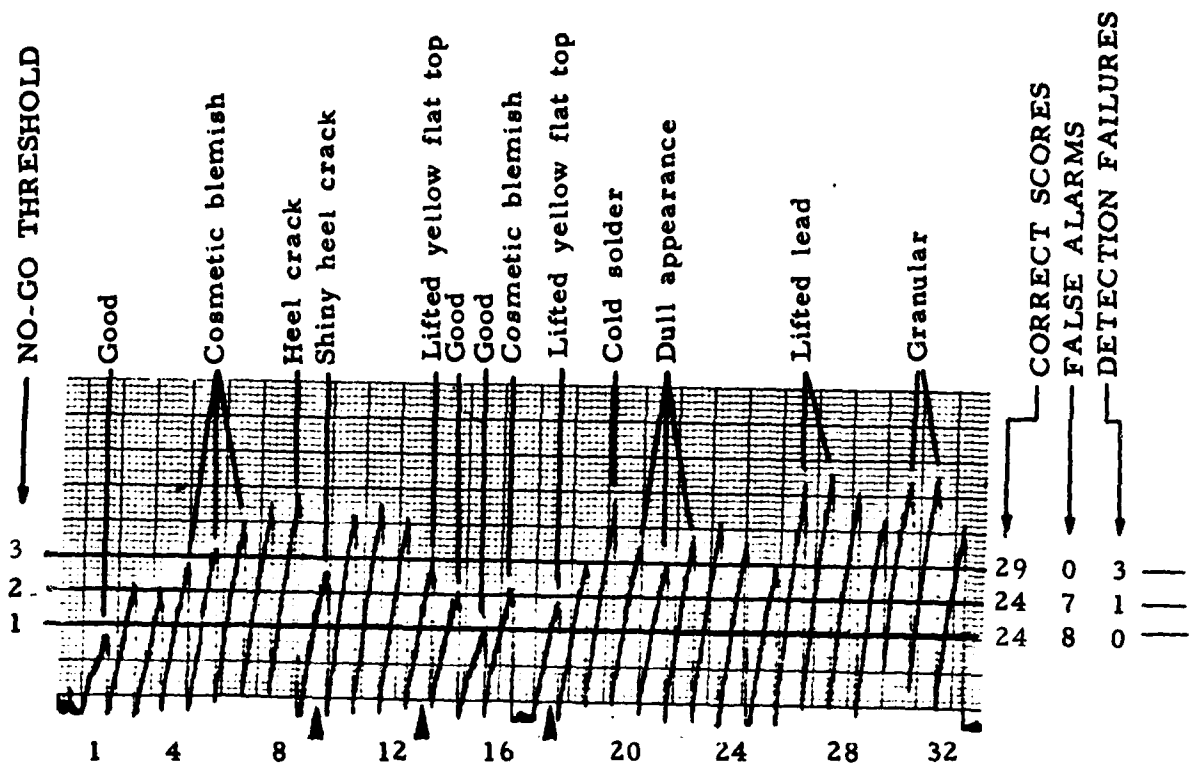


Figure 58. Effect of threshold level on trade-offs in scoring. Hypothetical case.

In this example, all thermal peaks above Level 3 are taken to signify true defects or cosmetic blemishes which are serious enough as to require touch-up.

All peaks below Level 3 represent acceptable joints except for the three obvious defects noted above: Peaks Nos. 9, 13 and 17.

However, the use of Level 3 as the threshold would cause three detection failures.

A lower threshold, such as at Levels 2 or 1, would reduce or eliminate the detection failures but would increase the number of false alarms.

We now have a choice as to where to place the decision level or "no-go threshold", and three such levels are shown.

Suppose it is decided that cosmetic-blemish peaks, as well as all other peaks above Threshold No. 3, identify joints which should be reworked or at least examined. If the computer were instructed to reject all peaks above Threshold No. 3, it would correctly identify 29 acceptable and no-go joints but would miss the three defects which are marked by arrows in Figure 58:

Peak No. 9: Shiny heel crack
Peak No. 13: Lifted yellow flat top
Peak No. 17: Lifted yellow flat top.

No good joints would be called bad, and so there would be no false alarms. If it is important to reduce the number of detection failures, then a lower threshold can be used, but this would increase the number of false alarms. At Level 2, for example, the shiny heel crack of Peak No. 9 will be detected, as well as lifted yellow flat top No. 13, but some of the acceptable cosmetic blemishes will become no-goes. And Peak No. 17 still qualifies as a detection failure.

In order to eliminate this last detection failure, the threshold can be reduced to Level 1, but this now increases the number of false alarms.

These effects on the various scores are tabulated to the right of the chart in Figure 58.

We make the above point in order to stress that the placement of the no-go threshold has an important bearing on the scores. The data to be shown were derived from the use of thresholds which, in our opinion, were appropriately placed. However, the

data could take on an entirely different character if the thresholds were to be shifted upward or downward. The particular result would be to change the balance between the numbers of false alarms and detection failures, with possible consequences on the overall number of correct scores.

We proceed to present the test results in summary form, this time by board number in numerical order rather than in the previous chronological sequence.

3.4.8.1 Test Results on Through-hole Joints

In Table 5 are tabulated the test results on feed-through joints, with some additional information. The latter refers to the right-hand column in the table in which we list the number of detection failures which are included in the unsafe-side disagreements.

The unsafe-side disagreements are of two types:

1. A joint which was visually rated as bad but which was called questionable by the system; and
2. A joint which was visually rated as bad or questionable but which was called good by the system.

The latter is of a more serious nature and we call it a "detection failure". The first type is less serious because a system rating of "questionable" would ensure that the joint was to be human-inspected in any event.

We hold laser-beam inhomogeneities to be responsible for a large proportion of the detection failures which are listed in Table 5 and we are confident that the scoring will be more favorable when the beam is later homogenized.

TABLE 5. SCORING SUMMARY FOR FEED-THROUGH JOINTS.

| Board No. | Types of joint | Number of joints tested | Number of correct scores | Number of safe-side disagreements | Number of unsafe-side disagreements | Number of detection failures |
|-----------|----------------------------|-------------------------|--------------------------|-----------------------------------|-------------------------------------|------------------------------|
| 1 | Mostly good; a few defects | 128 | 128 | 0 | 0 | 0 |
| 2 | Mostly insufficient solder | 126 | 101 | 20 | 5 | 3 |
| 3 | Cold joints, cracks | 124 | 118 | 4 | 2 | 2 |
| 4 | Insufficient solder | 118 | 114 | 1 | 3 | 1 |
| 5 | Pits, cavities, crevices | 127 | 113 | 10 | 4 | 4 |
| 6 | Burns | 128 | 121 | 7 | 0 | 0 |
| 7 | Assorted; subsurface voids | <u>98</u> | <u>96</u> | <u>2</u> | <u>0</u> | <u>0</u> |
| TOTALS: | | 849 | 791 | 44 | 14 | 10 |

Another possible contributor to the number of detection failures is our own inexperience in judging solder joint quality. We may have been too critical in rating certain defects as being more serious than they were rated by laser/thermal testing.

3.4.8.2 Test Results on Lap Joints

Earlier in this report we had described the use of an elongated laser beam spot to better match the elongated nature of the lap joint. We have pointed out that it would be preferable to match the infrared detector sensitive area to this shape as well, but that this must wait until a later time, when a special beam-splitter is to be installed.

Until that time, we are able to identify certain small defects on lap joints by exposing each joint three times, respectively, in the heel, central and toe regions.

This was done in some of the testing on Board 8B, in which a given solder joint was actually regarded as three separate targets, each having its own physical features and its own thermal signature.

The scoring results for lap joints are presented in Table 6. Although Board 8B contains only 112 joints, the various sections that were tested individually accounted for a total of 148 tests on this board.

There are two significant points about the resulting scores:

1. Although we have listed six detection failures, we point out that three of them were accidents due to positioning errors. The other three are uncorrectable errors due to highly reflecting defects such as lifted leads having exposed gold.

TABLE 6. SCORING SUMMARY FOR LAP JOINTS.

| Board No. | Types of joint | Number of tests | Number of correct scores | Number of safe-side disagreements | Number of unsafe-side disagreements | Number of detection failures |
|-----------|--|-----------------|--------------------------|-----------------------------------|-------------------------------------|------------------------------|
| 8 | Lifted leads, insufficient solder, cold joints, etc. | 105 | 99 | 2 | 4* | 4* |
| 8B | Similar to Board 8 | 148 | 143 | 0 | 3** | 2** |
| TOTALS: | | 253 | 242 | 2 | 7 | 6 |

* Two were corrected by re-positioning.

** One was corrected by re-positioning.

2. The number of safe-side disagreements is quite low. Although it is not true in this case, advantage can sometimes be taken of such a low count by lowering the no-go threshold so as to detect more defects while raising the "safe-side" count somewhat.

3.4.8.3 Discussion of Test Results

As a general statement, with limited reservations, our conclusions about the use of laser/thermal testing are very positive.

The reservations are:

1. The system is highly responsive to cosmetic blemishes (tool marks, splotches, small pits) which may be of little import in gauging solder-joint quality;
2. Certain, normally detectable defects escape notice when they happen to be highly reflecting; and
3. Defective lap-joint leads which are not centered on the pad can escape detection (although this problem may be eased in the future by various techniques).

On the other hand, the types of defect which are detected with high reliability include:

Lap joints:

Lifted leads

Heel cracks, half length or greater, with single exposure

Toe cracks, half length or greater, with single exposure

Heel cracks, 1/3 length, with three exposures

Toe cracks, 1/3 length, with three exposures

Cold-solder joints if dull

Insufficient solder joints if granular

Yellow flat tops.

In addition, there is a good possibility of the detection of partial heel or toe cracks by a single exposure when both the laser-beam spot and the infrared detector spot are elongated together.

Feed-through joints:

Insufficient solder, taking various forms:

Cavities, depressions, surface voids, shallow fillets,
no solder at all

Large subsurface voids (see Section 3.4.9.1)

Pits, crevices, blow holes (if centered)

Cold-solder joints if dull

Fractures at lead-solder interface (see Section 3.4.9.2)

Besides the above, generally any variation in visible appearance will be detectable by the laser/thermal method. There is also the possibility that the centering limitation on small defects will be removed after laser-beam homogenization.

In our Phase 2.2 proposal to USAF, we referred to our identifying, during the program, the range of defect severities which can be detected by our method. What we have learned is that an individual type of defect does not always occur by itself and, for a given degree of severity, the detectability may be either enhanced or inhibited by the presence of an accompanying defect type. For example, a 50% heel crack is generally detectable with a single, centered exposure if its surface is normal. If the surface is cloudy or dull, the lifted part of the lead may be shorter and yet detectable. If the surface is shiny, detection is more difficult and so a greater length of detachment may be required.

Interestingly, this interplay of defect types affects the human observer in the same way. A deep but shiny cavity in a feed-through joint which is difficult to detect by infrared is also more difficult to see. A cloudy, "insufficient-solder" lap joint which is readily detectable by infrared is also more highly visible.

As a practical matter, then, we make the following assertion about the required severity of a defect in order for laser/thermal detection to occur:

Generally speaking, if the defect of interest and any accompanying defective features happen to combine so as to be highly noticeable to the eye, then they will be highly detectable by the laser/thermal system. If a set of conflicting defects (such as a deep cavity with a shiny surface) render the defect less noticeable visually, it will also be more difficult to detect by laser/thermal testing. As a general rule, any defect which can be seen at all is capable of detection by laser/thermal means. An advantage is added in that large subsurface voids are also detectable by this method (see *infra*). The same ought to be true of large inclusions of foreign matter, of internal disconnections, and so forth, although this remains to be verified.

3.4.9 Specific Defect Types

During the course of this work, two types of defect in feed-through joints received special consideration, partly as being of particular interest to USAF and partly because they required a certain amount of experimentation in order that we perfect our techniques for preparing them artificially.

One of these was the large internal void, which is known to occur occasionally during wave soldering due to a variety of causes. This type of defect escapes visual inspection but its existence can be verified, destructively, through metallurgical sectioning. Its impact upon solder joint quality is to weaken the joint because of insufficient solder.

The other defect is the "cracked joint", a field failure which occurs after long periods of thermal cycling and mechanical vibration in which a separation occurs between the lead and the solder or between the solder and the hole barrel. The result is an intermittent or a broken electrical connection.

3.4.9.1 Internal Voids in Through-hole Joints

Our interest is confined to fairly large voids filling one-third or more of the volume of the plated-through-hole. Voids smaller than this would be difficult to detect with the short laser-beam exposures which we were using and would provide correspondingly less weakening of the joint.

Such voids are detectable by laser/thermal testing by virtue of the reduced solder mass upon which the laser beam impinges. The presence of solder at the far side of the void plays little part in the detection process and, for all practical purposes, the void could be simulated by a deep cavity in the hole, opposite to the test surface. Nonetheless, our purpose was to prepare actual voids such that they were not visually detectable, for purposes of realism.

(In later, Company-sponsored work subsequent to Phase 2.2, we have shown that far-side cavities of various depths are more readily detectable by longer laser exposures, such as one second or more, and the same is likely to be true of smaller voids than those in which we were interested in Phase 2.2. The minuteness of a detectable void would be in proportion to the amount of exposure time -- and to the reduction in inspection rate -- which

one is willing to use.)

Several methods of simulating internal voids were investigated without success. These included the application of solder flux only at the entrances to the hole, leaving the inside of the barrel unfluxed. It was hoped that the subsequent application of solder from both ends would leave a central void. However, we found that the slightest presence of flux would cause the solder to fill the hole completely when it was applied from the first side, through capillary action. Conversely, when attempts were made to cap the ends of the hole without the use of flux, no wetting action took place. Localized applications of flux and various solder resists were also tried, without avail.

The method which was finally adopted was the drilling away of the plated barrel by a No. 56 drill bit. The hole was then capped at both ends by soldering to the fluxed pads. The result was an oversized hole, containing a large void, but without an electrical lead; the simulation was therefore not an exact one.

Such a series of test joints was prepared on Board No. 3 and is shown in Figure 59. In the numbered sequence from 1 to 16, good joints in pairs are alternated with bad ones in pairs. The good ones, starting with Nos. 1 and 2, were normal plated-through-holes (PTH's) which were soldered without being drilled. In the resulting oscillogram, the sequence of thermal peaks should start with two low ones, followed by two high ones, and alternating in this way to the end. In all cases but one, the thermal peaks for the voids reach at least to mid-height on the oscillogram, there being some variation due to differences in solder

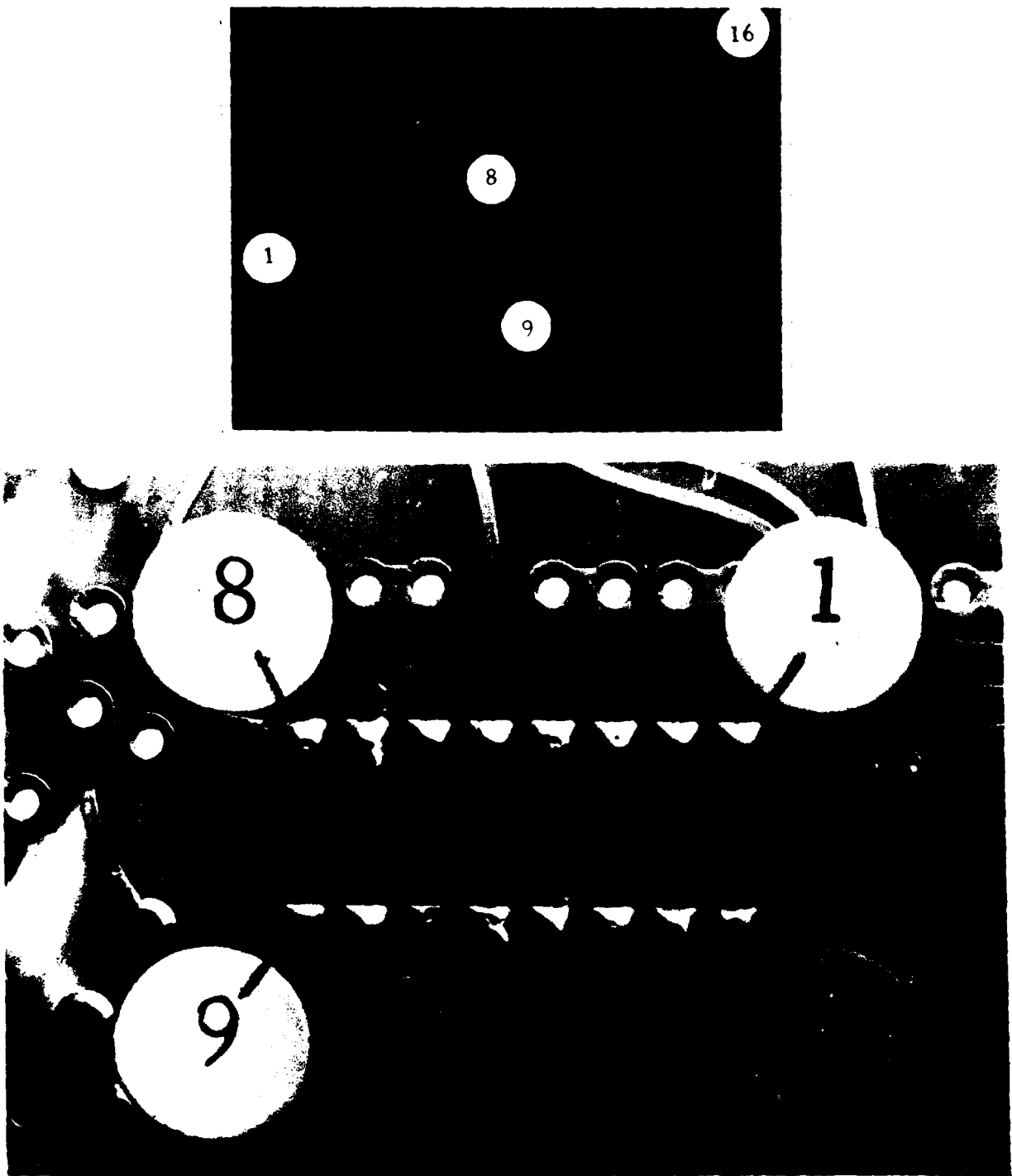


Figure 59. Thermal signatures and pictorial view of normal and void-type joints on Board No. 3. Note heat-sinking of Joint No. 11 by adjacent thermal mass which suppressed the expected high peak.

mass at the caps. The one exception is Joint No. 11 which, as seen in the photograph, is well "heat-sinked" to a massive land (or "etch") which probably cooled it during heating.

We note, also, in the oscillogram that thermal peaks Nos. 7, 8 and 12 are lower than for the other voids. A glance at the photograph shows that the corresponding joints are also in thermal contact with lands, although these are not as massive as with Joint No. 11. This evidence strongly suggests that there will be normal variations in "good" signatures, depending upon the amount of heat-sinking. These will be automatically accounted for in our final system where the reference signature for each joint will be stored separately.

After testing, the caps on the tested sides of Joints 1 through 16 were sliced off with a knife to verify the presence or absence of internal voids. Their appearance is seen in Figure 60.

As a matter of possible interest we show in Figure 61 a set of joints, prepared similar to those above, which were accidentally damaged by the laser beam during some preliminary tests using excessive exposure durations. Joint No. 9 is completely melted through and others show dimples indicating incipient cave-in. This set could not be used in further tests. Had the damage-prevention circuit been in operation, this incident would not have occurred.

3.4.9.2 Cracked Through-hole Joints

Early attempts to simulate this type of defect were discouraging. Thermal cycling of normal joints did not produce the

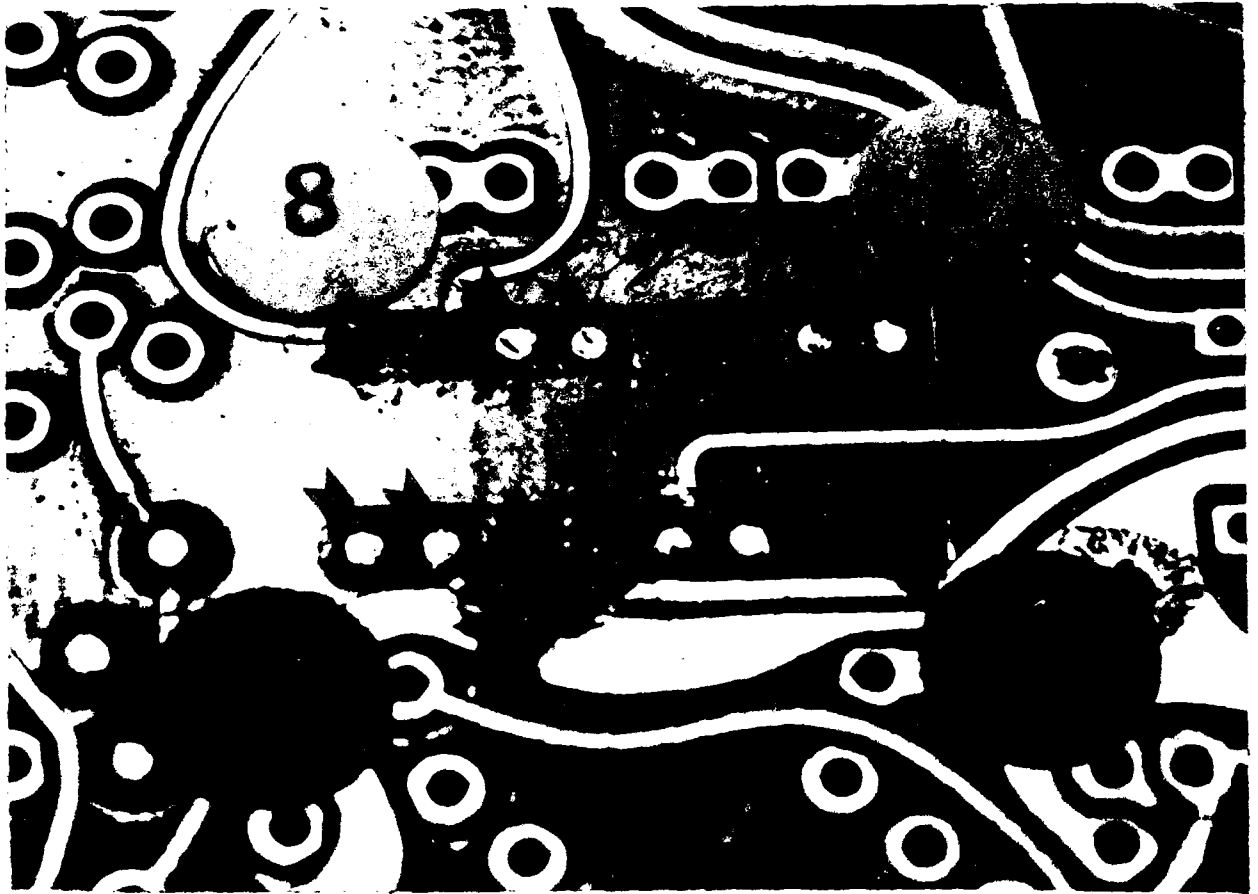


Figure 60. Joints shown in Figure 59 after removal of caps. Pairs of solid solder cores are seen (arrows) alternating with pairs of voids.

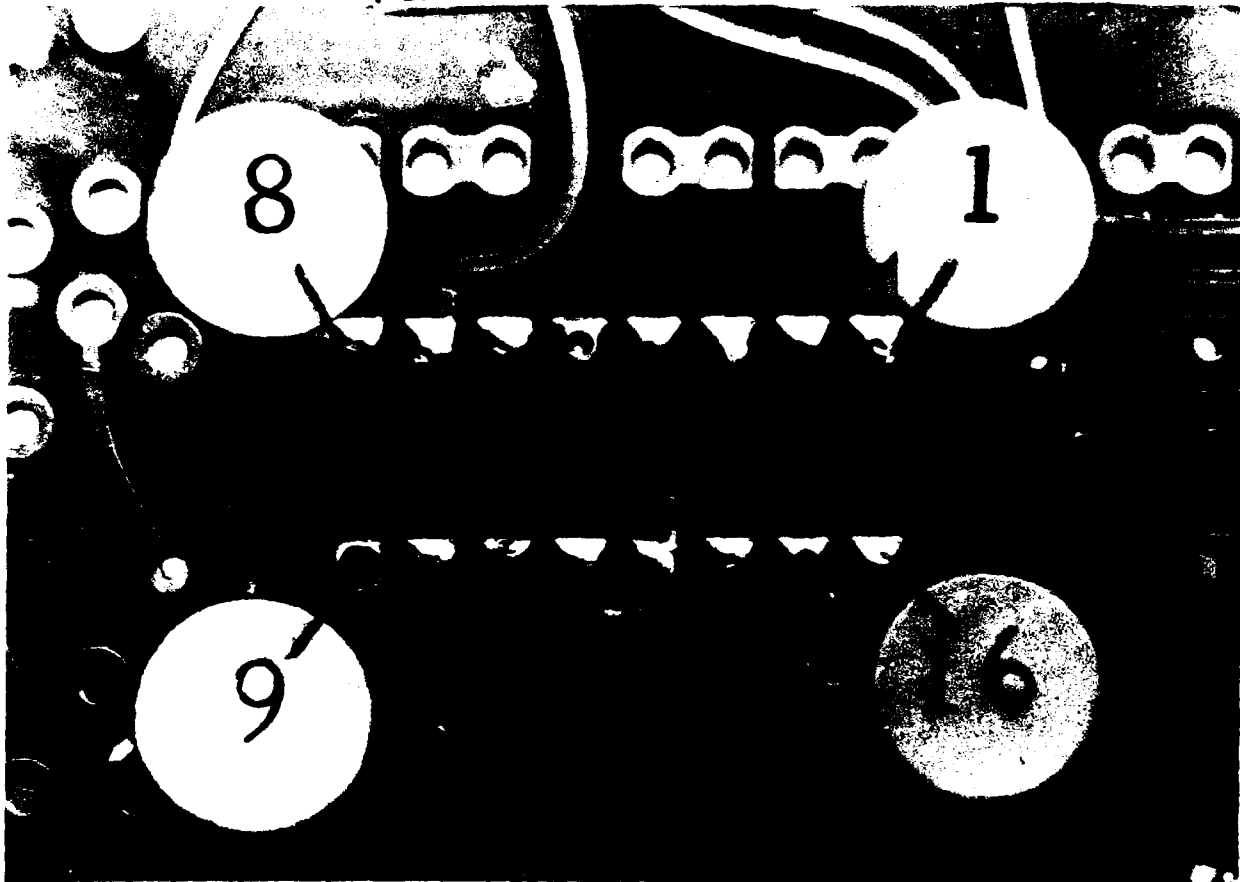


Figure 61. Example of laser-beam damage to an earlier set of void-type samples.

desired effect, even when the section of test board was alternately plunged from a vessel of hot oil into a container of liquid nitrogen and back again, for many cycles. Thermal cycling was applied by use of other heat and cold sources such as hot-air guns and pressurized cans of spray coolant, with similar ineffectiveness.

In a different test, several-pound weights were hung from simulated leads which passed through solder slugs in plated-through-holes, with the hope that, through cold-flow action, the leads would become loose. After several weeks without results, this test was abandoned.

In a discussion with the contract sponsoring office, agreement was reached that it might be reasonable to simulate solder cracks at the bases of protruding leads through the removal of solder by use of a fine-pointed tool. To this end, two feed-through joints in a group of eight normal ones were subjected to such a "surgical" procedure through the careful manipulation of a needle during examination under a stereomicroscope. Relatively short "cracks" were made, extending no more than a quarter of the way around each lead.

The resulting artificial cracks are shown in Figure 62 and the corresponding thermal signatures of the eight joints appear in Figure 63. The prominence of the thermal peaks corresponding to the defects, and the repeatability of the results during two separate passes, leave no doubt that the "cracks" have been reliably detected. It is necessary to point out, however, that had the cracks been located out of sight beneath a clinched

First scan Second scan

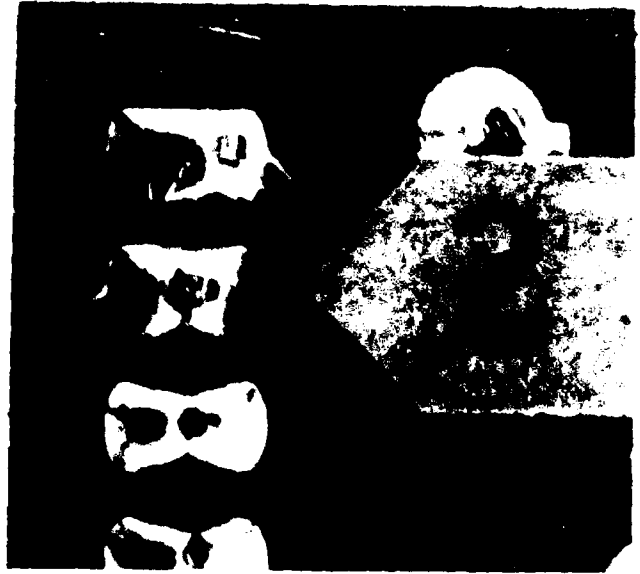
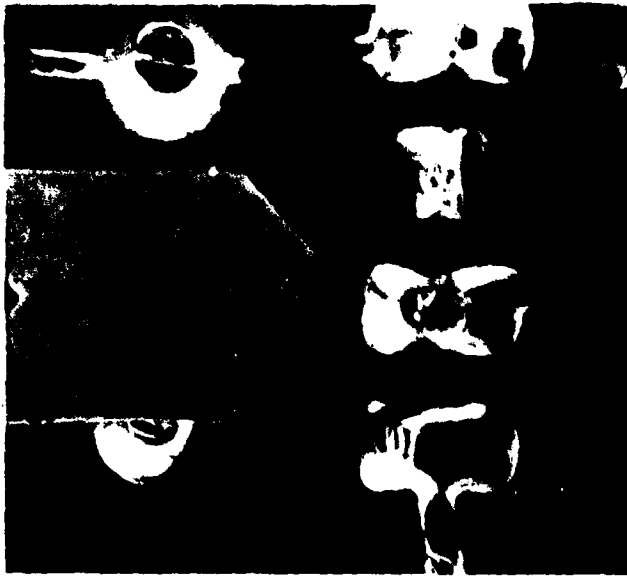
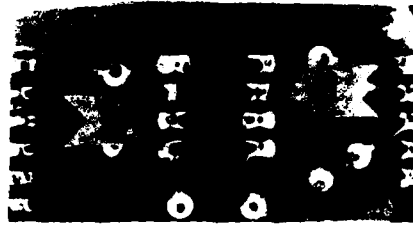


Figure 62. Two lead cracks (at arrows) simulated by removal of solder.

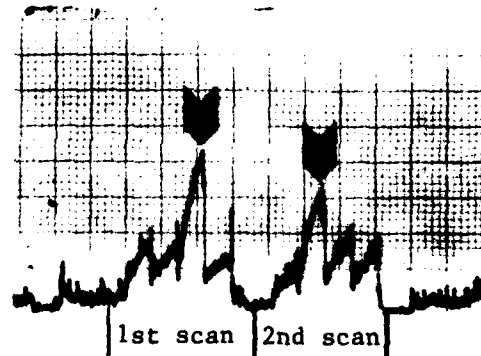
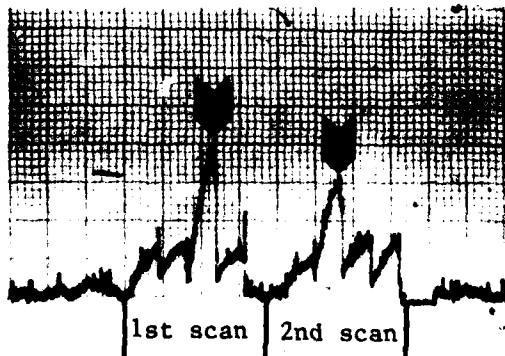


Figure 63. Separate thermal scans of eight joints containing the above cracks.

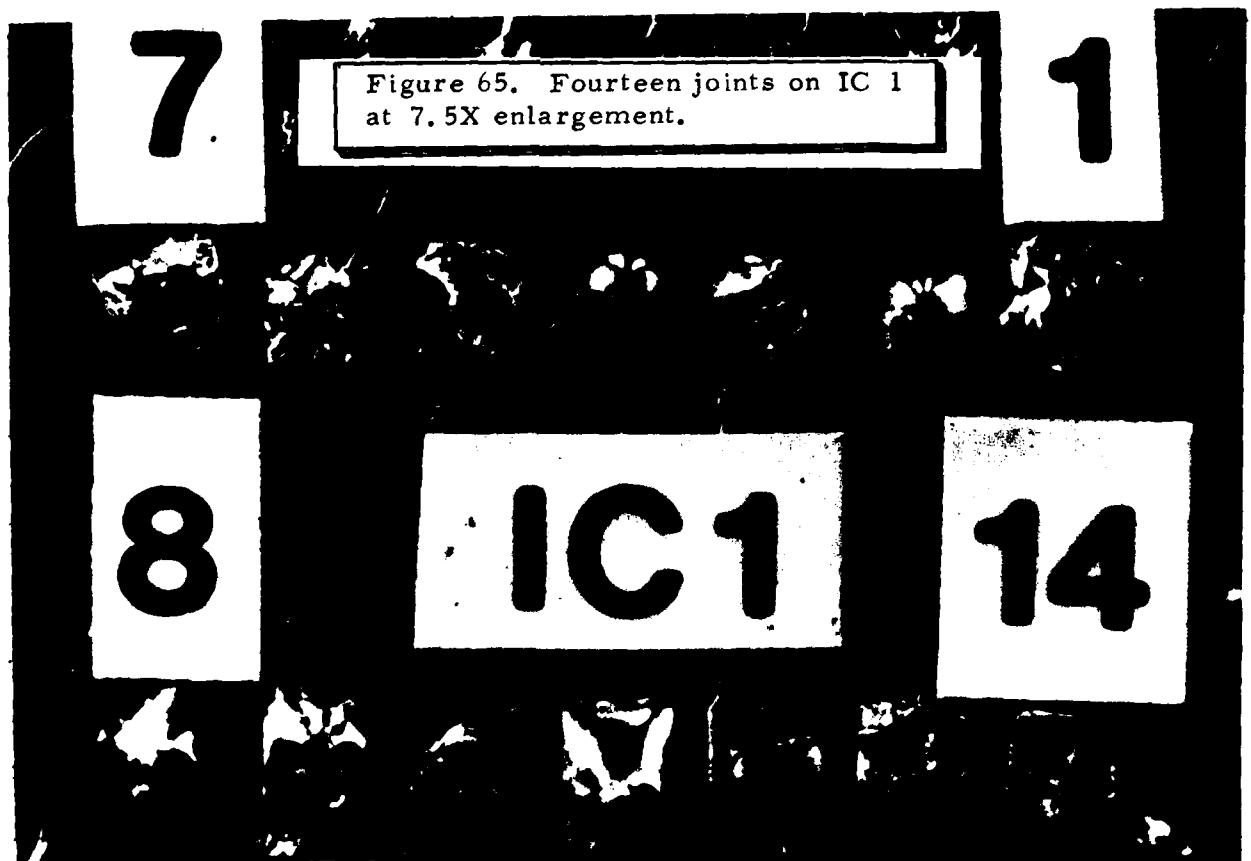
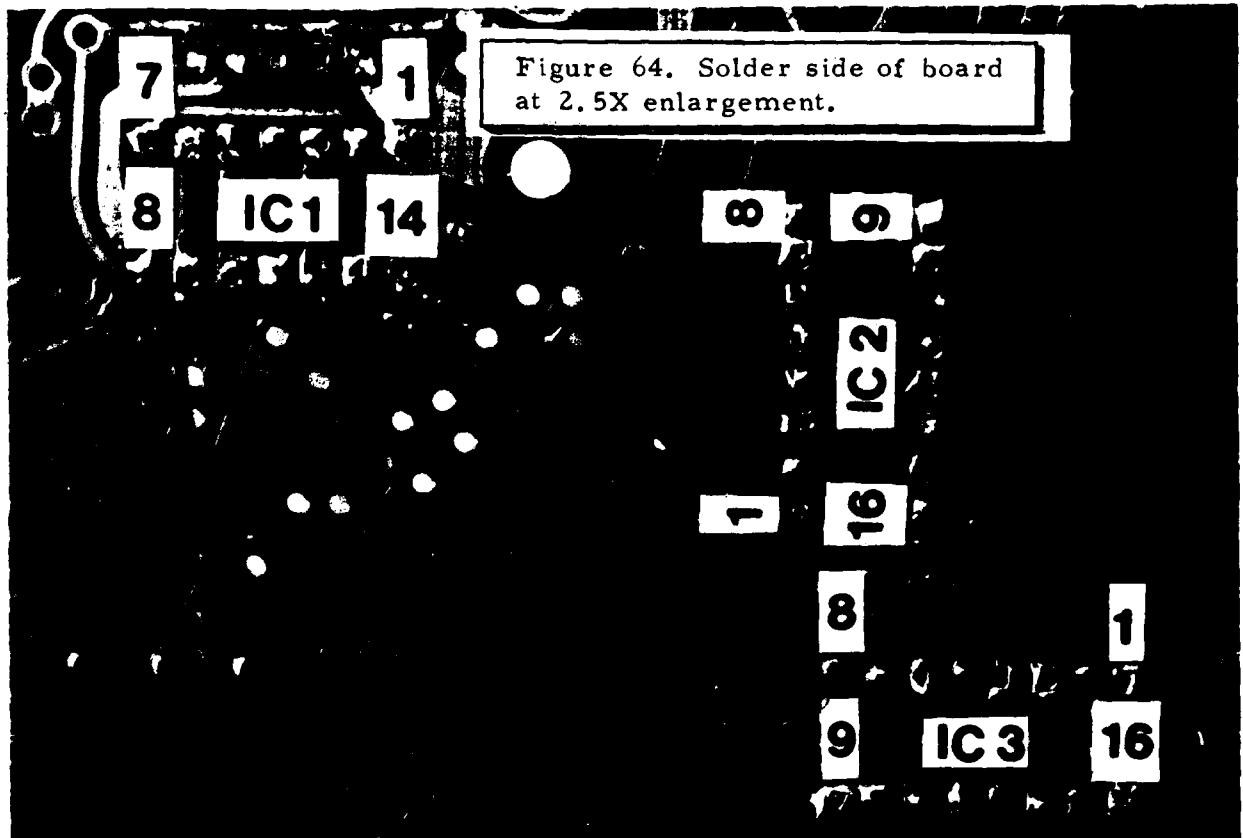
lead, they would not be detectable unless they were longer.

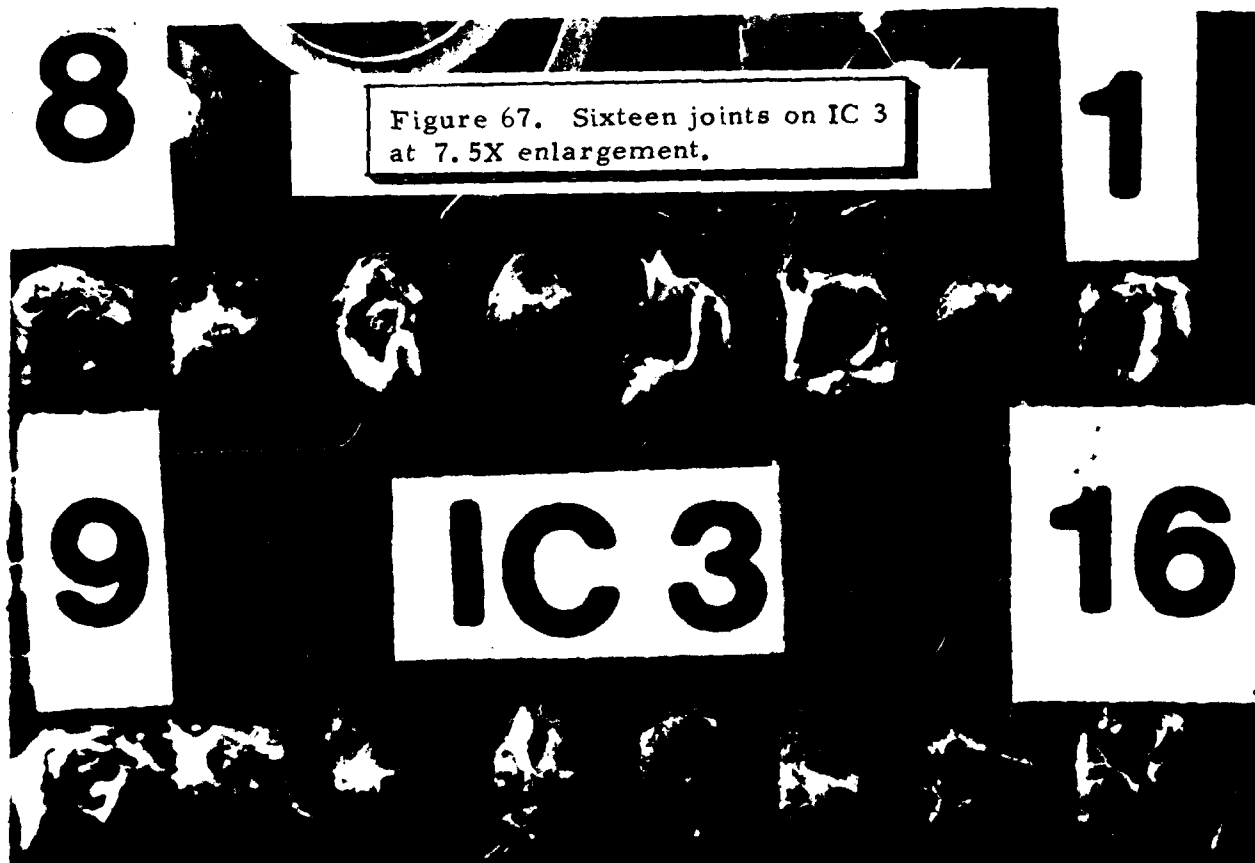
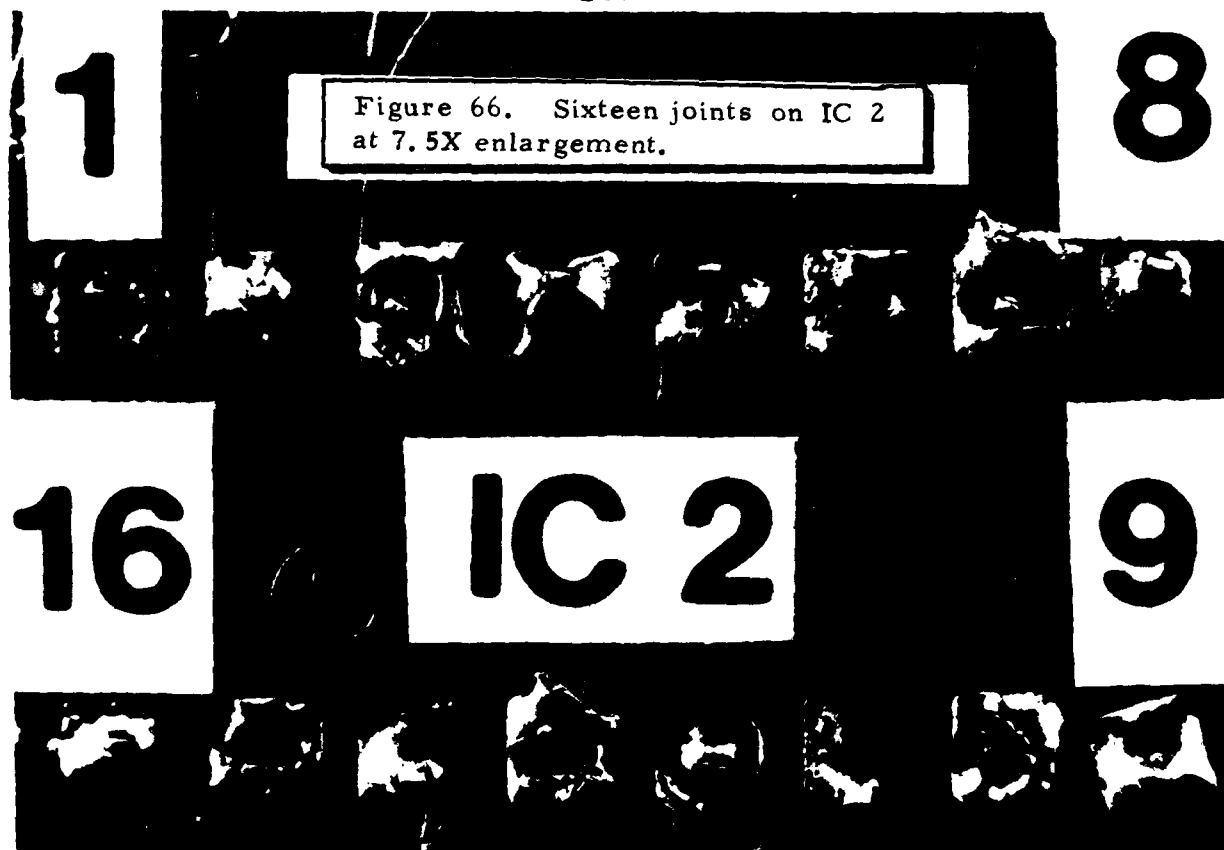
Greater success was enjoyed in our later attempts to simulate cracks by a different method. Several materials such as oils and waxes were examined for their effectiveness as solder resists for this application and generally proved to be either overly or insufficiently effectual. We ultimately came to the choice of a household furniture polish (Pledge) as a suitable material. When an IC lead was coated with the polish and was then soldered into a hole normally, the lead remained loose within the solder and was surrounded by a cylindrical void. The size of the intervening airspace between the lead and the solder could be controlled by varying the amount of solder which was applied.

Figures 64 through 67 show a number of samples prepared by this method and which were the subject of our laser/thermal tests. The photographs show an assortment of good and bad joints, with the bad ones showing a certain amount of variability in their appearances.

These samples were prepared by our mounting three ICs on a section of circuit board which had plated-through-holes. The ICs were numbered "1" through "3" and contained 14, 16 and 16 pins, respectively. Good and bad joints were then prepared randomly at the various pins. The solder side of the board is shown in the photographs at various magnifications.

The labeling of the individual joints in the photographs is as follows. Each numbered IC contains two rows, and the label with the IC-number is located between the rows. Additionally,





the end joints in each row are identified by a number-label placed above the corresponding joint. Between the numbered end-joints, one can easily count the unnumbered joints sequentially in order to identify a particular one.

After preparation, the board was mounted on the positioning table, the sample locations were programmed into the table controller, and the joints were laser/thermally tested in normal fashion. Fifty-millisecond exposures were used at a laser beam power level of five watts. The resulting sequence of thermal signatures is seen in Figure 68. The testing time for the 46 samples was 12.3 seconds, with most of this being accounted for by table motion.

On the chart in Figure 68, we have placed a dividing line between what we believe to be the normally low and the abnormally high thermal signatures. To assist the reader in interpreting the data we have indicated, by squares, those thermal peaks which are at or below the dividing line. Circles are placed at those peaks which appear above the line.

Our purpose, then, was to inspect the joints visually and to establish the correlation between high peaks and bad joints and between low peaks and good joints.

The joints were tested in sequence, from IC 1 through IC 3 and always starting with Pin 1, as shown by the labeling at the bottom of the chart. The sequence of thermal peaks may thus be easily compared with the sequences of solder joints seen on the actual board or in the photographs.

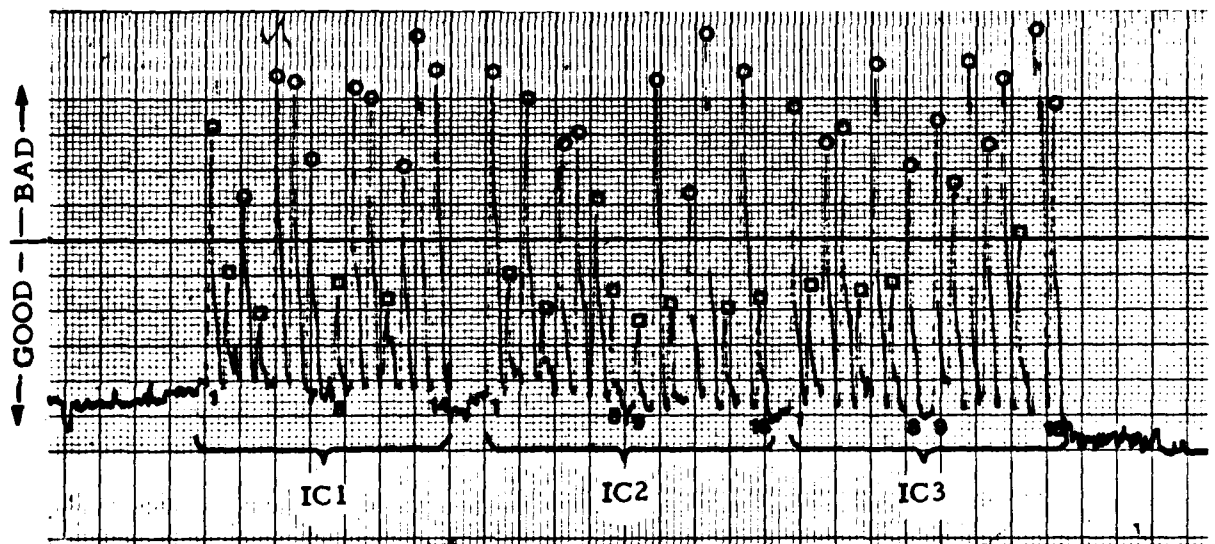


Figure 68. Thermal signatures of 46 joints including cracked ones.

Visual inspection of joint quality was carried out via a stereomicroscope and our judgments were recorded. These were then compared with the thermal data, and the results are tabulated in Table 7.

The asterisks in the table identify three cases of solder joints which were not cracked but which were of questionable quality, thus providing peaks which were either high or borderline.

In all other cases, there is perfect correlation between "high" and "low" peaks when compared with "cracked" versus "normal" solder joints.

3.5 System Optimization

Concurrently with the testing of solder joints and other activities in Phase 2.2, one of our objectives was to be alert to opportunities for improving the system design concept in order to achieve better performance. We have found, for example, (Section 3.4.6.2) that an elongated laser-beam spot would be more effective in averaging out local defects in lap joints. It would be equally desirable to lengthen the detector spot correspondingly, but this is not conveniently done in the present system design because the detector and laser-beam axes are not coincident.

If the reader will refer to Figure 7 in Appendix A which describes the system, he will notice a small mirror at the end of a rod-like holder just above the workpiece. This mirror directs both the HeNe and Nd:YAG laser beams downward toward the target, which can be seen as a luminous spot in the

TABLE 7. COMPARISON OF LASER/THERMAL TEST DATA WITH VISUAL ASSESSMENT OF SOLDER JOINT QUALITY.

| <u>Pin</u> | <u>Quality</u> | <u>Thermal Peak</u> | <u>Pin</u> | <u>Quality</u> | <u>Thermal Peak</u> | <u>Pin</u> | <u>Quality</u> | <u>Thermal Peak</u> |
|------------|----------------|---------------------|------------|----------------|---------------------|------------|----------------|---------------------|
| IC 1 | | | IC 2 | | | IC 3 | | |
| 1 | Bad | High | 1 | Bad | High | 1 | Bad | High |
| 2 | Good | Low | 2 | Good | Low | 2 | Good | Low |
| 3 | Bad | High | 3 | Bad | High | 3 | Bad | High |
| 4 | Good | Low | 4 | Good | Low | 4 | Bad | High |
| 5 | Bad | High | 5 | Bad | High | 5 | Good | Low |
| 6 | Bad | High | 6 | Bad | High | 6 | Bad | High |
| 7 | Bad | High | 7 | Bad | High | 7 | Good | Low |
| 8 | Good | Low | 8 | Good | Low | 8 | Bad | High |
| 9 | Bad | High | 9 | Good | Low | 9 | Bad | High |
| 10 | Bad | High | 10 | Bad | High | 10 | Bad | High |
| 11 | Good | Low | 11 | Good | Low | 11 | ** | High |
| 12 | Bad | High | 12 | * | High | 12 | Bad | High |
| 13 | Bad | High | 13 | Bad | High | 13 | Bad | High |
| 14 | Bad | High | 14 | Good | Low | 14 | *** | Low |
| | | | 15 | Bad | High | 15 | Bad | High |
| | | | 16 | Good | Low | 16 | Bad | High |

* This was not a cracked joint but was a shallow fillet which gave a high peak.

** This joint is shaped normally and would ordinarily have provided a low thermal peak. However, by microscope, it can be seen to have residual solder flux and a slightly hazy surface, both of which contributed to the high thermal peak.

*** This joint is similar to the one above. However, its thermal peak is just at the dividing line and we have classified it as "Low".

photograph. It will be seen that the laser optical path is several degrees away from the vertical axis along which the thermal radiation from the heated target proceeds to the infrared detector.

This was the irradiation geometry used during Phase 2.2. It is at variance with the more desirable geometry depicted in Figure 4 of Appendix A which existed in concept but which had not yet been implemented.

In order to be able to elongate the laser-beam and detector spots, and for other reasons as well, it was desirable to render their axes coincident. Therefore, a design effort was carried out under Phase 2.2 and the actual implementation was performed under Vanzetti company sponsorship after Phase 2.2 was completed.

The co-alignment design effort and other activities involving design improvements are discussed in the following sections.

3.5.1 Co-alignment of Optical Axes

In addition to providing for target-spot elongation when needed, co-alignment of the laser-beam and detector axes was desirable for other reasons. One of these concerns board-to-board target-height variations which could be brought about during tests on boards of various thicknesses (if these were not compensated for by mechanical mounting provisions). Such variations could be accommodated by a simple focusing adjustment if the optical axes were coincident but they would require, in addition, an angular adjustment of the laser-beam axis if this were not vertical.

Another reason for the desirability of vertical laser-beam incidence has to do with the testing of feed-through joints. When an IC is mounted on a circuit board prior to soldering, its leads along opposite edges are most often clinched in opposite directions in order to secure the IC to the board for ordinary handling. The non-perpendicular laser-beam incidence, during testing, can thus introduce an asymmetry in the irradiation optics for joints whose leads are oppositely clinched. And if the clinching angle is such as to bring a lead close to the incident angle of the laser beam, shadowing and other unwanted effects can occur. (For boards whose ICs are all oriented in the same direction, the board can be oriented on the positioning table such that the clinch angles are bisected by the incident beam, thus restoring symmetry. However, not all manufactured boards exhibit parallel orientation of the IC axes.)

Our design study involved a consideration of various ways of implementing the co-alignment of the optical axes. One simple method, using an ordinary first-surface mirror as an insertable element, is shown in Figure 69. It assumes that the HeNe laser spot is needed only during the manual entry of solder-joint locations into the table controller. During testing, the mirror is withdrawn and the YAG and detector axes are combined by use of a small permanent mirror on a larger IR-transmitting substrate. This latter element makes use of the disparity in beam diameters for the laser and thermal-infrared paths. However, it poses the problem that the YAG beam must be focused by a lens which

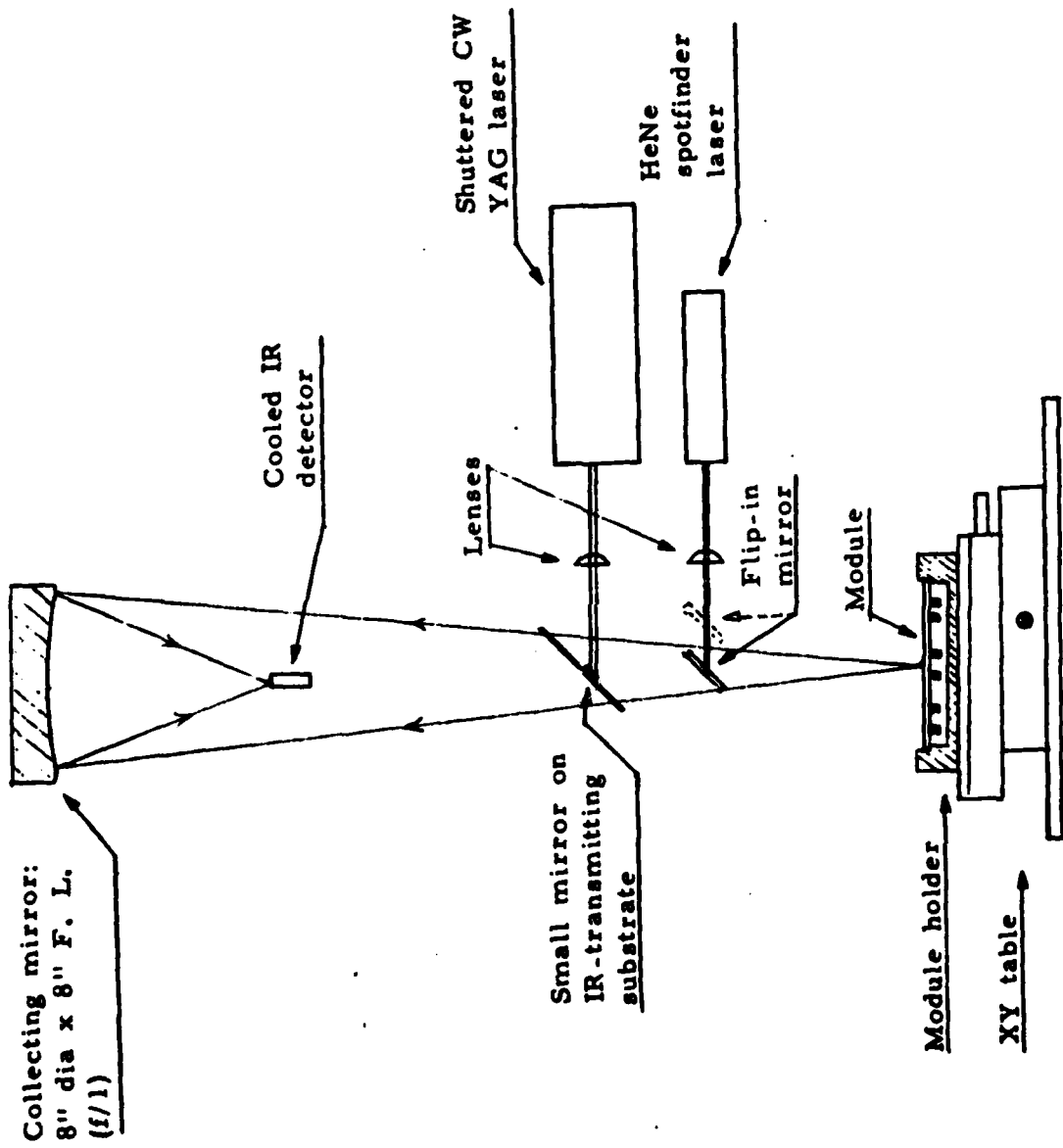


Figure 69. One method of bringing the laser and detector axes into coincidence.

is some distance from the target. This requires the use of a relatively long-focus lens which, through diffraction considerations, can restrict one to spot sizes larger than needed for solder-joint testing. The multimode laser-beam divergence is stated as being 10 milliradians. In order to form a diffraction-limited image no larger than 0.020", let us say, the lens can be no farther than two inches from the target. One can reduce the beam divergence by use of a beam-expanding telescope which increases the beam diameter, but this would require the use of a larger mirrored area on the IR-transmitting substrate, thus reducing the transmittance of thermal infrared.

Another, often-used method of combining two optical paths makes use of a partial mirror or "beamsplitter", that is, one which is partly reflecting and partly transmitting. If such a mirror is fabricated from dielectric interference-layer coatings, it can be made to have negligible absorption. Its transmittance and reflectance values can be tailored to be 50% each or any other combination totaling 100%. Such mirrors can be used with optical beams of comparable diameters. However, they exact a toll in power transmission, as we can understand by referring to Figure 69. A "50-50" mirror could be used, for example, in place of the upper of the two 45° mirrors in the figure. Half of the laser radiation which reached it would be reflected downward to the target; the other half would be transmitted and would be lost. Of the emitted thermal radiation from the target, half would pass through to the detector and half would be lost in the direction of the laser. The compounding

of these losses can be costly either in terms of reduced system sensitivity or the need for a higher-powered laser.

The beamsplitter to which we refer above is assumed to be of the neutral density type, that is, one which is equally efficient at all wavelengths. There is another type of interference-layer beamsplitter which is called "dichroic" because it is wavelength sensitive. Such a device can be designed to be a highly reflecting mirror in one wavelength region and a highly transmissive window in another region. Its use is allowed where one wishes to combine (or separate) two optical beams having well-separated spectral compositions. It is ideally suited to our present case where the YAG radiation is at $1.06\text{ }\mu\text{m}$ and where the thermal radiation is in the 2- to $5\text{-}\mu\text{m}$ region. One requires merely a dichroic which is highly reflecting to the YAG beam and which is clear in the longer wavelength region.

The name "dichroic" stems from the "two-color" nature of the device's behavior.

Figure 70 is a later diagram than Figure 69 and shows how the dichroic beamsplitter would be used. It also shows the two laser beams being rendered parallel by mirrors and being brought together at the entrance face of an optical fiber which will be discussed in the following section. The dichroic element is highly reflective for both laser beams.

Dichroic beamsplitters are commercially available having absorptivities of less than 0.01 percent. However, they are not ordinarily designed for use at wavelengths as great as those of interest to us. Our optimization effort therefore

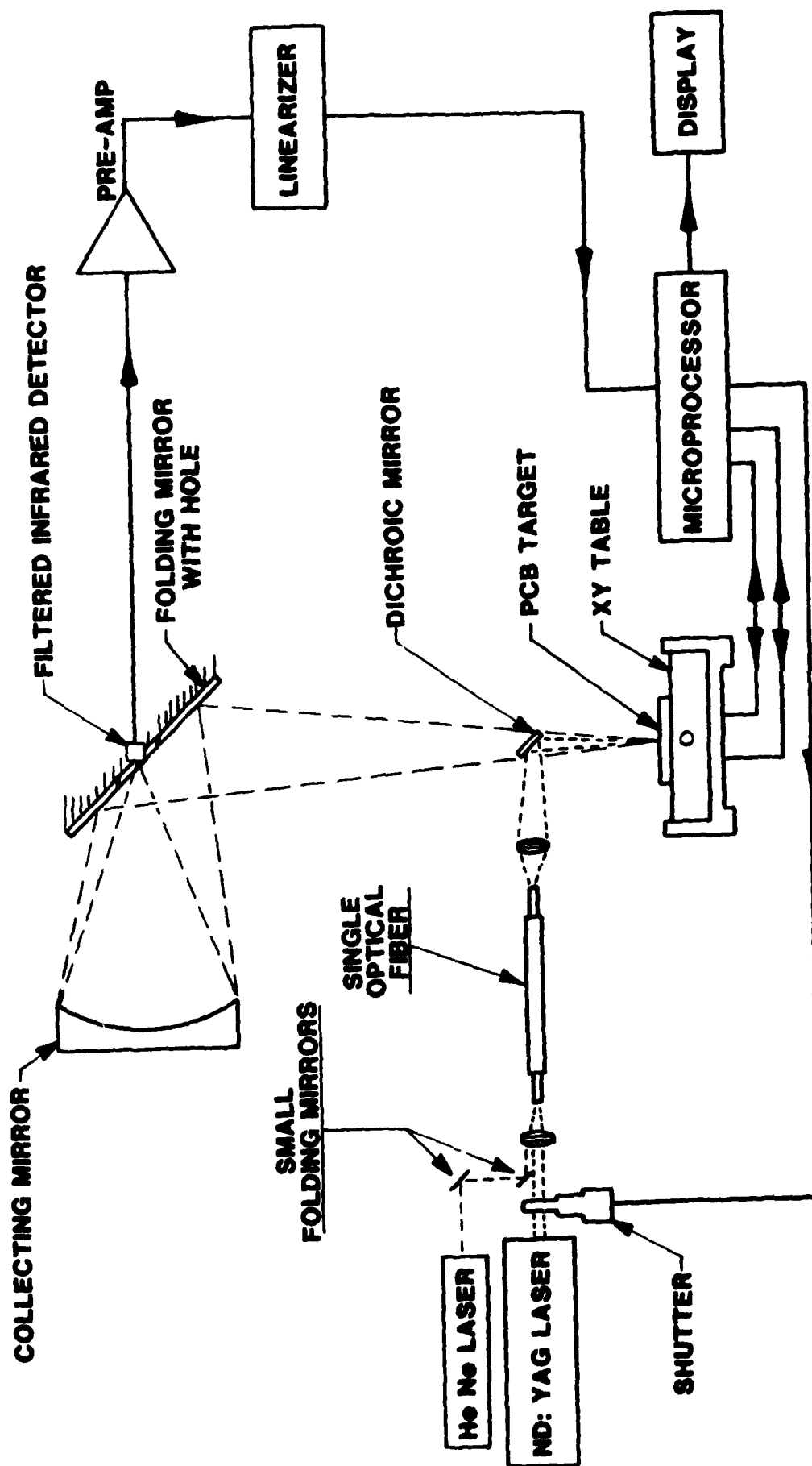


Figure 70. Use of a dichroic mirror to bring separate optical axes into coincidence.

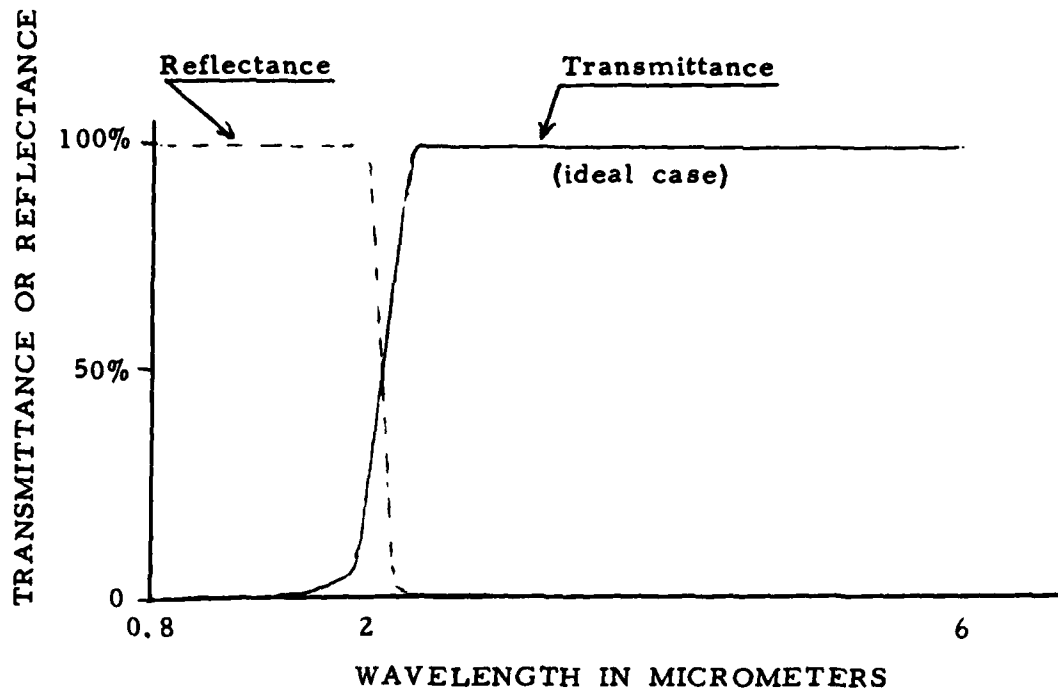
included consultations with several manufacturers in order to explore feasibility and to arrive at a realistic set of specifications. Two out of six manufacturers contacted indicated that they would be capable of meeting our special infrared requirements.

Figure 71 presents the beamsplitter specifications which were arrived at in Phase 2.2. The spectral curves appearing above the specifications represent the idealized case of perfect reflectance in one wavelength region and perfect transmittance in another. The reflectance and transmittance specifications listed below the curves are more in keeping with what is realizable in practice.

As was indicated, such a beamsplitter was procured and installed after Phase 2.2 was completed and its performance has been more than satisfactory. There has not yet been an opportunity to carry out further beam-spot elongation studies for use with lap joints but we look forward to doing so in the future. Elongation could be carried out by use of an insertable, or "flip-in", cylindrical lens, with a rotational capability if this were needed to accommodate joints which were oriented at right angles to each other on the same board. The flip-in and rotational features could be automated in a later system.

3.5.2 Laser-beam Homogenization

As a second step in the system-optimization effort, we have considered the use of a flexible optical fiber in coupling radiant power from the YAG laser to the target, instead of irradiating the target via an air path as we had customarily done. Four improvements would be brought about by this method:



SPECIFICATIONS FOR A TYPICAL DICHROIC MIRROR

Substrate: Sapphire
 Angle of Inc: Film designed for use at 45° incidence
 Polarization: Random
 Size: 1.500" dia +0.000-0.010" x 0.040" max thickness
 Clear aperture: 1.250" min dia
 Durability: Adherence, adhesion and humidity per MIL-M-13508
 Reflectance: Greater than 95% at 1.06 μm
 Transmittance:
 Average of 70% from 1.06 to 5.0 μm
 (Average transmittance will drop from 70% average to 1% over the spectral range from 5.0 to 7.0 μm)
 (Transmittance at less than 1.06 μm is unspecified)
 Absorption: Less than 0.01% from 1.06 μm to 5.0 μm .

Figure 71. Spectral reflectance, transmittance and specifications for a typical dichroic mirror.

1. The laser-beam radiation path would be automatically protected over most of its length, which would be advantageous from the standpoint of personnel hazards. The earlier use of lengths of metallic tubing to enclose the beam over much of its path had the following disadvantages:

- a. Parts must be machined, including couplings, which must then be fitted together and secured. When it occasionally becomes necessary to remove the protection, such as for servicing or for special tests, a sufficient length of the laser beam is exposed along its air path, requiring special alertness by the operator in avoiding exposure to eyes or skin, with the risk of accident.
- b. The rigid nature of the protective tubing can allow the transmission of mechanical vibrations from the laser to the XY table unless shock-mounting precautions are taken. The vibrations are generated within the laser head by the continuous passage of cooling water and air through its various parts. The use of a flexible optical fiber provides a "built in" shock-mounting feature.

2. The laser head may be mounted remotely from the temperature-sensitive target zone. This is so as to avoid unwanted heat from the laser head which may warm the solder joints unintentionally or which may cause false infrared signals to reach the detector. Although remote mounting is possible by use of folded optical paths which make use of fixed mirrors, each such mirror would have to be specially mounted in order to be precisely adjustable in angle so that the laser beam will strike the target exactly. Also, the use of a long folded path can enhance the effects of mechanical vibration and cause beam-spot jitter at the target. A flexible, enclosed optical path through a transparent fiber suffers no such limitation.

3. The use of a fiber allows a precise way of identifying the beam-spot location at the target. One need merely disconnect the input end of the fiber from the laser and inject light from a visible source over the same path, whereupon a visible light spot will be seen exactly in the position where the infrared spot is aimed. This avoids the need for the flip-in mirror which was considered earlier (see Figure 69). The use of the flip-in mirror imposes an aiming requirement, with the possibility of accidental aiming errors, whereas the use of the "backlighted" fiber automatically guarantees aiming accuracy.

In practice, continuous backlighting could be implemented by various means so that one need not actually remove the fiber from the laser in order to do this. One such means is indicated in Figure 70.

Should the HeNe laser be mis-aimed in the design concept of Figure 69, the operator would be unaware that the two laser spots were no longer in registration in the target area, resulting in programming errors and possibly in damage to the substrate until the error was noted. In the Figure 70 concept, mis-aiming of the HeNe beam would result in little or no red light being visible in the target area, which would alert the operator to the problem.

4. Finally, it was hoped that the use of an optical fiber would result in greater uniformity of the power distribution within the focused laser-beam spot, a problem which has only been mentioned in passing in this report.

A feature of all lasers is that the power density distribution over the cross section of the beam is noticeably irregular, and this irregularity is preserved when the beam is focused to a spot by use of ordinary lenses. The nature of the irregularity is such that there is often an intensity maximum, or "hotspot", at the center, falling off toward the edges, with a random grain structure superimposed on the whole pattern.

When the beam cross-section is imaged upon a solder joint, a problem develops if the surface contains microscopic blemishes such as scratches, pinholes, etc. If the hotspot or one of the more intense image areas in the grain structure happens to coincide with the blemish, a higher-than-normal thermal signal will result. A slight relative displacement of the beam spot with respect to the target (by no more than 0.001" or 0.002") can change the signal amplitude markedly. Normal vibrations in the positioning table (due to the flow of cooling water and air within the laser head) cause oscillations to be superimposed upon the thermal signal during heating.

In the testing of feed-through joints containing tiny blow holes or other minute blemishes, the ability of the laser/thermal system to detect these depends strongly upon whether the central hotspot does or does not fall upon the blemish.

The non-uniformities of laser beams have been of concern to other laser-applications workers and several methods of "homogenizing" the beams have been proposed. In one of these, the beam is passed through a section of either a bent glass rod or an optical fiber which is curved through 90 degrees or more.

Within the bent element, the optical rays comprising the beam are multiply reflected through random angles, thus following separate paths through the element. The result is that the original beam is "scrambled" and loses its structured pattern by the time it emerges from the element. The output end face thus appears uniformly irradiated, and the re-imaging of this end face produces a uniform laser beam spot at the target.

Our approach, then, was to select an optical fiber, on the basis of composition, diameter and length, which would have the best chance of bringing about the above four improvements, and to evaluate its performance. The fiber selected was a two-foot length of "communications fiber", No. QSF-600A, supplied by Quartz Products, Inc., of Plainfield, NJ. This is high-purity fused silica which is clad with a tough, Teflon coating to provide strength and small bending radii without breakage. A 0.024" diameter was chosen for the optical core, being large enough that the entire laser beam could be readily focused into it. At the output end, the 0.024"-diameter radiant end face could in turn be re-imaged upon the target area to provide any convenient spot size over a reasonable range.

A separate transmittance measurement verified the supplier's claim that the absorption loss within this length of fiber was too small to be measurable.

A special support structure was prepared for the output end of the fiber, containing a focusing (objective) lens and a mirror which would direct the output beam downward to the target. The structure is seen in Figure 72.

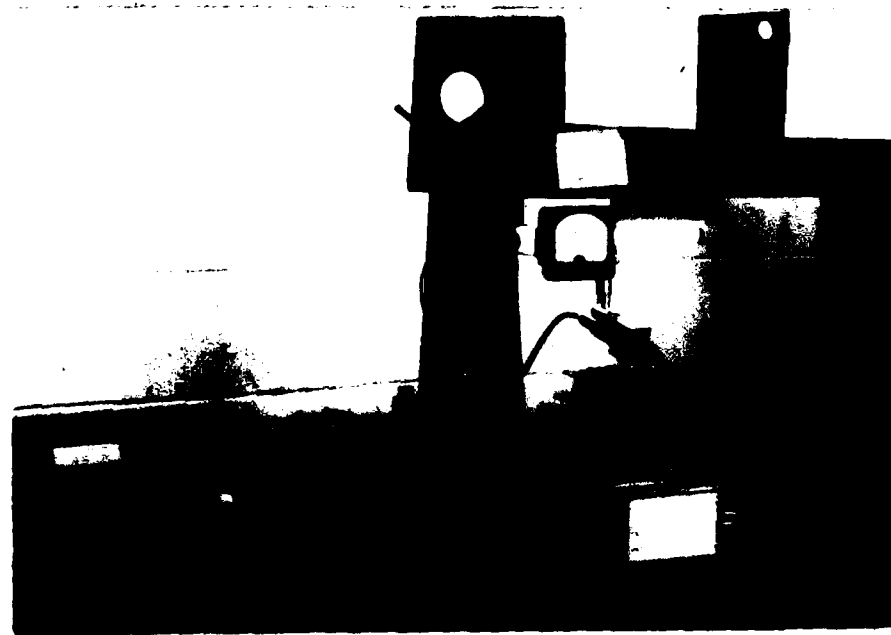
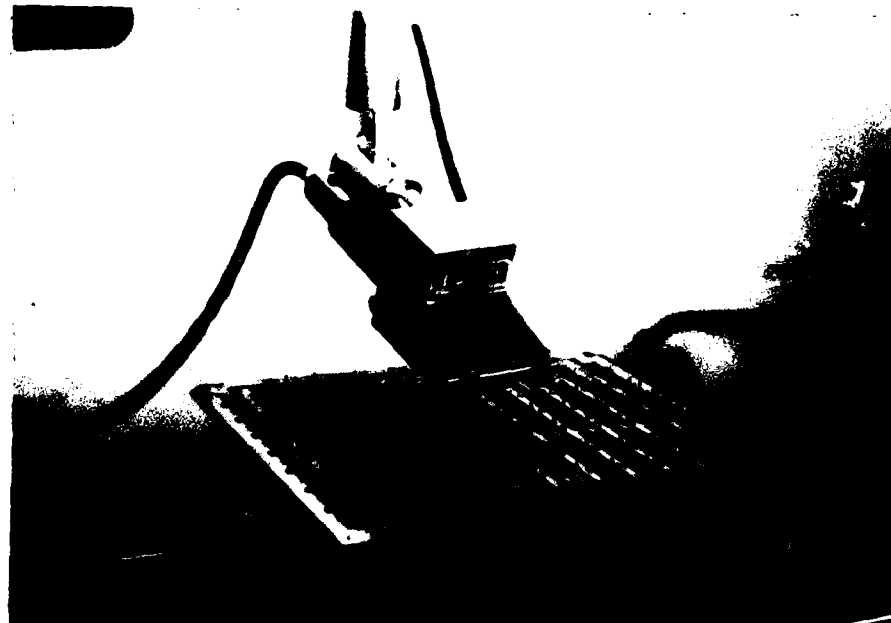


Figure 72. Near and far views of fiber optic assembly being tested for location programming and for target heating.

At the input end, a precision mechanical positioner was provided so that the fiber could be placed exactly at the focus of a small lens placed in the laser output beam. The positioner was a three-axis micrometer movement by whose use the input power to the fiber could be maximized.

When the solder-joint locations were to be programmed into the XY table controller, white light was injected into the input end of the fiber and appeared as a focused spot at the target. After programming was completed, the source was removed so that the laser beam could enter the fiber. (In later developments subsequent to this contract, the simultaneous illumination method shown in Figure 70 was implemented.)

The installation of the optical fiber occurred late in Phase 2.2 and so its advantages were not available during most of the solder-joint testing which was carried out in this phase. However, independent testing of the fiber did indeed verify that the desired objectives were achieved and that there seemed to be no reason to modify the design. One problem was experienced in the form of the gradual deterioration of the input end face due to overheating by the laser beam, partly due to the burning of the Teflon cladding by the edge of the beam spot. This necessitated occasional repolishing of the end face. In later work, subsequent to Phase 2.2, the Teflon was carefully removed for a short distance back from the end face, thus eliminating this problem.

Separate optical measurements also verified that the efficacy of the fiber as a homogenizer was complete; that is, when the non-uniform, granular laser beam entered the fiber, it emerged as a uniform disc of radiation within which there is no measurable structure.

The use of an optical fiber is thus recommended as a permanent design feature of the laser/thermal testing system.

3.5.3 Laser-beam Power Considerations

In earlier phases of this program we were concerned with lap joints on flat pack IC's and we had determined that an inspection rate of ten joints per second might reasonably be attained with a six watt laser.

Since that time, our attention has turned to the more massive feed-through joints, which require more laser power for the same heating rate, and it is clear that ten joints per second will not be achieved with the present laser.

As a part of the Phase 2.2 optimization study, it was appropriate for us to carry out some testing in order to arrive at an idea of what a practical laser power level might be. For that purpose, two Vanzetti Company personnel visited a major laser manufacturer in New York state on 26 March 1981 in order to conduct tests on solder joints with 50-watt laser whose output power could be adjusted downward. Our purpose was to find a high enough laser-beam power level for more rapid heating than with 6 watts, but yet not enough to damage the solder surface or to change it in any way.

As a preliminary test, a solder joint was selected at random and was exposed to a 140-mSec pulse of a highly focused beam spot which was expected to damage the joint. The laser power had been reduced to 30 watts and the beam was concentrated into a 0.012" diameter spot near a corner of an approximately 0.070" square solder joint. As was anticipated, a pinhole was formed at the central hot spot and is seen in Figure 73. No laser-beam homogenization was used in any of these tests.

Through a series of tests such as this, we determined that if the laser-beam power were dropped to nine watts, there was no solder damage with a 140-mSec exposure even if the beam were focused to as small a diameter as 0.006". Similarly, at 20 watts of power and with a 0.010" spot diameter, no damage was seen with reasonably short exposures such as 17 mSec. With the spot defocused to a 0.040" diameter (by removal of the lens), the 20-watt beam caused no solder damage during a 50 mSec exposure, provided that it was centered on the solder. However, a slight spillover of the edge of the spot onto the substrate would damage the latter. The full effect of such damage is seen in Figure 74 where the entire beam spot was intentionally placed on the substrate in two different exposures.

These test results established that, with the proper spot size and exposure durations, solder damage could be avoided by use of laser-beam power levels in the range from nine to twenty watts. The next question was, which was the most desirable end of this relatively wide range? It appeared that, with lower powers, two advantages might be gained:

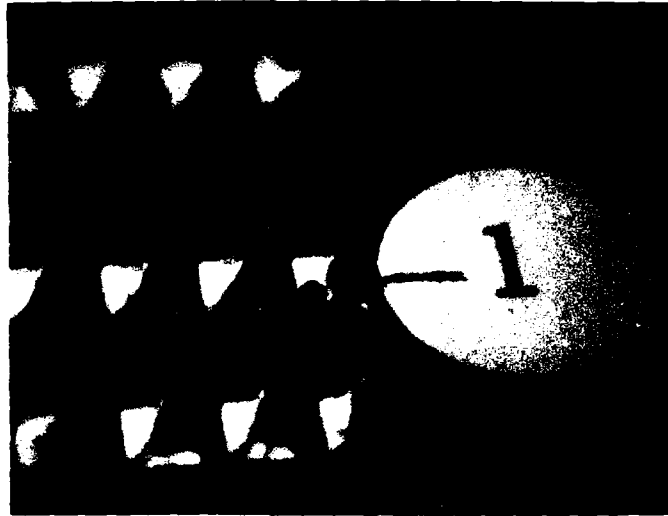


Figure 73. Small pit was intentionally formed at corner of solder joint marked "1" by intense laser-beam pulse.



Figure 74. Burn marks formed by intentional exposures directly on the substrate material (indicated by pencil marks on label).

1. The requisite longer exposure durations (perhaps between 50 and 100 mSec) would provide more time for heat-penetration into the target in order to reveal hidden defects, and

2. The longer exposures at lower power levels would reduce the possibility of sudden accidental damage to the substrate and would also provide a safer margin for damage prevention by giving the damage-prevention circuit more time to operate.

The only question about the use of the lower power levels might be, would they provide enough thermal signal to the infrared detector during a reasonably short exposure?

A test series was then conducted in which 9-watt exposures of various durations were used on solder joints while temperatures were observed with a Vanzetti Thermal Monitor. The sensitivity of this device is appreciably less than that of the INSPECT optical detector and required a minimum of 140°F at a blackbody target in order for any signal to be observed at all. This corresponds to an even higher target temperature for a non-blackbody target such as solder, whose emissivity may be as low as 0.1 or 0.2. It required no more than a few tests for us to determine that 9-watt pulses of between 50 and 100 mSec with a defocused beam spot would provide more than adequate signals to the Thermal Monitor. These signals would be much more than needed for the highly sensitive INSPECT detector, and so even shorter exposures might be used if they were sufficiently long for heat penetration. This question will be answered during the design phase for the final system.

In a final test series with the same laser, the 9-watt beam was refocused to a diameter of 0.015" in order to provide a somewhat more hazardous situation as far as board damage might be concerned, and some tests of board damage were carried out. One test result was that a commonly used light-green FR-4 laminate (our Sample No. 16 from the earlier board-damage tests) showed no damage with exposures as long as 140 mSec. However, a different green FR-4 (our Sample No. 13) did exhibit a large burn mark at 140 mSec and a small one even at 18 mSec. The results for board materials of other colors were between these two extremes.

We conclude, from these "worst case" tests with a nine-watt beam, that:

1. The beam spot should not be focused as small as 0.015" unless lower powers than nine watts are being used;
2. Steps should be taken to ensure spot-centering on the solder and not on the substrate;
3. The use of the damage-prevention circuit should be implemented to avoid accidental board damage.

3.5.4 Other Considerations

To conclude our discussion of system optimization, we remind the reader that we have already pointed out, in Section 3.4.6.3, the desirability of maintaining proper focus for the laser-beam spot, an adjustment which may have to be made for each board thickness unless provision is made to maintain fixed target heights. The best focus is not necessarily the sharpest one, and some intentional defocusing may be in order, especially when beam homogenization is not used, so that the target is covered

more uniformly and the system does not respond to minute blemishes. The matter of the best focal condition with homogenized beams remains to be examined in a later phase of this work.

We have also indicated, in Sections 3.4.6.2 and 3.4.6.4, the advantages of beam-spot elongation and, alternatively, of multiple exposures along the lead length in the case of lap joints. The elongation method remains to be further investigated with the laser and detector axes being made coincident. Point-by-point testing along a lap joint is a matter of programming at the time rather than a design consideration, but it is listed here as a possibly useful technique.

Finally, the use of the damage-prevention circuit of Section 3.2 is recommended as a means of improving the system performance by eliminating the possibility of damage to the various board surfaces.

4.0 PROGRAM REVIEW

In summary of the program highlights, the following objectives were achieved:

1. A total of 1,074 solder joints were prepared for the tests which are reported on here, in addition to preliminary samples which were made as we perfected our fabrication techniques. Results are tabulated on 1,148 tests on these joints in addition to preliminary test results which are detailed in the text.
2. Laser-beam damage tests were carried out on 60 samples of laminate materials, showing a wide variability in damage susceptibility.
3. A damage-prevention circuit was implemented and was shown to operate successfully with laser-beam powers up to six watts. (It was later shown to be effective with beam powers as high as 20 watts on easily damaged black FR-4 material.)

4. Two types of conformal coating were tested on solder joints and on laminates and were found to have desirable, rather than undesirable, effects upon the test results.
5. Other testing procedures were explored besides the usual single exposure with a round laser-beam spot. These included tests with an elongated spot as well as multiple exposures on lap joints with round spots.
6. Improvements were made in the system design concept, comprising the generation of a method for co-aligning the laser-beam and detector axes (which was later implemented) and the installation of an optical fiber in the laser-beam path which brought about homogenization of the beam spot and other advantages.
7. Separate tests revealed that the optimal laser-beam power for most tests on solder joints would be ten watts or less.

Of the 1,148 test results which appear in Tables 5, 6 and 7, ninety-four percent of the laser/thermal data points agreed with human judgment in assessing the qualities of the individual joints. In 46 cases, the laser/thermal assessment was more critical than the human observer and in 21 cases it was less critical. Of the 21 cases, we count 16 of these as detection failures because a "bad" or "questionable" joint was rated as "good"; in the other five, a "bad" one was rated "questionable" and would have to be checked visually in any case.

It must be remembered that there is a certain amount of arbitrariness in the human assessment of solder-joint quality, and there is further arbitrariness in defining the thresholds which separate the thermal peaks into various categories. A change in these decision levels would revise our scores either upward or downward.

We expect, also, that closer agreement between human and automatic assessment will result when tests are carried out with the homogenized laser beam as it impinges vertically upon the target.

5.0 RECOMMENDATIONS

Our primary recommendation is that the present work be carried forward and that the implementation of a prototype of the final testing station should begin. We are aware that the sponsor is already giving this serious consideration and we are prepared to offer our assistance in any way.

We also make a recommendation regarding what action is to be taken after the "no-go" solder joints have been identified. We have separately proposed to the sponsor that a verification station be designed and implemented so that a human inspector might visually check all no-goes which have been identified by the system. The station would be comprised of a separate positioning table under the control of the main computer. This would allow the operator to examine each no-go in sequence, at will and under push-button control, while the laser/thermal system proceeded to test other boards. Stereomicroscopic viewing would allow close inspection of each no-go by means of a recently developed 3-D projection display, in color, which does not require viewing through eyepieces or the use of other encumbrances.

In the meantime, work has proceeded under Vanzetti Company sponsorship, since the time that Phase 2.2 was completed, as we continue to verify the system capability and to improve

upon the design concept. Some of the testing of simulated cracked feed-through joints, reported herein, was carried out under the continuing program, as was the installation of the optical fiber, which has eliminated the hotspot problem and others. Installation of a dichroic beamsplitter for the co-alignment of the laser and detector axes has also been done since Phase 2.2. Recently, a "main computer" has been integrated into the system which now performs many functions automatically which were once required of the human operator. This includes automatic sorting of thermal peaks into "good" and "bad" categories. A 30-watt Nd:YAG laser is now in use (at reduced power) and provides more satisfactory operation than did the earlier six-watt laser.

6.0 CONCLUSION

In closing, we offer a final statement about the general capability of the laser/thermal testing method. The method combines the use of two phenomena in distinguishing between normal solder joints and deviations from normality:

1. Reflectance differences, such as due to cloudy surfaces, pits, cracks, and other light-absorbing or light-scattering features which are likewise visible to the human eye; and
2. Heat-penetration differences between a normal joint and one whose surface is not in thermal contact with the normal amount of heat-sinking, thus causing a more rapid heat buildup in the surface. This would apply to feed-through joints with large gas bubbles beneath the surface, to poorly bonded flat-pack leads, and to similar hidden defects. (Recent work of ours, since Phase 2.2, has revealed that longer-than-normal exposures, up to one second or more, will allow sufficient depth of heat penetration to permit the detection of voids well below the surface of a feed-through joint.)

However, as was pointed out in Section 3.4.8.3, the system is still slightly sensitive to small cosmetic defects, which can be an advantage if such defects are cause for rejection. If they are not, the system decision level must be raised so that the thermal peaks for such blemishes are below the threshold and fall into the "acceptable" category, thus requiring greater severity of defect in the rejectable joints. Also, a joint containing a combination of surface features which tend to drive the thermal peak in opposite directions will work against the defect-detection process. An example would be a depressed but shiny surface in a feed-through joint (which could likewise escape human detection) or a lifted lap-joint lead with an exposed gold surface.

Aside from these matters, which may have a low probability of occurrence in actual solder joints, we believe that our test results have been quite positive for solder joint defects of ordinary interest, as was reviewed in Section 3.4.8.3.

We believe that the results of our earlier and future work in solder joint testing will benefit the entire "solder-joint inspection" community as well as the United States Air Force who has provided the initial and encouraging financial support which has stimulated this development.

The enthusiasm and inspiration of J. H. Ele of the SM-ALC/MMIREA office are especially appreciated.

APPENDIX A

We present, on the following pages, a reproduction of a paper which was presented at the Cleveland Electronics Conference (CECON '80) on May 21, 1980. The paper describes the principle and operation of the laser/thermal testing system which is the subject of this report.

LASER INSPECTION OF SOLDER JOINTS

Riccardo Vanzetti, Alan C. Traub and Alan A. Richard

Vanzetti Infrared & Computer Systems, Inc.
607 Neponset Street, Canton, Massachusetts
U. S. A. 02021 617/828-4650

ABSTRACT

The prototype of an automatic system has been developed for the inspection of solder joint quality on printed circuit boards. The process uses laser-pulse heat injection and infrared thermal sensing, both under microprocessor control. Each joint is warmed slightly by a timed exposure from a six-watt laser, during which its thermal signature is obtained via an infrared sensing system. The latter uses a cryogenically cooled indium antimonide detector and is sensitive to temperature changes of 0.05°C . Joints which differ in certain physical properties exhibit different thermal signatures which are sorted out by the computer. The method is presently being used both on lap-type joints at integrated circuit leads and on feed-through joints in plated-through holes.

INTRODUCTION

In the manufacture of printed circuit boards, it is essential that each solder joint meet certain standards of mechanical quality in order to remain electrically intact during possible prolonged use in adverse environments. Circuit boards are often put to uses in which they are physically handled, dropped, vibrated, thermally cycled, and so forth. Although electrical testing of a newly made board may reveal that the board is intact at the moment, visual inspection is often used to assess the quality and survivability of each joint.

The preparation of a solder joint involves several variables such as the degree of cleanliness, proper application of flux, optimal solder temperature, and so forth. As in most manufacturing operations there is the likelihood of operator error, improper machine settings, materials quality variations and other adverse influences which lead to cold joints, insufficient solder, solder voids, blow holes, poor attachments, and to many other sources of ultimate joint failure under duress.

There are two problems connected with the use of visual inspection of joint quality, both of which can be eased by use of the laser/thermal method described here. The first is that not all types of defect are visible, such as solder voids or poor bonds. The second is the known variability of human judgment in making decisions about joint quality. It is known, in the inspection field, that an inspector will often change his decision level according to batch quality. A bad batch of samples may result

in more liberal decisions than otherwise, whereas a good batch can cause the inspector to become more critical.

PRINCIPLE OF OPERATION

The laser/thermal method singles out variations in one or the other of two physical properties which often indicate defective joints:

Variations in thermal mass;
Variations in surface absorption.

As an example, Figure 1 shows, in cross section, a normal lap-type joint compared with one having insufficient solder and a void beneath the lead. It is evident that the defective joint will warm up faster than the good one when exposed to the same laser pulse duration and intensity.

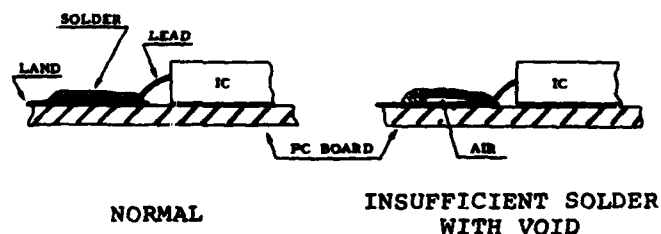


Figure 1. Examples of good and bad lap joints.

Similarly, Figure 2 shows a normal feed-through joint and one with insufficient solder. Here again it is clear that the latter will reach a higher final temperature than the former. In this case, the higher heating rate is further enhanced by the cavity-like nature of the joint which thus serves as a light-trap. The incident laser beam undergoes several reflections before escaping the cavity, repeatedly adding heat to the joint each time.

Variations in surface absorptivity are commonly associated with certain other types of defect. These include the dull or granular finishes of a cold joint, discolorations due to overheating, and exposed gold surfaces not covered by solder. Dull and discolored surfaces exhibit higher peak temperatures whereas lower ones are associated with exposed gold.

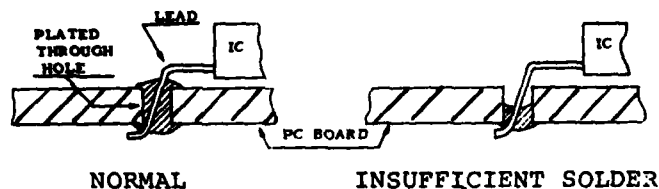


Figure 2. Examples of feed-through joints.

By well-known principles of infrared radiation, the temperature rise during laser warming may be observed remotely. This is carried out by an optical collecting system which focuses the emitted radiation onto a sensitive infrared detector. The amplified detector signals may be displayed on an oscilloscope and would have the appearances shown in Figure 3 for various types of joint.

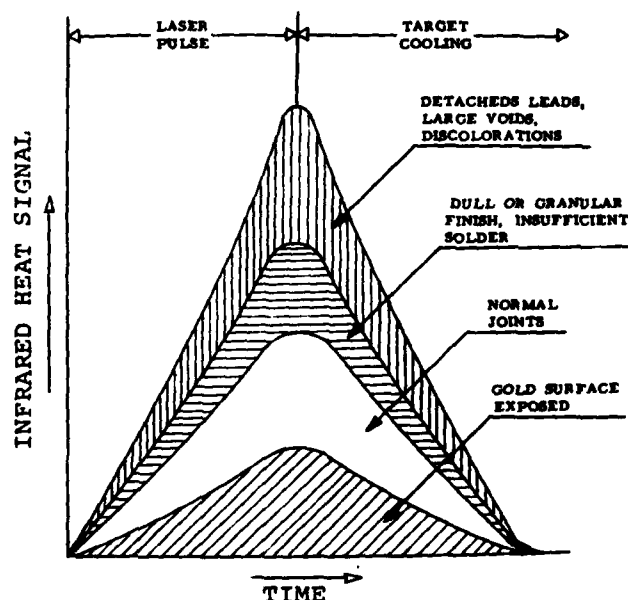


Figure 3. Solder joint variations are revealed by different peak temperatures.

Alternatively, the signals may be directed to a microprocessor where they may be sampled for peak-temperature values or at various points along the heating curve to determine uniformity of heating or other properties. The computer also controls the operation of an XY positioning table and the firing of the laser shutter, besides printing out the identities or locations of joints whose thermal properties fall outside of a designated acceptance

band.

A schematic diagram of the system is shown in Figure 4. Because the beam from the neodymium:YAG heating-laser is invisible, a red-light beam from a small helium-neon laser is brought into coincidence with it at the target point as a convenience in finding this point visually. This is necessary only when the XY-locations of joints on a new board are being manually programmed into the computer.

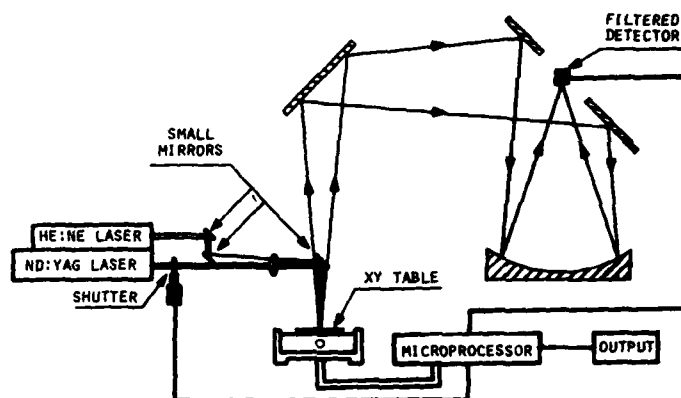


Figure 4. Infrared system measures warming during laser pulse.

Once a given type of board is programmed, other boards of that type may be tested without further programming. The program may be stored on tape so that boards of various configurations may be alternated.

The infrared collecting and detection system is sensitive to temperature changes of 0.05°C , so that the temperature of a test joint need be raised by only a few degrees above ambient temperature in order for a complete thermal signature to be achieved. The detector is optically filtered to exclude most of the laser radiation, so that essentially the thermal infrared from the joint itself will be detected.

A block diagram of the system appears as Figure 5, showing the interfacing of the processor with the rest of the system.

THE MICROPROCESSOR

Our laboratory prototype was implemented with an Intel Development System, Model 230. The processor performs all of the controlling functions and computations. Two SBC multibus compatible boards were added to this. The first was a high speed analog to digital converter used to input the thermal data from the infrared detector. The input rate can be as high as 16 KHz, which is more than sufficient for our purposes. The second board was a general purpose parallel digital interface board used to input and output the control signals.

The positioning table is interfaced to the processor through the digital interface board. Separate signals are supplied to jog the table in

The X and Y directions. These signals are open-loop because the table stepping motors simply respond to input pulses and do not provide feedback. Care must thus be taken in writing the software so that the jog pulses do not exceed the stepping rate.

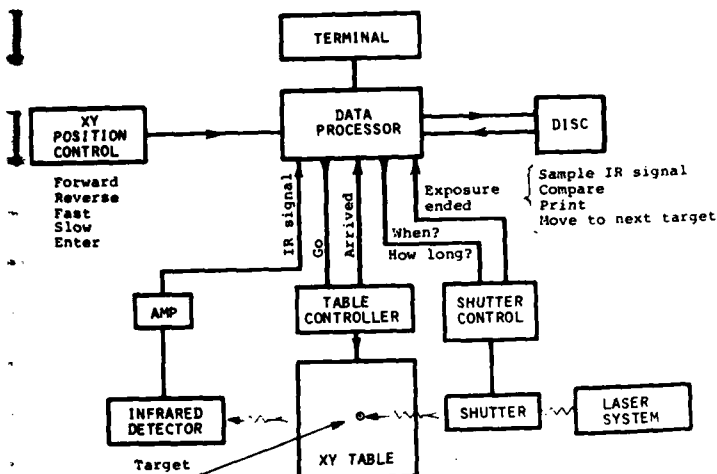


Figure 5. Block diagram of system.

Several closed loop signals are sent to the table motors. The first is the start-of-board command in which the circuit board under test is moved so that the first test joint falls into position, to which all subsequent positions are referred. The second closed loop signal is the end-of-board command, and the third is for advancing the table to intermediate points and signaling its arrival

at each. For each joint, the arrival signal causes a digital signal to open the laser shutter for a predetermined exposure duration. During this time, via a separate photodetector downstream of the shutter, the laser intensity and pulse duration are monitored. The intensity information may be used for automatic gain control computations in order to account for possible laser power fluctuations during or between exposures. At the end of the pulse, the processor is notified to index the table to the next joint.

At present, the detailed table commands are provided by a commercial controller which is provided with the table, but under the general supervision of our processor. One of its principal functions is, upon each indexing, to compute an up-ramp and a down-ramp for each axis so that the table will accelerate and decelerate properly in order to arrive smoothly at its destination. Later, the functions of the table controller will be taken over by the main processor.

The program is written in the higher level language of PLM. This allows easy manipulation of the numbers inside the processor, as well as the ability to output printed reports on the system console. Assembly language sub-programs are used to speed up and pre-process the thermal data prior to actual analysis.

At present, the system software makes decisions about data based on pre-set high-low acceptance limits on the peaks of the thermal signatures. More versatile algorithms are possible, however, and will be used if needed. These can be used to derive



Figure 6. Laboratory system used in feasibility study.

information about the first and higher time derivatives of the thermal signatures, to take action if there are discontinuities in these, and so forth.

EXPERIMENTAL RESULTS

The prototype system is currently in the form of a laboratory setup, as shown in Figure 6. Beams from the two lasers at the left enter apertures in the side wall of the supporting structure which holds the XY table and, in the cabinet above it, the infrared detection system. The beams are combined and re-directed via mirrors and are focused on the target (see light-spot in Figure 7). To the right of the structure is the table controller in which the successive target positions are programmed. This is in turn controlled by a main processor (not shown) which also fires the YAG laser shutter, processes and prints out the thermal data, and carries out other functions. The oscilloscope provides visual displays of the thermal data and is used in preparing the accompanying oscillograms.



Figure 7. Sample board on XY table.

Figure 7 is a view of the table with a sample board on it. Above the target, a small mirror corrects the laser beams downward after they proceed from the focusing lens in the holder at the left.

Figure 8 is a composite oscillogram showing thermal signatures at four different locations along an irregular joint with an uneven solder distribution. The straight lines near the top show the creation of the laser pulse as seen by a separate detector. In this and in the following cases, the pulse durations were 0.6 second or greater. It is seen, however, that the differences in the curves were readily noticeable much earlier in the warming cycle, so this exposure duration will not be necessary in the production environment.

In the curves, the lower ones are indicative of the more massive solder regions while the upper ones indicated lower thermal masses. Ripples in the traces were due to a temporary vibration problem which has since been remedied.

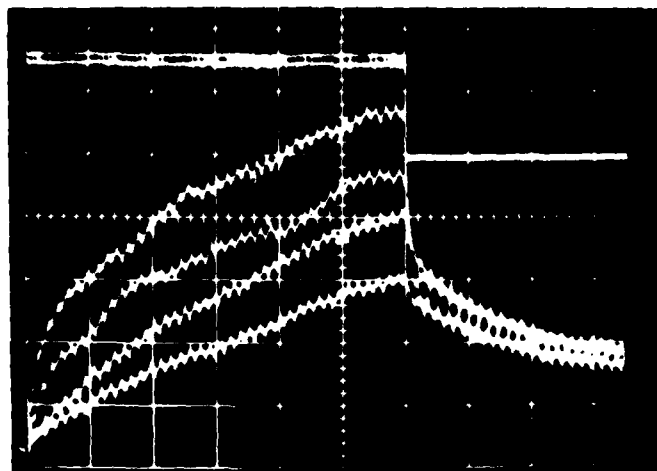


Figure 8. Variations in solder mass along a single lap joint.

On the same horizontal scale, Figure 9 shows a high thermal signature for a detached portion of a lead, compared with a lower trace which shows the intact part. Again the difference is noticeable early in the cycle.

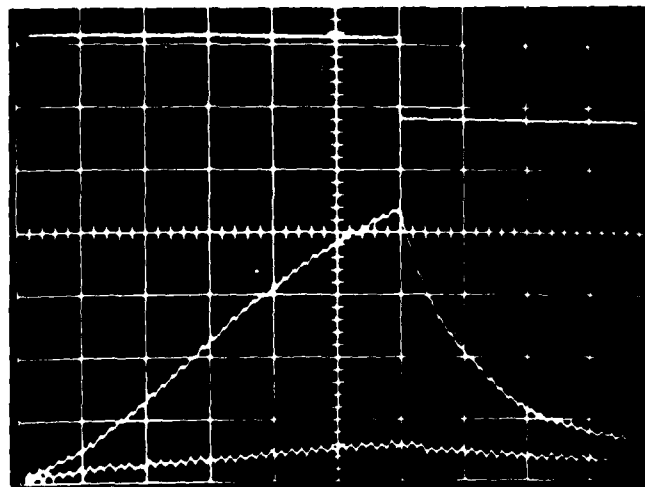


Figure 9. Lifted heel of lap joint shows higher thermal peak than center.

A similar exposure duration was used in preparing Figure 10, in which greater warming is shown by the cold joint than by the normal one. The difference was detectable within 50 mSec of exposure initiation; the long exposure was used for demonstration purposes.

A slower oscilloscope sweep was used in Figure 11 which shows a sequence of thermal signatures from a set of feed-through joints. These were more massive than the lap joints tested and exposures of 1.2 seconds were used. Again, the lower curves represent more massive joints, the higher ones showing either cold joints, voids, blowholes, insufficient solder, discolorations, or other defects.

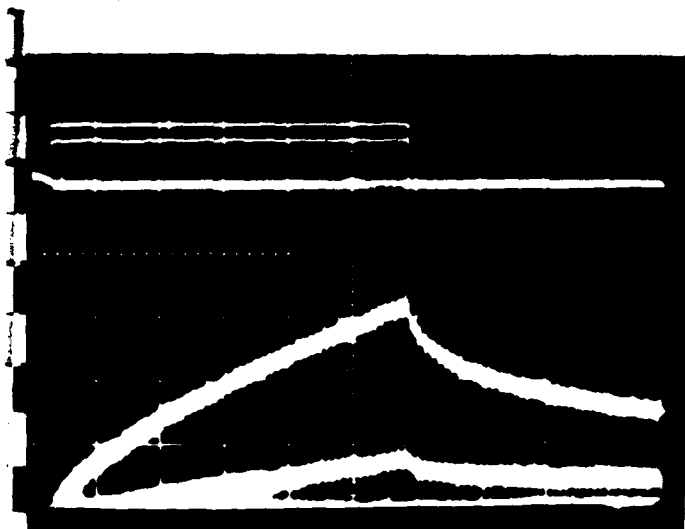


Figure 10. A cold lap joint (upper curve) and a normal one.

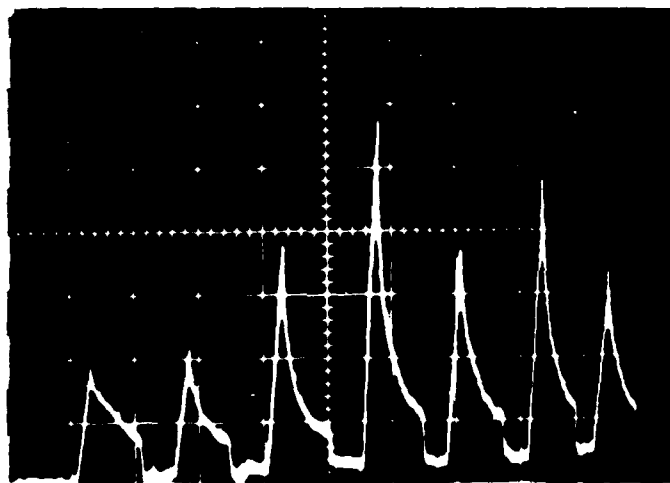


Figure 11. Seven feed-through joints of varying quality.

In these examples, the actual temperatures reached by the test joints seldom exceeded 100°F.

The developmental system currently uses a six-watt Nd:YAG laser. In most of our tests, as in those discussed here, the laser was operated at two to three watts. During full-power tests, heating rates increased approximately in proportion to the power increase. In most cases, defective joints could be recognized in 50 to 100 mSec. With a laser of higher power, the inspection time would decrease proportionately, up to the point where surface damage might occur before the heat had time to penetrate the solder mass in order to probe it.

A custom-designed positioning table is used which can access adjacent joints within 50 mSec. With laser powers tailored to provide 50 mSec exposures or less, testing rates of ten adjacent joints per second or more will be achievable by this method.

The average testing rate will be somewhat lower, considering board-loading time plus travel time between non-adjacent joints.

The rejection of faulty joints is performed by the processor on the basis of a threshold level which is programmed into it for each type of joint. For each board, the processor stores not only the XY coordinates of each joint but its normal range of thermal peaks. When a peak falls outside of the acceptance range, the coordinates of that joint are printed out for later repair. Alternatively, a dye marker could be applied at or near the joint, or any of several other possible methods could be devised for visually displaying to a repair operator the locations of faulty joints as found by the system.

TYPICAL APPLICATION

The average inspection rate of the developmental system is potentially twice that of the human inspector. The principal advantage of the system, however, is that it is a more reliable decision maker than the inspector. The judgment of the latter is subject to variation according to whether an especially good batch or an especially bad batch of items is being inspected, and it is always limited to the visible features of the items.

The potential cost/effectiveness of an operational system is illustrated by a hypothetical case. We assume that a given circuit board manufacturer produces a half million square feet of board per year with an average density of 1,500 feed-through joints per square foot. According to the actual experience of one such manufacturer, about 25 inspectors (single shift) would be required to keep pace with this production rate. Their average inspection rate would be about four joints per second, or half the expected average rate of the automatic equipment.

One automated system could thus replace two inspectors, so that 12 or 13 systems could accommodate the annual production. In these quantities, such a system might cost the customer \$75,000 besides maintenance. If an inspector earns \$5 per hour with a 150% overhead rate, his yearly cost is about \$25,000 per year, so that \$50,000 could be saved in the first year (except for maintenance). If a system were used for three shifts per day, the savings would be tripled.

Besides the savings, we emphasize the advantage of consistency of judgment as well as the detectability of hidden defects.

PROGRAM STATUS

The prototype system is presently in the form of a laboratory setup. Product development will begin at the end of a testing program which is now under way. Large-scale statistical testing of various types of defective joint will determine which types can be detected by this method and how severe each type of defect must be for reliable

detection. During the tests, such optical parameters as laser-beam spot size and power density, spot shape and exposure duration will be optimized for various solder joint configurations.

These designs will be finalized after the tests, and units will be implemented for further tests under operational conditions.

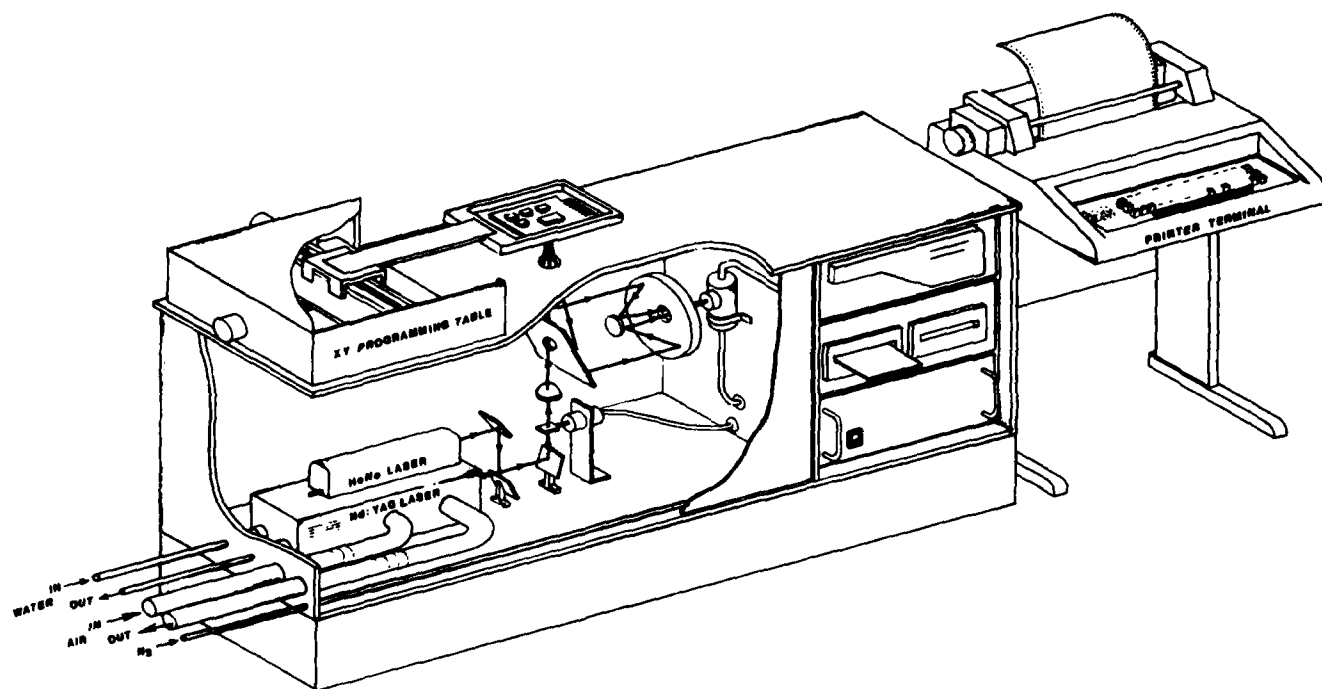


Figure 12. Artist's Concept: Solder Joint Inspection System for Feed-Through Joints

A design concept for one type of production unit is depicted in Figure 12. This unit is intended for assembly line use after the wave soldering process, for boards using feed-through joints. Testing is thus done from underneath so that the board may remain right side up. For lap joints, testing will be done from above, using a configuration similar to that shown earlier in Figure 4.

ACKNOWLEDGMENT

We are grateful for the cooperation of Messrs. Hamman, Shilliday and others at Battelle-Columbus Laboratories which funded the early development of this method, and we acknowledge the enthusiasm, encouragement and financial support of John Ele of the USAF Sacramento Air Logistics Center at McClellan AFB.